

Spring 5-14-2016

Application of an Ionic Liquid Column to the Analysis of Flavor and Fragrance Ingredients

Nicole L. Curto

nicole.harmuth@student.shu.edu

Follow this and additional works at: <https://scholarship.shu.edu/dissertations>



Part of the [Analytical Chemistry Commons](#)

Recommended Citation

Curto, Nicole L., "Application of an Ionic Liquid Column to the Analysis of Flavor and Fragrance Ingredients" (2016). *Seton Hall University Dissertations and Theses (ETDs)*. 2176.
<https://scholarship.shu.edu/dissertations/2176>

Application of an Ionic Liquid Column to the Analysis of Flavor and Fragrance Ingredients

by

Nicole L. Curto

THESIS

Submitted to the Department of Chemistry and Biochemistry at Seton Hall University in partial fulfillment of the requirements for the degree of Master of Science.

May, 2016

© 2016 Nicole L. Curto

We certify that we have read this thesis and that in our opinion it is adequate in scientific scope and quality as a thesis for the degree of Master of Science.

Approved



Nicholas H. Snow, Ph.D., Research Advisor



Yuri Kazakevich, Ph.D.
Member of Defense Committee



Alexander Fadeev, Ph.D.
Member of Defense Committee



Cecilia Marzabadi, Ph.D.
Chair, Department of Chemistry and Biochemistry

Acknowledgements

None of this would have been possible without the numerous people who have supported me over the years. I am beyond thankful to Villanova University's Department of Chemistry for giving me such a solid foundation in Chemistry. After graduating in 2010, I promised myself I would go back to pursue a Master's degree and in 2012 I found myself at Seton Hall University. I am so grateful to all the professors I have had the pleasure of learning from, and for the opportunities the department has provided me during the course of my time at SHU.

I started working at International Flavors & Fragrances in 2010 and immediately fell in love with the industry. It is because of the opportunities I had at IFF that I decided to attend Seton Hall and pursue a Master's degree under Nicholas Snow's direction. I am grateful for the financial support IFF has given me over the years. Even more so, I owe so much, to so many people who coached me through numerous exams, papers, classes, and research headaches. I am so appreciative of the compassion and support from my managers, Danielle DiNallo and Robert Cannon. You have both been continual sources of inspiration, from your knowledge of expertise to long conversations about life. I value our professional relationships but our friendships even more. Thank you.

Dr. Snow, it has been quite a journey, and it only seems fitting that I followed in Danielle's footsteps as a student in your lab. Thank you for reminding me what I loved so much about academia. Being part of the Separations Group has been a lot of fun and I am so grateful for all of your guidance and input throughout the years. You have not only expanded my knowledge about chromatography, but have challenged me to think of things differently, and appreciate all facets of chemistry involved. While I have enjoyed our numerous discussions

about GC, I will miss our conversations about daily life and business the most. I think it is here that some of the most important lessons can be found, and I thank you for imparting your wisdom and exploring these aspects of life with me, as well.

One of the greatest things about graduate school is the people you meet along the way. I am so lucky to have met some wonderful people who made the “pain” of graduate school just a little sweeter. Julianne Berger and Michelle Schmidt, I am so grateful we ended up at the same school at the same time. You have made this journey something to be proud of and I can’t thank you both enough for the countless pep talks and laughs we’ve had along the way. I am beyond proud of both of you and continually find myself inspired by you. This is just the beginning for us. Tom Del Mastro, I am so thankful that your path led you to the Separations Group. Our back and forth discussions about the flavor & fragrance industry have been instrumental to my research project, and have challenged me to look at the industry from another point of view. I could not have accomplished this without your input, support, and friendship these past few years. I am hoping our paths continue to cross throughout our careers in the F&F industry.

My family and friends made this all worth it. Thank you to my parents for inspiring me every day to love what you do and do what you love. I will never have half as much knowledge as you do talent, but I will continue to try to make you proud every day in my own unique ways. Your love and encouragement has been my rock since day one.

Last but not least, I dedicate this entire chapter of my life to my husband. You are the kindest, sweetest man and I am so lucky to have you by my side through it all. Your love and support is what kept me going throughout my years at SHU. Everything I do, I do for you and because of you. This accomplishment is *ours*. Thank you will never be enough.

Table of Contents

Acknowledgments	ii
List of Figures	vii
List of Tables	xi
Abstract	1
1 Introduction	3
1.1 Flavor and Fragrance Materials.....	3
1.2 Gas Chromatography Column Phase Selection	4
1.3 Development of Ionic Liquid Columns.....	8
1.4 Stationary Phase Retention Mechanisms	12
1.4.1 Traditional Column Phases	12
1.4.2 Ionic Liquid Stationary Phases	13
1.4.3 Polarity and Selectivity	14
1.4.4 Grob Test	16
1.4.5 Kovats Retention Indices	16
1.4.6 Rohrschneider-McReynolds Classification of Stationary Phases.....	19
1.4.7 Inverse Gas Chromatography	23
1.4.8 Abraham Solvation Parameter	23

1.5	Polarity Scale for Ionic Liquid Columns.....	26
1.6	Thermodynamics and van't Hoff	29
1.7	Polyol-Induced Extraction.....	31
2	Experimental Procedure	32
2.1	Materials.....	32
2.2	Instrumentation for pure chemical characterization.....	32
2.3	Liquid/Liquid Extraction of Mead	33
2.4	Polyol-Induced Extraction of Mead	33
2.5	Instrumentation for Analysis of Extracts	34
3	Results and Discussion	35
3.1	Polarity Study of Molecules with a Common Hexane Backbone.....	35
3.2	Homologous Series Study	45
3.3	Alcohols	46
3.4	Aldehydes.....	55
3.5	Acids.....	64
3.6	Ethyl Esters	73
3.7	Alkanes.....	82
3.8	Polyol-Induced Extraction.....	91
3.8.1	Organoleptics	91
3.8.2	GC-FID Analysis	92

4	Conclusions and Future Work	95
5	References	98
6	Appendix	102
6.1	Raw Data from Polarity Study	102
6.1.1	SLB-IL60 data	102
6.2	Raw Data for Alcohols.....	113
6.2.1	SLB-IL60: Alcohols.....	113
6.2.2	HP-20M: Alcohols	117
6.3	Raw Data for Aldehydes	119
6.3.1	SLB-IL60: Aldehydes.....	119
6.3.2	HP-20M: Aldehydes	122
6.4	Raw Data for Acids	124
6.4.1	SLB-IL60: Acids.....	124
6.4.2	HP-20M: Acids	127
6.5	Raw Data for Ethyl Esters	130
6.5.1	SLB-IL60: Ethyl Esters.....	130
6.5.2	HP-20M: Ethyl Esters	133
6.6	Raw Data for Alkanes	136
6.6.1	SLB-IL60: Alkanes.....	136
6.6.2	HP-20M: Alkanes	139

List of Figures

Figure 1: The general structure of polysiloxane	5
Figure 2: The structure for a 100% dimethylpolysiloxane stationary phase.	6
Figure 3: The general structure for polyethylene glycol (PEG)	7
Figure 4: The phase structure of SLB-IL60, 1,12-di(triisopropylphosphonium)dodecane bis(trifluoromethylsulfonyl)imide	11
Figure 5: The chemical structure of squalane.	21
Figure 6: Polarity Scale for IL stationary phases. Adapted from Sigma-Aldrich. ¹	28
Figure 7: van't Hoff plots of different polarity aldehydes with a common hexane backbone on SLB-IL60 (A) and HP-20M (B) columns.	37
Figure 8: van't Hoff plots of different polarity ketones with a common hexane backbone on SLB-IL60 (A) and HP-20M (B) columns.	38
Figure 9: van't Hoff plots of different polarity alcohols with a common hexane backbone on SLB-IL60 (A) and HP-20M (B) columns.	39
Figure 10: van't Hoff plots of different polarity lactones with a common hexane backbone on SLB-IL60 (A) and HP-20M (B) columns.	41
Figure 11: van't Hoff plots of different polarity esters with a common hexane backbone on SLB- IL60 (A) and HP-20M (B) columns.	42
Figure 12: van't Hoff plots for 2-hexylthiophene on SLB-IL60 (A) and HP-20M (B) columns.	43
Figure 13: van't Hoff plot of a homologous series of primary alcohols on the SLB-IL60 column. The corresponding table shows the ln k values at various temperatures for a homologous series of primary alcohols on the SLB-IL60 column.	47

Figure 14: van't Hoff plot of a homologous series of primary alcohols on the HP-20M column. The corresponding table shows the $\ln k$ values at various temperatures for a homologous series of primary alcohols on the HP-20M column.	48
Figure 15: A plot of ΔG° vs T for a homologous series of primary alcohols on the SLB-IL60 column. The corresponding table shows the ΔG° values at various temperatures for a homologous series of primary alcohols on the SLB-IL60 column.	49
Figure 16: A plot of ΔG° vs T for a homologous series of primary alcohols on the HP-20M column. The corresponding table shows the ΔG° values at various temperatures for a homologous series of primary alcohols on the HP-20M column.	50
Figure 17: A plot of the ΔS° and ΔH° values and their absolute differential values on the SLB-IL60 and HP-20M columns for a homologous series of primary alcohols.	52
Figure 18: A plot of ΔG° vs the number of carbon atoms for a homologous series of primary alcohols at various temperatures on the (A) SLB-IL60 column and the (B) HP-20M column.	54
Figure 19: van't Hoff plot of a homologous series of alkyl aldehydes on the SLB-IL60 column. The corresponding table shows the $\ln k$ values at various temperatures for a homologous series of alkyl aldehydes on the SLB-IL60 column.	56
Figure 20: van't Hoff plot of a homologous series of alkyl aldehydes on the HP-20M column. The corresponding table shows the $\ln k$ values at various temperatures for a homologous series of alkyl aldehydes on the HP-20M column.	57
Figure 21: A plot of ΔG° vs T for a homologous series of alkyl aldehydes on the SLB-IL60 column. The corresponding table shows the ΔG° values at various temperatures for a homologous series of alkyl aldehydes on the SLB-IL60 column.	58

Figure 22: A plot of ΔG° vs T for a homologous series of alkyl aldehydes on the HP-20M column. The corresponding table shows the ΔG° values at various temperatures for a homologous series of alkyl aldehydes on the HP-20M column. 59

Figure 23: A plot of the ΔS° and ΔH° values and their absolute differential values on the SLB-IL60 and HP-20M columns for a series of alkyl aldehydes..... 61

Figure 24: A plot of ΔG° vs the number of carbon atoms for a homologous series of alkyl aldehydes at various temperatures on the (A) SLB-IL60 column and (B) HP-20M column. 63

Figure 25: van't Hoff plot of a homologous series of alkyl carboxylic acids on the SLB-IL60 column. The corresponding table shows the $\ln k$ values at various temperatures for a homologous series of alkyl carboxylic acids on the SLB-IL60 column..... 65

Figure 26: van't Hoff plot of a homologous series of alkyl carboxylic acids on the HP-20M column. The corresponding shows the $\ln k$ values at various temperatures for a homologous series of alkyl carboxylic acids on the HP-20M column. 66

Figure 27: A plot of ΔG° vs T for a homologous series of alkyl carboxylic acids on the SLB-IL60 column. The corresponding table shows the ΔG° values at various temperatures for a homologous series of alkyl carboxylic acids on the SLB-IL60 column. 67

Figure 28: A plot of ΔG° vs T for a homologous series of alkyl carboxylic acids on the HP-20M column. The corresponding table shows the ΔG° values at various temperatures for a homologous series of alkyl carboxylic acids on the HP-20M column. 68

Figure 29: A plot of the ΔS° and ΔH° values and their absolute differential values on the SLB-IL60 and HP-20M columns for a homologous series of alkyl carboxylic acids..... 70

Figure 30: A plot of ΔG° vs the number of carbon atoms for a homologous series of alkyl carboxylic acids at various temperatures on the (A) SLB-IL60 column and (B) HP-20M column. 72

Figure 31: van't Hoff plot of a homologous series of ethyl esters on the SLB-IL60 column. The corresponding table shows the $\ln k$ values at various temperatures for a homologous series of ethyl esters on the SLB-IL60 column. 74

Figure 32: van't Hoff plot of a homologous series of ethyl esters on the HP-20M column. The corresponding table shows the $\ln k$ values at various temperatures for a homologous series of ethyl esters on the HP-20M column..... 75

Figure 33: A plot of ΔG° vs T for a homologous series of ethyl esters on the SLB-IL60 column. The corresponding table shows the ΔG° values at various temperatures for a homologous series of ethyl esters on the SLB-IL60 column..... 76

Figure 34: A plot of ΔG° vs T for a homologous series of ethyl esters on the HP-20M column. The corresponding table shows the ΔG° values at various temperatures for a homologous series of ethyl esters on the HP-20M column. 77

Figure 35: A plot of the ΔS° and ΔH° values and their absolute differential values on the SLB-IL60 and HP-20M columns for a homologous series of ethyl esters..... 79

Figure 36: A plot of ΔG° vs the number of carbon atoms for a homologous series of ethyl esters at various temperatures on the (A) SLB-IL60 and (B) HP-20M column. 81

Figure 37: van't Hoff plot of a homologous series of alkanes on the SLB-IL60 column. The corresponding table shows the $\ln k$ values at various temperatures for a homologous series of alkanes on the SLB-IL60 column. 83

Figure 38: van't Hoff plot of a homologous series of alkanes on the HP-20M column. The corresponding table shows the $\ln k$ values at various temperatures for a homologous series of alkanes on the HP-20M column..... 84

Figure 39: A plot of ΔG° vs T for a homologous series of alkanes on the SLB-IL60 column. The corresponding table shows the ΔG° values at various temperatures for a homologous series of alkanes on the SLB-IL60 column. 85

Figure 40: A plot of ΔG° vs T for a homologous series of alkanes on the HP-20M column. The corresponding table shows the ΔG° values at various temperatures for a homologous series of alkanes on the HP-20M column..... 86

Figure 41: A plot of the ΔS° and ΔH° values and their absolute differential values on the SLB-IL60 and HP-20M columns for a homologous series of alkanes..... 88

Figure 42: A plot of ΔG° vs the number of carbon atoms for a homologous series of alkanes at various temperatures on the (A) SLB-IL60 column and (B) HP-20M column. 90

Figure 44: Chromatograms of the mead extracts on the SLB-IL60 column. Chromatogram A is the dichloromethane extract and chromatogram B is the acetonitrile extract..... 93

Figure 45: Chromatograms of the mead extracts on the HP-20M column. Chromatogram A is the dichloromethane extract and chromatogram B is the acetonitrile extract..... 94

List of Tables

Table 1: Grob test mixture probes and their functions, adapted from Grob and Barry. ¹²	18
Table 2: The McReynolds test probes and their measured interactions. Adapted from Grob and Barry. ¹²	22
Table 3: Descriptors and their properties used in the solvation parameter. Adapted from CF Poole, ⁶ JL Anderson, ¹⁵ and LM Sprunger. ²⁷	25
Table 4: Experimental P (polarity) and PN (polarity number) for various stationary phases. Adapted from Sigma-Aldrich. ¹	27
Table 5: Analytes chosen for comparison on the SLB-IL60 and HP-20M columns. All molecules have a common hexane backbone and are shown in order of elution from the HP-20M column. ³⁶	
Table 6: Calculated selectivities for peak pairs on the SLB-IL60 and HP-20M column phases..	44
Table 7: ΔH° and ΔS° values for a homologous series of primary alcohols on the SLB-IL60 and HP-20M columns.	53
Table 8: ΔH° and ΔS° values for a homologous series of alkyl aldehydes on the SLB-IL60 and HP-20M columns.	62
Table 9: ΔH° and ΔS° values for a homologous series of alkyl carboxylic acids on the SLB-IL60 and HP-20M columns..	71
Table 10: ΔH° and ΔS° values for a homologous series of ethyl esters on the SLB-IL60 and HP-20M columns.	80
Table 11: ΔH° and ΔS° values for a homologous series of alkanes on the SLB-IL60 and HP-20M columns.	89
Table 12: SLB-IL60 data from increasing polarity study.	102
Table 13: HP-20M data from increasing polarity study.	108

Table 14: Raw data for a homologous series of primary alcohols on the SLB-IL60 column. ...	113
Table 15: Raw data for a homologous series of primary alcohols on the HP-20M column.....	117
Table 16: Raw data for a homologous series of alkyl aldehydes on the SLB-IL60 column.	119
Table 17: Raw data for a homologous series of alkyl aldehydes on the HP-20M column.	122
Table 18: Raw data for a homologous series of alkyl carboxylic acids on the SLB-IL60 column.	124
Table 19: Raw data for a homologous series of alkyl carboxylic acids on the HP-20M column.	127
Table 20: Raw data for a homologous series of ethyl esters on the SLB-IL60 column..	130
Table 21: Raw data for a homologous series of ethyl esters on the HP-20M.....	133
Table 22: Raw data for a homologous series of alkanes on the SLB-IL60..	136
Table 23: Raw data for a homologous series of alkanes on the HP-20M.....	139

Abstract

Traditional, polar (polyethylene glycol/wax) stationary phase gas chromatography columns pose challenges for flavor and fragrance analysis particularly in regards to thermal instability at high temperatures, degradation when exposed to water, unchanging selectivity, and relatively short shelf lives. Recently, capillary columns using ionic liquids as stationary phases have become available. Ionic liquid columns offer a potential combination of high polarity and high temperature stability with unique selectivity. An in depth discussion about the history and development of column phase characterization, with specific emphasis on selectivity and polarity, will allow for a critical look at the polarity scale currently employed to characterize ionic liquid stationary phases.

Performance of an SLB-IL60 column was compared to a traditional HP-20M wax column, with focus on classic thermodynamic parameters – Gibbs free energy, enthalpy, and entropy. This comparison explores retention mechanisms and thermodynamic properties of the ionic liquid stationary phase versus its historical (wax) counterpart. A thorough analysis of these fundamental chemistry parameters developed a strong foundation for a comparison of selectivity and polarity. Ionic liquid columns were found to have similar retention mechanisms for homologous series of primary alcohols and ethyl esters. Thermodynamics revealed differences for homologous series of alkyl aldehydes, alkyl carboxylic acids, and alkanes in regards to retention mechanisms on the SLB-IL60 and HP-20M columns. In addition, a new polyol extraction technique was employed for the extraction of mead (an alcoholic beverage consisting of fermented honey). This extract was compared on both stationary phases to a traditional liquid/liquid extract of the mead. Comparing the activity of flavor and fragrance compounds on

ionic liquid and wax stationary phases demonstrated the applicability of ionic liquid columns to the flavor and fragrance industry.

1 Introduction

1.1 Flavor and Fragrance Materials

The flavor and fragrance industry plays an important role in modern life. From snacks and beverages to laundry detergents, cleaning solutions, and perfumes it is difficult to navigate through the day without touching an ingredient that was born in a Research & Development facility. As the industry gets more and more competitive, flavor and fragrance houses are challenged to create unique products that win in the marketplace. These materials are traditionally small, volatile molecules with low molecular weights, making gas chromatography (GC) the instrument of choice for analysis. A majority of molecules are oxygen containing – ketones, aldehydes, and esters account for a large portion of the portfolios. A slight change in the chemical structure - a double bond rearrangement, branch placement - can result in a significant impact on the organoleptic quality. However, molecular weights and physiochemical properties may go unchanged, thus making separation on traditional GC phases challenging. Analysts are continually challenged with finding robust, quantitative methods for product development, market product analysis, and new molecule discovery. These methods must cover a wide range of polarity with unique separations which generally requires the use of both polar and non-polar column phases to get a full profile of the product. Compounds that are difficult to quantitate on traditional, non-polar phases typically require the use of a wax phase column to obtain optimum chromatography. In this regard, new column chemistries that provide unique selectivity and cover a wide range of polarity would be ideal for analysis of flavor and fragrance materials.

1.2 Gas Chromatography Column Phase Selection

Polysiloxane polymer stationary phases were introduced in the early 1950s followed by polyethylene glycol stationary phases in the mid-1950s. These phases are liquid polymers that have applications in both packed column and capillary column analysis. The general structure for polysiloxane follows the format shown in Figure 1. A typical GC column stationary phase used for the analysis of flavor and fragrance materials is Agilent DB-1 which is 100% dimethylpolysiloxane, the structure of which can be found in Figure 2.

The general structure for polyethylene glycol follows the format shown in Figure 3. A typical GC column used for the analysis of flavor and fragrance materials, which will be used as a comparison column throughout this research, is Agilent HP-20M. The column phase has a molecular weight of 20,000 which corresponds to approximately 450 repeating C₂H₄O units.

Modifications to the general column phase structures led to the introduction of numerous GC stationary phases to the market place, but the chemistry remained relatively stagnant for the next 60 years. These stationary phases have a number of limitations, starting with active hydroxyl groups at the polymer termini. When exposed to water and oxygen, analysts are challenged to deal with column phase degradation, particularly for wax phases at elevated temperatures. In addition, the chemistry to make the column phases allows little room for altering the selectivity, making enhanced and unique separations a rather oblique option. Lastly, PEG phases are only stable up to approximately 280 °C, making it difficult to analyze analytes at elevated temperatures.¹ In 2008, Supelco introduced the first ionic liquid stationary phase, bringing to light a new age of technology to the industry that addressed the traditional column phase limitations.

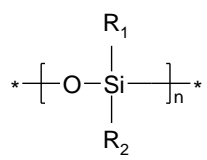


Figure 1: The general structure of polysiloxane

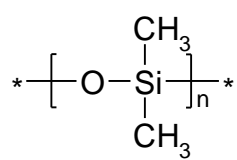


Figure 2: The structure for a 100% dimethylpolysiloxane stationary phase.

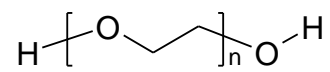


Figure 3: The general structure for polyethylene glycol (PEG)

1.3 Development of Ionic Liquid Columns

Ionic liquids (ILs) are salts that traditionally include an organic cation (nitrogen or phosphorous containing) and an organic or inorganic anion. They are liquid at room temperature with melting points at or below 100 °C. Physiochemical properties of ionic liquids include high viscosity, wide liquid range, low volatility, and high thermal stability.^{2,3,4} Yao⁴ reported that the viscosities of most ILs are often 1-3 orders of magnitude higher than traditional organic solvents. In order for an ionic liquid to be considered as a stationary phase, the material should have high viscosity that remains consistent over a wide temperature range. Hydrogen bonding and van der Waals-type interactions between the cation and anion of the IL govern the visco-properties. In addition, it is important to consider the surface tension of the IL. Values ranging from 30 to 50 dyne/cm typically exhibit superior wettability on the wall of untreated capillary columns.⁴ Historically, when the oven temperature is increased a rise in the baseline is observed, which signifies the volatilization and decomposition of the stationary phase. This is a direct indication of the thermal stability of the stationary phase, and it affects the operating temperature range and lifetime of the GC column.⁴ In many cases, the upper temperature limit of the IL is established by the thermal stability of the ionic liquid rather than its vapor pressure.⁵

Since the physical characteristics of ILs include high thermal stability, negligible vapor pressure, and high viscosity, ILs make excellent candidates for capillary GC phases. In order to be further considered for column phases, the IL should wet glass surfaces, have high viscosity to resist film disruption at high temperatures, and have adequate solubility in a volatile organic solvent to facilitate column coating.⁶ Ionic liquids have been shown to have good wettability in regards to fused silica capillaries. Their stability when exposed to oxygen and water makes ILs even more of particular interest. As previously mentioned, traditional GC column phases such as PEG and

siloxane-based phases decompose when exposed to oxygen and water, whereas ionic liquids are essentially unaffected. ILs have extended temperature ranges, higher polarity (which is said to be infinitely tunable), low column bleed, and unique selectivity. In 1999, Armstrong and coworkers⁷ reported the dual nature of IL stationary phases, suggesting that they separated nonpolar analytes as if they were nonpolar stationary phases, while also separating polar analytes as if they were polar stationary phases.

Ionic liquids have been extensively studied for approximately 15 years now, and because the possible combinations of cations and anions are nearly infinite, the number of publications is quite extensive. A simple search in the literature for “ionic liquids” results in 55,775 references. Refining this search to only include publications containing “chromatography” results in 2,518 references, the first of which was published in 1999.⁷ The goal of this research is not to reiterate all of the work on ILs that has been done thus far, but rather to explore the retention mechanisms and thermodynamic properties of ionic liquids in comparison to their historical counterparts, namely PEG. These concepts will be explored in the sections to follow.

It is important to note that Supelco (Sigma-Aldrich) has an extensive guide available online* for column selection. Using this guide and based on the work done by Cagliero⁸ and Ragonese⁹ regarding the analysis of flavor and fragrance compounds using IL columns, it was decided to focus the research efforts on SLB-IL60. This column phase is said to be useful for the analysis of alcohols, ketones, terpenes, sulfur compounds, amines, aromatic amines, esters and ethers, edible oils, beverages, volatiles, essential oils, and flavor & fragrance aromas.¹ In addition, IL columns such as the SLB-IL60, which exhibit intermediate polarity similar to PEG stationary

* http://www.sigmaaldrich.com/content/dam/sigma-aldrich/docs/Supelco/Posters/1/ionic_liquid_gc_columns.pdf

phases, are said to be suitable for the “analysis of volatile and semivolatile analytes possessing a wide range of polarities”² which is ideal for flavor and fragrance analysis. Cagliero and coworkers⁸ reported the attractiveness of IL stationary phases for the analysis of flavors and fragrances, referring to their extended application to a wide polarity range. The authors studied the performance (efficiency, separation capability, inertness/activity) of allergen and pesticide mixtures on available IL columns. Performance was measured by determining average peak width, peak asymmetry, adsorption and the calculated separation measure (the number of consecutive non-overlapping peaks within an arbitrary time interval) for the standard mixtures. They reported similar performance of IL60 to OV-1701. They also reported adsorption of alcohols and polar compounds. Overall, they found that SLB-IL60 offered an improvement over conventional columns by increasing the number of peaks separated by nearly 50%.⁸

The chemical name of SLB-IL60 is 1,12-di(triethylphosphonium)dodecane bis(trifluoromethylsulfonyl)imide¹ and its chemical structure is shown in Figure 4. The structure makes it very apparent that ionic liquid molecules possess very different chemical and physical properties compared to its polysiloxane and PEG counterparts.

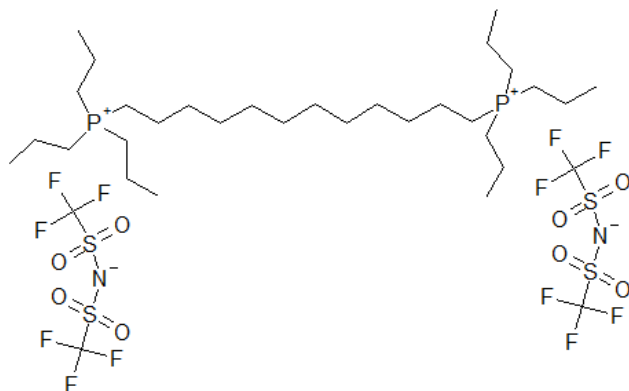


Figure 4: The phase structure of SLB-IL60, 1,12-di(triethylphosphonium)dodecane bis(trifluoromethylsulfonyl)imide .

1.4 Stationary Phase Retention Mechanisms

1.4.1 Traditional Column Phases

The interaction of a solute with the column stationary phase directly correlates with the time it takes for the solute to elute – this is its retention time. The goal with any GC analysis is to effectively and efficiently separate all components in a sample. Separations occur due to different volatilities and/or the interactions of the solutes with the stationary liquid phase.¹⁰

More specifically, separation is typically influenced by three factors – boiling point, molecular weight, and chemical structure. Under standard gas chromatography conditions the mobile phase does not participate in retention mechanisms, and is solely responsible for transporting solutes through the column.¹¹ The retention mechanisms for liquid stationary phases are generally well understood. When a chromatographer refers to the retention mechanism of a stationary phase, s/he is really alluding to the selectivity of the stationary phase, which can be defined as its capacity to enter into intermolecular interactions.¹¹ In essence, this is a measure of a solute's solubility in the stationary phase.¹⁰ Selectivity (α) is a comparison of two analytes in regards to each other, and is mathematically defined by equation 1 as

$$\alpha = \frac{t_{R2} - t_0}{t_{R1} - t_0} \quad (1)$$

where t_{R2} is the retention time of the second eluting compound, t_{R1} is the retention time of the first eluting compound, and t_0 is the retention time of an unretained peak. The interactions of the solute and the stationary phase influence the separation factor α via van der Waals cohesive forces. Dispersion forces, inductive forces, orientation force and hydrogen bonding account for these cohesive forces. All of these are a measure of forces between dipoles, whether they are induced or permanent.¹² Non-polar analytes generally exhibit dispersion forces, which are the

weakest intermolecular force and are universal and independent of temperature.¹⁰ However, even n-alkanes in polar liquids will experience induction and dispersion interactions showing that no solute interacts by a single interaction mechanism.¹⁰ Induction and orientation forces decrease with increasing temperature and at high temperatures disappear entirely as all orientations of the dipoles become equally probable.¹⁰ Polar solutes generally experience the strongest interactions through orientation forces and hydrogen-bonding.

Clearly the capacity for a solute to undergo numerous interactions with a stationary phase makes it difficult to define selectivity in regards to only one variable. Chromatographers have been trying to address this, essentially for as long as gas chromatography has been around, which will be discussed in subsequent sections. Poly(siloxane) and poly(ethylene glycol) stationary phases occupy only a small fraction of the selectivity space,¹¹ meaning there is room to expand and develop stationary phases with unique selectivities.

1.4.2 Ionic Liquid Stationary Phases

The retention mechanisms for ionic liquids are more complex, due mainly to the fact that they are capable of undergoing a number of different intermolecular interactions.¹³ While these salts are liquid at room temperature, it must be kept in mind that they are exactly that – *salts*. Their traditional (liquid) counterparts are polymers and so it becomes very apparent that the surface chemistry of these stationary phases will be quite different and must be considered extensively. Poole⁶ reported that ionic liquids are the most hydrogen-bond basic of stationary phases and the only significant hydrogen-bond acidic stationary phases currently available for gas chromatography. Examining the structure for SLB-IL60 (Figure 4), one can see that the anion is highly hydrogen basic.

It is well known and accepted that ionic liquid columns undergo multiple solvation mechanisms.^{2,8,13,14,15} Anderson's work¹⁴ on imidazolium-based ILs showed that the anion contributes the most to the unique selectivity of IL stationary phases, and also plays a critical role in regards to separation efficiency. The discussion around IL retention mechanisms frequently refers to the hydrogen bonding capacity of the stationary phase and the solute. The anion appears to have a direct impact on the hydrogen-bond basicity and dipolarity of the ionic liquid.¹⁵ The cation influences the ability of the IL to interact via non-bonding and pi-electrons.¹⁵ Hydrogen basic anions were found to produce asymmetrical peaks when analyzing analytes such as alcohols or carboxylic acids.¹⁴ In addition to that, hydrogen-bonding solutes such as alcohols are retained largely by interfacial adsorption, more so than any other polar compounds.⁸ Cation and anion pairs are numerous, making it difficult to pinpoint specific retention mechanisms since they directly influence the dispersion forces and hydrogen-bond acidity interactions.¹⁵ However, a number of general conclusions have been made in regards to ionic liquid stationary phases thus far: Moderately polar and polar compounds are mainly retained by gas-liquid partitioning,⁵ while low polarity to non-polar compounds are generally retained by interfacial adsorption.^{5,8}

1.4.3 Polarity and Selectivity

There is an apparent dichotomy in gas chromatography between polarity and selectivity. These terms are continually referred to in the literature to describe stationary phases and at times are used interchangeably, though this is improper use of the terms. Poole^{6,8} defined polarity as the capacity of a solvent for all possible intermolecular interactions, or more commonly as the solvent strength of the stationary phase. Selectivity is defined⁶ as the relative capacity of compared solvents for a particular intermolecular interaction. It is primarily determined by

differences in analyte vapor pressure and the strength of solute-solvent interactions.¹⁶ Polarity can also be defined thermodynamically as the capacity of a solvent for various intermolecular interactions corresponding to the partial molar Gibbs free energy of solution.⁸

The difference between these two terms becomes clearer when studying ionic liquids. Two stationary phases can have essentially the same polarity and yet produce very different separations. A comparison¹⁴ of two ILs to two common commercial GC stationary phases showed that the polarities of the ILs were very similar to each other and to the OV-22 stationary phase, yet had very different separations. Armstrong and coworkers^{3,7} alluded to this when stating that IL stationary phases seemed to separate non-polar analytes like a non-polar stationary phase and polar analytes like a polar stationary phase. They referred to this as *dual-nature selectivity*, unique to ionic liquid stationary phases.

The general consensus in the literature is that polarity does not accurately measure the properties of a stationary phase.^{8,11,13} Polarity scales are generally an average or a summation of all possible solute-solvent interactions. Therefore, it is expected that stationary phases with similar chemistries would have similar polarities, but based on experimental observations do not adequately capture the unique selectivities. These scales are even more so problematic as there is no single probe solute molecule that can capture one particular intermolecular interaction, but rather each captures several possible interactions. This makes it particularly difficult to attribute specific solvent-solute interactions to any one type of molecule. In fact, there is no molecule that is uniquely polar that can be used to probe polarity.

There are numerous solvent selectivity scales for stationary phase classifications, but the Rohrschneider-McReynolds system and Abraham solvation parameter model are the only two that have been applied to ionic liquids thus far⁶ and will be discussed in subsequent sections.

1.4.4 Grob Test

Capillary column performance can be evaluated using the Grob mixture. The probes selected were chosen to measure column activity, specifically by monitoring peak shapes for indications of adverse adsorptive effects and the acid-base character of a column.¹² Table 1 outlines the role each probe plays in the Grob mixture. As column stationary phases advanced, the test mixture was updated by Luong, and is considered a more demanding test of column inertness.⁶

1.4.5 Kovats Retention Indices

Absolute retention times are essentially irrelevant in comparative GC analyses, specifically because experimental errors, fluctuations in the chromatography, and changes in the chromatographic parameters all directly affect retention times. In order to address the need for comparative gas chromatographic retention data, the Kovats approach assigns a retention index value, I , to each analyte. The Kovats approach employs the use of a homologous series of n-alkanes, and each n-alkane is assigned a value of 100 times its carbon number. For example, hexane, octane, and decane have I values of 600, 800, and 1000, respectively. The choice of n-alkanes was not only based on their relative availability but also on their very low polarity and their freedom from hydrogen bonding.¹⁷ The retention index of an analyte at an isothermal column temperature can be calculated using the following equation:

$$I = \frac{100n + 100[\log t'_{r(\text{unknown})} - \log t'_{r(n)}]}{\log t'_{r(N)} - \log t'_{r(n)}} \quad (2)$$

where I is the Kovats retention index, t'_r is the adjusted retention time of the unknown, $t'_{r(n)}$ is the adjusted retention time of the closest n -alkane eluting before the unknown, and $t'_{r(N)}$ is the adjusted retention time of the closest n -alkane eluting after the unknown. In this regard, retention indices normalized instrumental variability in gas chromatographs, allowing retention data generated on different systems to be compared.¹² The use of retention indices obtained for an analyte on two orthogonal GC stationary phases is an inexpensive alternative to Mass Spectrometry for the positive identification of an unknown.

It is worth mentioning that Kovats retention indices were initially developed for isothermal gas chromatography. However, the equation was later expanded to also be employed in temperature programmed gas chromatography (TPGC), which is discussed elsewhere.¹⁸ For TPGC, it was suggested that a secondary reference set is sometimes beneficial in obtaining retention indices. Here van den Dool and Kratz suggested the use of ethyl esters as a secondary reference set.¹⁸

<u>Probe</u>	<u>Function</u>
n-alkanes	column efficiency
fatty acid methyl esters	separation number; column efficiency
1-octanol	detection of hydrogen-bonding sites, silanol groups
2,3-butanediol	silanol group detection
2-octanone	detection of activity associated with Lewis acids
nonanal	aldehyde adsorption other than via hydrogen bonding
2,6-dimethylphenol	acid-base character
2,6-dimethylaniline	acid-base character
4-chlorophenol	acid-base character
n-decylamine	acid-base character
2-ethylhexanoic acid	irreversible adsorption
dicyclohexylamine	irreversible adsorption

Table 1: Grob test mixture probes and their functions, adapted from Grob and Barry.¹²

1.4.6 Rohrschneider-McReynolds Classification of Stationary Phases

McReynolds system is the most widely used system to classify stationary phases. This system employs the use of 10 probe molecules, each having different functionality, and thus different implications for column phase interactions. A similar approach was previously implemented by Rohrschneider with five probes, McReynolds took it one step further adding five additional probes.¹⁹ A detailed explanation of the probes and their measured interactions is available in Table 2. Squalane was chosen as the reference (non-polar) stationary phase against which all other measurements would be (and still are) compared. The chemical structure for squalane can be found in Figure 5. Each probe's I value is measured on the stationary phase in question, and a ΔI value for the probe is obtained according to equation 3.

$$\Delta I = I_{stationary\ phase} - I_{squalane} \quad (3)$$

This indicates the degree of a specific probe interaction changing in regards to that column phase. A sum of these values suggests the overall polarity of the stationary phase. This is the founding principle of the Rohrschneider-McReynolds method – intermolecular interactions are assumed to be additive.¹¹

When applied to IL stationary phases, a few issues with this approach surfaced. The first is that the method utilizes probe molecules that are highly volatile^{6,14,16} and therefore often elute with the dead volume of the column. In 2009, Anderson¹⁴ pointed out that this model is dependent on single solvation interactions of the probe molecules with the column phase, but the retention is rather due to several simultaneous interactions making it difficult to fully characterize individual solvation interactions. In this regard, the Rohrschneider-McReynolds approach is only useful to the extent that it elucidates some of the different interactions ILs have with the probe molecules.

This method also fails to address the contribution of interfacial adsorption,¹⁶ which was extensively studied and the magnitude of errors were reported by Poole and coworkers.^{8,20} This is an issue because the reference n-alkane index markers are generally retained on polar stationary phases by interfacial adsorption. Meanwhile, the probes are generally retained by partitioning.^{6,8,11,20,21} It is also important to remember that probe molecules that represent a single intermolecular interaction do not exist, and each solute is retained by several simultaneous intermolecular interactions, therefore making it difficult to draw conclusions about individual solvation processes. Because of these reasons, researchers have been discontented with this proposed method for determining column polarity, despite its widespread use. In 1999, Abraham¹¹ stated that the Rohrschneider approach is unsound for stationary phase characterization, drawing attention to the fact that it may be a “useful model for retention that is simultaneously a poor model for characterizing phase selectivity.” Previous work has been done that also recognized the inconsistencies with n-alkanes in the determination of index values, and 2-alkanones were suggested as an alternative due to the fact that they partition with all phases and provide a more reasonable estimate of polarity for phases that do not show significant partitioning of the n-alkanes²². In 2014, Poole⁶ went as far as to discourage the use of the Rohrschneider-McReynolds system, particularly in regards to classifying ionic liquid stationary phases.

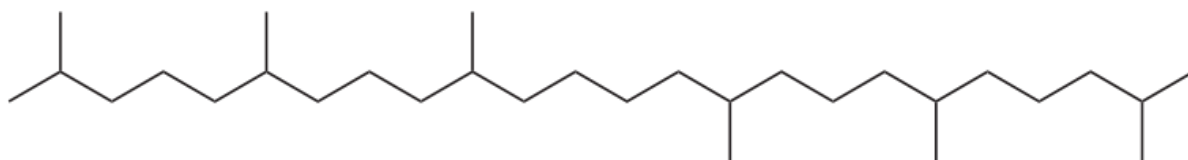


Figure 5: The chemical structure of squalane.

<u>McReynolds</u> <u>Probe</u>	<u>Rohrschneider</u> <u>Probe</u>	<u>Function</u>
benzene	benzene	electron density for aromatic and olefinic hydrocarbons
n-butanol	ethanol	proton donor and proton acceptor capabilities
2-pentanone	2-butanone	proton acceptor interactions
nitropropabe	nitromethane	dipole interactions
pyridine	pyridine	strong proton acceptor interactions
2-methyl-2-pentanol	-	substituted alcohol interactions
iodobutane	-	polar alkane interactions
2-octyne	-	unsaturated hydrocarbons
1,4-dioxane	-	proton acceptor interactions
cis-hydrindane	-	dispersion interactions

Table 2: The McReynolds test probes and their measured interactions. Adapted from Grob and Barry.¹²

1.4.7 Inverse Gas Chromatography

Traditionally gas chromatography is used to classify volatile compounds. When the analyte of interest is a large non-volatile molecule, traditional GC will not suffice. In inverse gas chromatography (IGC), the stationary phase becomes the sample and known volatile probes are used to investigate the material's properties.¹⁷ It is particularly useful when studying surface interactions, phase transitions, and physical properties of analytes.²³ IGC is often used in the development of ionic liquid stationary phases, as their interactions with a multitude of compounds are measured to better classify the column phase. In essence, this is being done with the McReynolds probes, but little method development has been done elsewhere to address the applicability of IGC to polarity determinations.

1.4.8 Abraham Solvation Parameter

The Abraham solvation parameter model is a theory that is based on a cavity model of solvation and assumes that retention occurs only by gas-liquid partitioning.^{6,11,24} The model is a linear free energy relationship that has a three step process for the solvation of a solute, which includes first a cavity being created in the solvent (the ionic liquid), reorientation of the solvent molecules around the cavity, and then introduction of the solute into the cavity.^{11,13} This is where the various solute-solvent interactions occur, and they will be different for each solute molecule based on the chemical functionality of the molecules (acidic, basic, electron donating/withdrawing, aromatic functional groups).

The Abraham solvation parameter method is supposed to succeed where the McReynolds classification system seems to fail, as previously discussed. In order to account for multiple possible intermolecular interactions as well as interfacial adsorption of the n-alkanes,¹⁶ the

Abraham solvation parameter method was developed and is currently the principle method used for column characterization.⁵ The theory adheres to equation 4:

$$\log k = c + eE + sS + aA + bB + \ell L \quad (4)$$

where k is the retention factor (determined chromatographically), E, S, A, B, L are descriptors that characterize solute properties, and e, s, a, b, ℓ are constants that describe the stationary phase properties. The literature contains solute descriptors for a number of probe molecules over a range of functional groups.²⁵ Once the retention factors and solute descriptors are defined, multiple linear regression analysis is used to obtain the stationary phase constants.²⁵ All of the solvation parameter model terms are explained in more detail in Table 3.

So long as Abraham solvation descriptors are known for a particular solute and stationary phase, predictions can be made¹¹ and retention data can be analyzed appropriately. As of 2002, approximately 3500 compounds had solute descriptor data available.²⁴ In general, this method has mainly been applied to stationary phase classification.^{11,24,26,27}

Symbol	Description	Measurement
c	Retention Factor	Experimentally, from chromatographic data
E	Excess molar fraction	<i>For liquids:</i> calculated from the refractive index and characteristic volume. <i>For solids:</i> experimental or calculated from an estimated refractive index
S	Dipolarity/polarizability	Experimental, from chromatographic or liquid-liquid partition data
A	Hydrogen-bond acidity	Experimental, from chromatographic or liquid-liquid partition data
B	Hydrogen-bond basicity	Experimental, from chromatographic or liquid-liquid partition data
L	Gas-liquid partition coefficient on hexadecane at 25 °C	Back-calculated from gas chromatographic data acquired at temperatures > 25°C
e	Interaction with π and n electrons of the solute	Multiple linear regression analysis
s	Dipolarity/polarizability	Multiple linear regression analysis
a	Hydrogen-bond acidity	Multiple linear regression analysis
b	Hydrogen-bond basicity	Multiple linear regression analysis
ℓ	Ability to separate adjacent members of a homologous series	Multiple linear regression analysis

Table 3: Descriptors and their properties used in the solvation parameter. Adapted from CF Poole,⁶ JL Anderson,¹⁵ and LM Sprunger.²⁷

1.5 Polarity Scale for Ionic Liquid Columns

Ragonese and coworkers⁹ proposed a method for calculating the polarity of IL stationary phases that is actively applied by Sigma-Aldrich (Supelco) for characterizing their commercially available IL column phases. It is based on McReynolds method and employs the use of the first five test probes, namely benzene, *n*-butanol, 2-pentanone, nitropropane, and pyridine. The first step is to calculate the *I* value for each probe on the IL stationary phase. Next, McReynolds constants (ΔI) are determined from the *I* values of the probes on the IL stationary phase and on squalane. A sum of the McReynolds constants leads to a polarity value, *P*. From here the polarity values are normalized to SLB-IL100 (*P*=4437) to obtain a Polarity Number, *PN*, as shown in equations 5 and 6.

$$P_x = \sum \Delta I \quad (5)$$

$$PN_x = 100 \times \frac{P_x}{P_{SLB-IL100}} \quad (6)$$

The experimental values obtained for a number of stationary phases (from non-polar to extremely polar) are shown in Table 4. At the time of developing this polarity scale, SLB-IL100 was the most polar column phase known. Since then, several additional phases have been introduced to the market place with higher polarity than SLB-IL100. A visual representation of the polarity scale for commercially available IL column phases in comparison to traditional column phases is shown in Figure 6.

Column Phase	McReynolds Constants					P	PN
	Benzene	n-Butanol	2-Pentanone	Nitropropane	Pyridine		
SPB-Octyl	17	-20	6	19	6	28	1
SPB-35	175	113	151	225	175	839	19
Supelco Wax	334	509	375	601	505	2324	52
SLB-IL59	338	505	549	649	583	2624	59
SLB-IL60	362	492	525	679	564	2622	59
SP-2560	510	724	652	913	773	3572	81
SLB-IL82	532	676	701	921	808	3638	82
TCEP	622	871	772	1072	957	4294	97
SLB-IL100	602	853	884	1017	1081	4437	100
SLB-IL111	766	930	957	1192	1093	4938	111

Table 4: Experimental P (polarity) and PN (polarity number) for various stationary phases. Adapted from Sigma-Aldrich.¹

POLARITY SCALE

<i>Traditional Phase</i>		<i>PN</i>	<i>Ionic Liquid Phase</i>
	Extremely Polar	120	
		110	SLB-IL111
TCEP	Highly Polar	100	SLB-IL100
		90	
SP-2560		80	SLB-IL82
		70	
SupelcoWax	Polar	60	SLB-IL61
		50	SLB-IL60 SLB-IL59
		40	
SPB-35	Intermediate Polar	30	
		20	
	Non-Polar	10	
SPB-Octyl		0	

Figure 6: Polarity Scale for IL stationary phases. Adapted from Sigma-Aldrich.¹

1.6 Thermodynamics and van't Hoff

A fundamental parameter of any chromatographic separation is the retention factor. This variable is dimensionless, independent of column flow, and independent of column dimensions.²⁸ Therefore, it is useful to calculate retention factors when comparing analytes on columns with different stationary phases and different dimensions. Retention factors are determined by the following equation:

$$k = \frac{t_r - t_0}{t_0} = \frac{t'_r}{t_0} \quad (7)$$

where t_r is the retention time of the analyte, t_0 is the retention time of an unretained peak and t'_r is the adjusted retention time. In a chromatographic process, retention is a measure of the equilibrium of an analyte between the mobile and stationary phases. In this regards, the equilibrium constant, K is proportional to k . There is also a direct correlation between retention factor and temperature, which becomes evident through an analysis of Gibbs free energy, where the Gibbs free energy change refers to the solvation thermodynamics of a solute between the mobile phase and stationary phase.²⁵ Gibbs free energy is defined in equations 8 and 9.

$$\Delta G^\circ = -RT \ln K \quad (8)$$

$$\Delta G^\circ = \Delta H^\circ - T\Delta S^\circ \quad (9)$$

Substituting equation 8 into 9 and rearranging produces equations 10 and 11.

$$-RT \ln K = \Delta H^\circ - T\Delta S^\circ \quad (10)$$

$$\ln k = \frac{\Delta S^\circ}{R} - \frac{\Delta H^\circ}{RT} \quad (11)$$

In equation 10 it becomes evident that $\ln k \propto \frac{1}{T}$. Calculating $\ln k$ for each analyte at different temperatures and plotting $\ln k$ vs $\frac{1}{T}$ will produce a van't Hoff plot. This is useful for comparing individual column performance.

Gibbs free energy, ΔG , can also be calculated for each analyte at a specific temperature using equation 3. One can calculate the equilibrium constant from the retention factor and the column phase volume ratio, β , as defined in equations 12 and 13,

$$\beta = \frac{(r_c - d_f)^2}{2r_c d_f} = \frac{r_c}{2d_f} \quad (12)$$

$$K = k\beta \quad (13)$$

where r_c is the column radius, and d_f is the film thickness. For the columns used in this research, the following values were calculated for β : Agilent HP-20M, $\beta = 266.7$; Sigma-Aldrich SLB-IL60, $\beta = 312.5$. Based on equation 9, a plot of ΔG° vs T will give a straight line with the equation $y = mx + b$. This can be used to determine the enthalpy, ΔH° , and entropy, ΔS° , values for a particular analyte on each column from the y-intercept and slope, respectively. Dose²⁹ showed that the enthalpy and entropy of the phase transition from mobile phase to stationary phase can be assumed to be independent of temperature.

ΔG° for a series of homologs allows one to derive a linear free-energy relationship between the free-energy and the number of carbon atoms in the straight alkyl chain.³⁰ Graphic representation of the thermodynamic properties for homologous series allows for a visual analysis and comparison of two different stationary phases.

Previously, the solvation thermodynamics of seven probe molecules were calculated by measuring the retention factors at six different temperatures to compare various ionic liquid

stationary phases,²⁵ but to the best of the author's knowledge, were not compared to PEG stationary phases.

1.7 Polyol-Induced Extraction

Recently, a patent³¹ was filed by colleagues at Seton Hall University claiming the use of polyols for the extraction of water from (miscible) organic liquids. This method was developed in the response to the 2008 shortage of acetonitrile (ACN), and the increasing need for green chemistry in the laboratory. Polyols are non-toxic (with the exception of ethylene glycol), inexpensive, biodegradable, and recyclable making them ideal candidates for green chemistry applications. Traditionally, purification is achieved using distillation, dehydrating agents, and recrystallization, processes which usually involve numerous steps and can create hazardous waste. The inventors showed that the method successfully extracts water from organic liquids with purity levels upwards of 98% or greater and the polyol can be recovered in greater than approximately 95% yield. This applies to a range of organic liquids that are partially to fully miscible with water, with significant emphasis on acetonitrile, due to the aforementioned reason.

While this method's initial intent was to successfully and safely separate organic liquids and water, another colleague at Seton Hall University took the extraction method one step further and applied the technique to the extraction of essential oils from natural products.³² Here, the miscibility of acetonitrile and water was exploited to effectively extract the compounds of interest, and the polyol was used to successfully induced separation of the organic and aqueous phases to obtain an acetonitrile extract suitable for GC/MS analysis. Work was done to determine the optimal temperature for increased phase separation, with an extensive look at the thermodynamic parameters of the acetonitrile/water/polyol system.

With the foundation laid for application of this extraction technique to flavor and fragrance materials, it was decided to compare PIE to a traditional liquid/liquid extraction technique. The two extracts were then compared using both the SLB-IL60 and HP-20M column phases to discern any uniqueness in 1) the extraction techniques and 2) the column selectivities.

2 Experimental Procedure

2.1 Materials

A majority of the flavor/fragrance ingredients were provided from an in-house stock supply at International Flavors & Fragrances. Ingredients that could not be obtained in-house were obtained from Sigma-Aldrich (Saint Louis, MO). In addition, pentane, sorbitol, acetonitrile, and dichloromethane were also obtained from Sigma-Aldrich. Methane gas was from Matheson Gas Products, Inc (Basking Ridge, NJ). The SLB-IL60 ionic liquid column was graciously provided by Sigma-Aldrich. A 500 mL bottle of Swinger (13% ABV), a traditional mead with wildflower honey, was purchased locally at Melovino Craft Meadery (Vauxhall, NJ).

2.2 Instrumentation for pure chemical characterization

Two Agilent 6850 Gas Chromatographs (GC) equipped with Flame Ionization Detectors (FID) were used to obtain chromatographic data on two columns. The first GC was set up with a traditional polyethylene glycol (PEG) wax phase from Agilent Technologies (Santa Clara, CA), HP-20M with the following dimensions, 50 m x 0.32 mm x 0.30 μ m. The second GC had a Sigma-Aldrich (Saint Louis, MO) SLB-IL60 30 m x 0.25 mm x 0.20 μ m Ionic Liquid column installed. Both instruments were set up with hydrogen as the carrier gas and run in constant flow mode at 2 mL/min. The inlets contained a split/splitless liner and 0.2 μ L injections, split 100:1 were made for all solutions. The inlet temperature was set to 250 $^{\circ}$ C. All gas chromatographic

runs for pure chemical characterization were done isothermally at varying temperatures including 50 °C, 75°C, 115°C, 150°C, 200°C, and 250 °C. Methane was used to determine the dead volume of both columns at each of the isothermal temperatures. Three injections of methane at each isothermal temperature were performed to calculate the average retention time of the unretained peak. This value was used to obtain the adjusted retention times for all compounds at the varying isothermal temperatures. Retention times for each chemical were collected in triplicate at each temperature on both column phases.

2.3 Liquid/Liquid Extraction of Mead

The mead was extracted at a 1:1 ratio using dichloromethane. 80 mL of DCM were added to 80 mL of mead in a separatory funnel. The vessel was capped and shaken vigorously for 2 minutes. The mixture formed an emulsion, which was left to settle for 5 minutes. The emulsion was then transferred to four glass tubes and centrifuged at 3500 RPMs for 10 minutes. The aqueous layer was decanted off and the organic DCM layer was collected in an 8 oz bottle for storage. The extract was stored in a freezer until ready for analysis. Prior to analysis the extract was concentrated under nitrogen (g) to a final weight of approximately 10 grams.

2.4 Polyol-Induced Extraction of Mead

The mead was extracted at a 1:1 ratio with acetonitrile. 80 mL of acetonitrile were added to 80 mL of mead in a separatory funnel. The vessel was capped and shaken vigorously for 2 minutes. 2 g of sorbitol were then added and shaken again until completely dissolved. The vessel was placed upright in a freezer at -20 °C for 20 minutes. The aqueous (bottom) layer was discarded and the organic, acetonitrile layer was collected in an 8 oz jar for storage. The extract was stored in a freezer until ready for analysis. Prior to analysis the extract was concentrated under a stream of nitrogen (g) to a final weight of approximately 25 grams.

2.5 Instrumentation for Analysis of Extracts

The same two gas chromatographs described in section 2.2 were used for GC-FID analysis of the extracts. The extracts were injected at 1 μ L with a 5:1 split ratio. The oven temperature ramp program started at 40 °C and increased at 2 °C/min up to 225 °C (HP-20M), 275 °C (SLB-IL60) with a 10 minute hold time.

3 Results and Discussion

3.1 Polarity Study of Molecules with a Common Hexane Backbone

An initial study was done to evaluate the interactions of molecules with increasing polarity on the SLB-IL60 and HP-20M columns. A series of analytes (15 in total) with a common hexane backbone was selected, starting from hexane to hexanoic acid, and also included a sulfur containing compound, 2-hexylthiophene. A detailed list of these analytes, along with their chemical structures, is provided in Table 5. For the SLB-IL60 column the temperatures studied were 50 °C, 75 °C, 150 °C, 200 °C, and 250 °C. For the HP-20M column, the temperatures studied were 50 °C, 75 °C, 150 °C, and 200 °C. The temperature limit of HP-20M is 250 °C, so to avoid column phase degradation this temperature was avoided during analysis. The SLB-IL60 has a higher temperature limit of 300 °C, thus 250 °C could safely be used for analysis. Stability at higher temperature limits is an obvious benefit of the ionic liquid column phase. van't Hoff plots were created for each class of compounds (aldehydes, ketones, esters, lactones, alcohols, and thiophenes) on both column phases and compared side by side. Figure 7A and 7B show van't Hoff plots with very different slopes and y-intercepts, indicating that the retention thermodynamics of aldehydes are quite different on both column phases. van't Hoff plots of the ketones, Figure 8A and 8B, have slightly different slopes and y-intercepts on the two column phases, which suggests that the retention thermodynamics differ slightly for ketones on SLB-IL60 and HP-20M. Interestingly, differences in slopes and intercepts are almost non-existent for alcohols on the two phases, as seen in Figure 9A and 9B. In fact, even the $\ln k$ values are almost identical at each temperature for all 4 analytes. The $\ln k$ values only differ slightly from one column phase compared to the other.

Analyte	Chemical Structure
hexane	
3-hexanone	
hexanal	
ethyl hexanoate	
hexyl acetate	
hexanol	
ally hexanoate	
cis-4-hexenol	
hexyl butyrate	
hexyl isovalerate	
cis-3-hexenyl isovalerate	
2-hexylthiophene	
hexyl hexanoate	
cis-3-hexenyl cis-3-hexenoate	
hexanoic acid	

Table 5: Analytes chosen for comparison on the SLB-IL60 and HP-20M columns. All molecules have a common hexane backbone and are shown in order of elution from the HP-20M column.

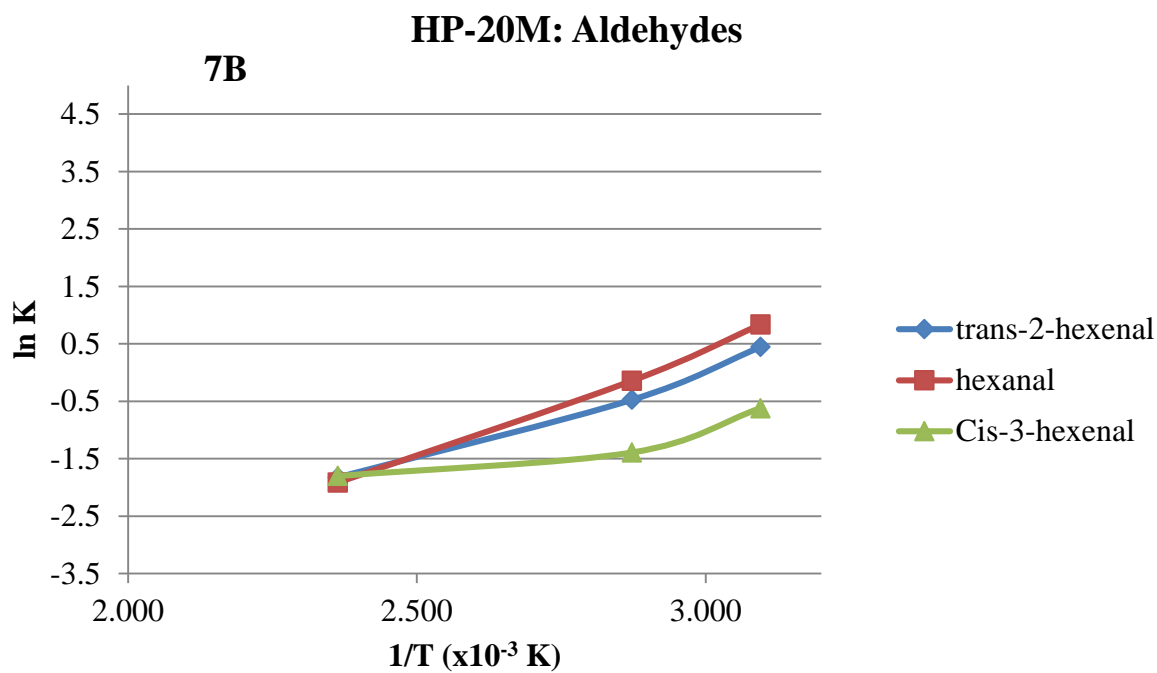
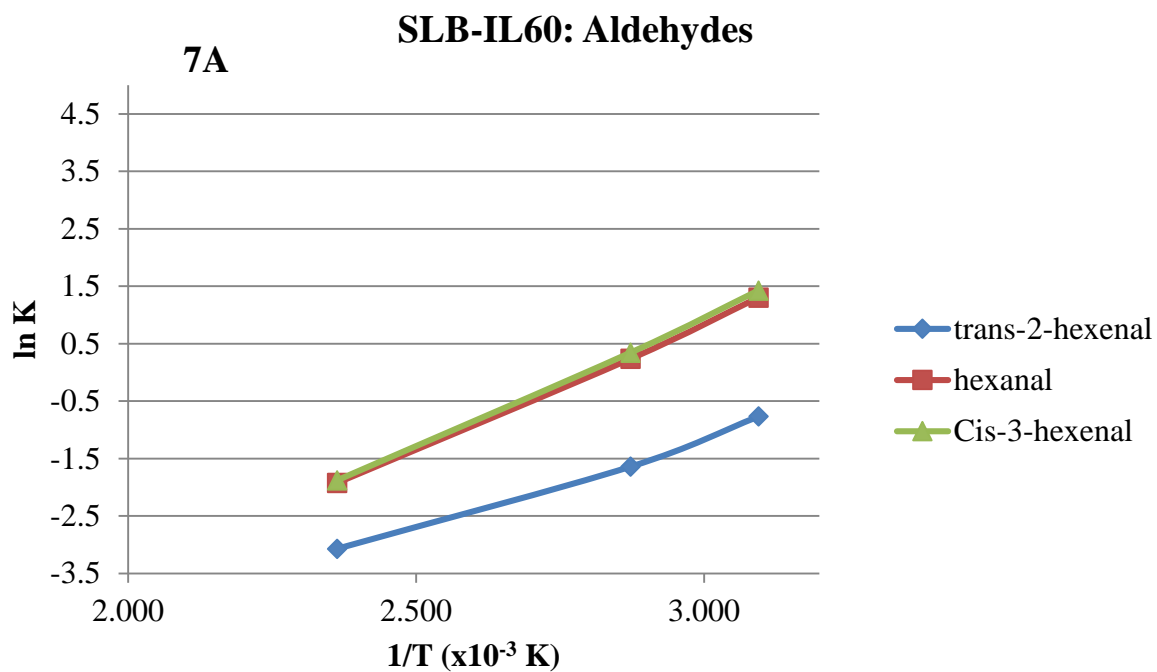


Figure 7: van't Hoff plots of different polarity aldehydes with a common hexane backbone on SLB-IL60 (A) and HP-20M (B) columns.

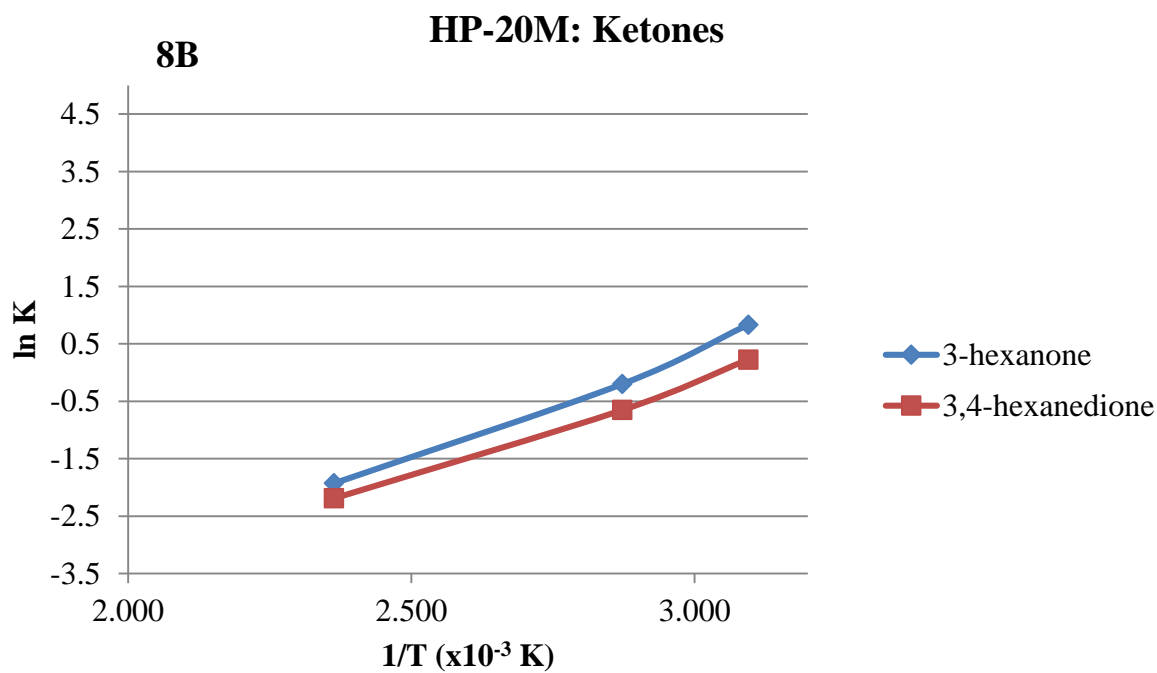
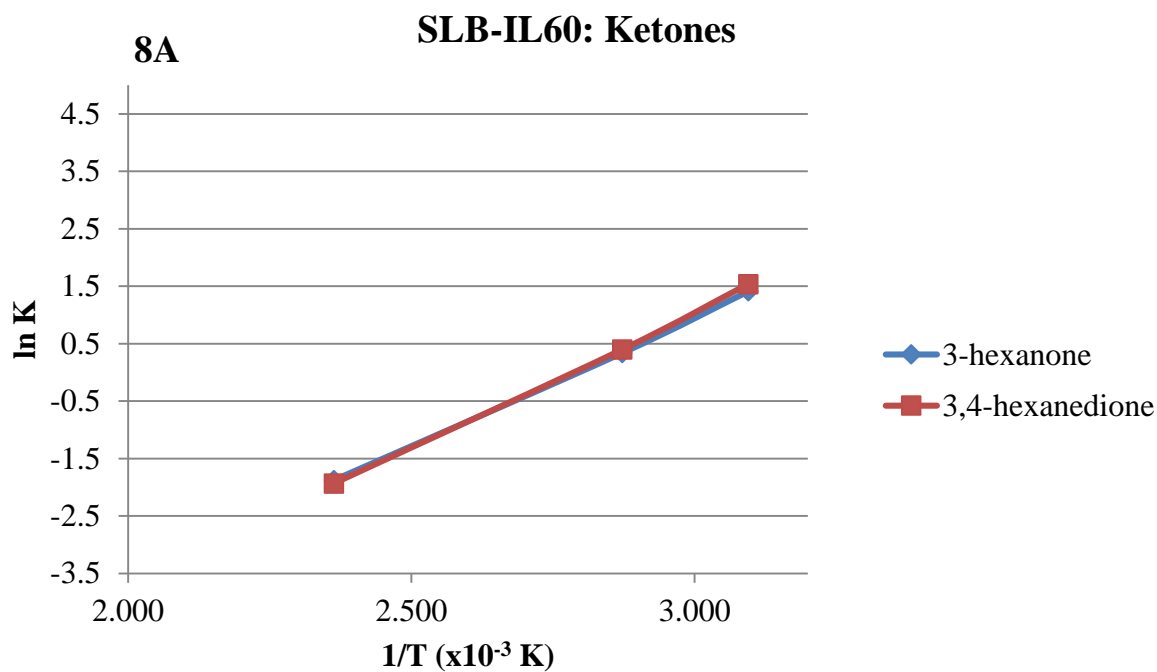


Figure 8: van't Hoff plots of different polarity ketones with a common hexane backbone on SLB-IL60 (A) and HP-20M (B) columns.

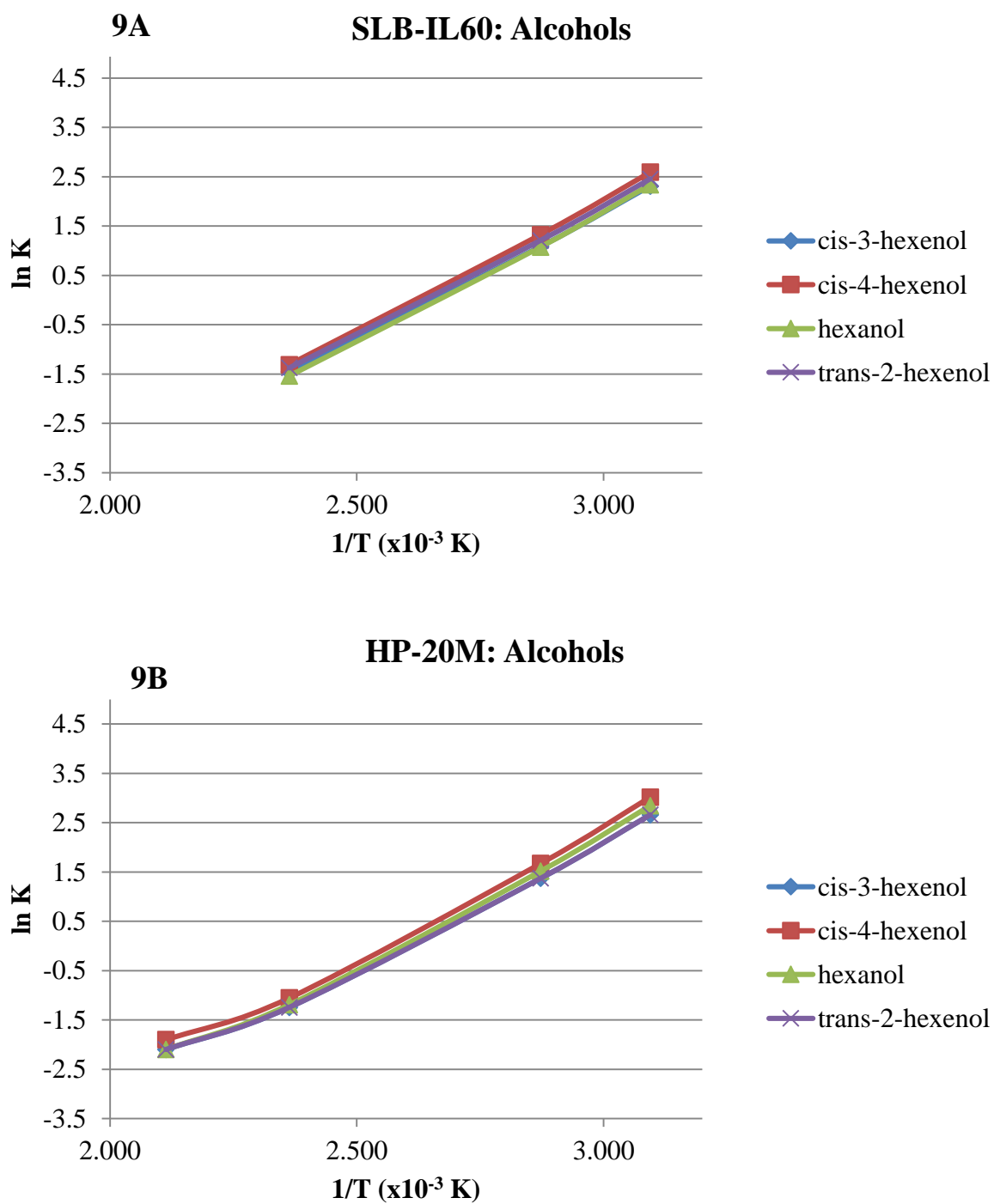


Figure 9: van't Hoff plots of different polarity alcohols with a common hexane backbone on SLB-IL60 (A) and HP-20M (B) columns.

The lactones were difficult to analyze on the SLB-IL60 column, specifically at lower temperatures as they were obstinately retained on the column. This in itself suggests that the retention thermodynamics are quite different for both column phases. This is further demonstrated in the slope and y-intercept differences on the van't Hoff plots in Figure 10A and 10B.

A number of the esters also posed the same challenge with retention on the SLB-IL60 column at lower temperatures. Again, this immediately suggests different retention thermodynamics for both column phases. A quick glance at the van't Hoff plots shown in Figure 11A and 11B visually suggests that the SLB-IL60 and HP-20M column phases are retaining the compounds differently. The slope and y-intercept values for a majority of the compounds are quite different, further confirming this theory.

Lastly 2-hexylthiophene was analyzed on the SLB-IL60 and HP-20M columns to compare non-oxygen containing molecules. A comparison of the slopes and y-intercepts of the van't Hoff plots show in Figure 12A and 12B alludes that the retention thermodynamics do not differ by much. Further investigation of this class of compounds needs to be done to draw any additional conclusions.

Selectivities for peak pairs on each column phase were also calculated according to equation 1. The results are reported in Table 6. A number of the peak pairs had very different α values, and in some cases the elution orders switched for a particular peak pair, such as hexyl acetate and hexanol.

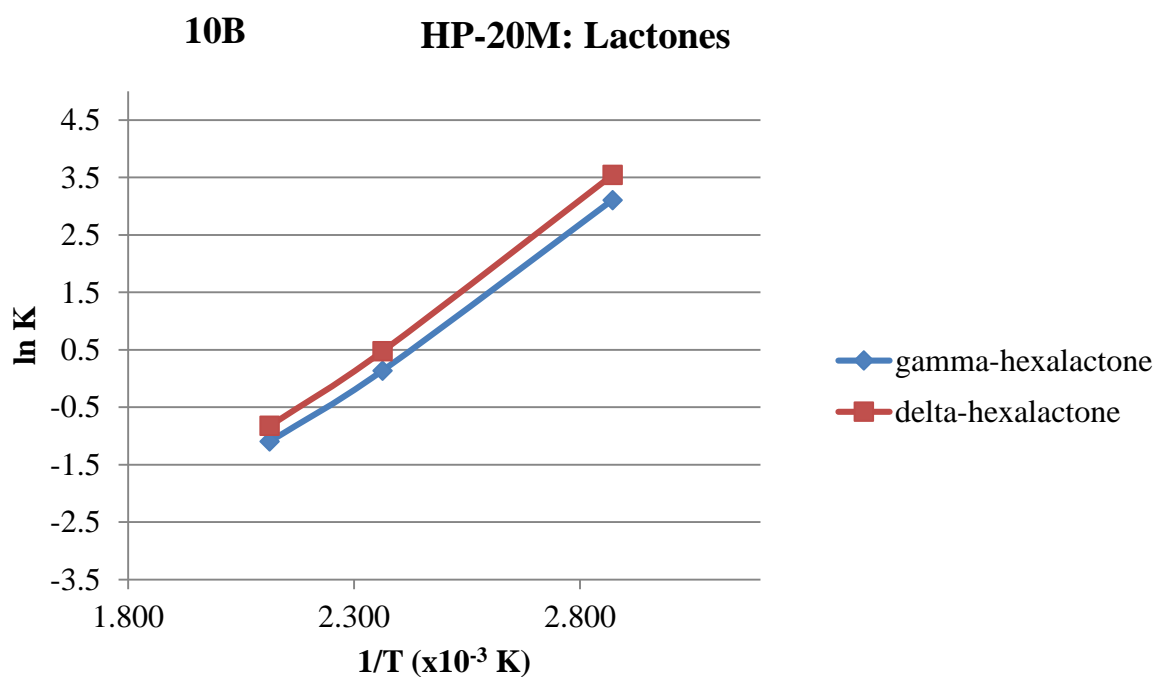
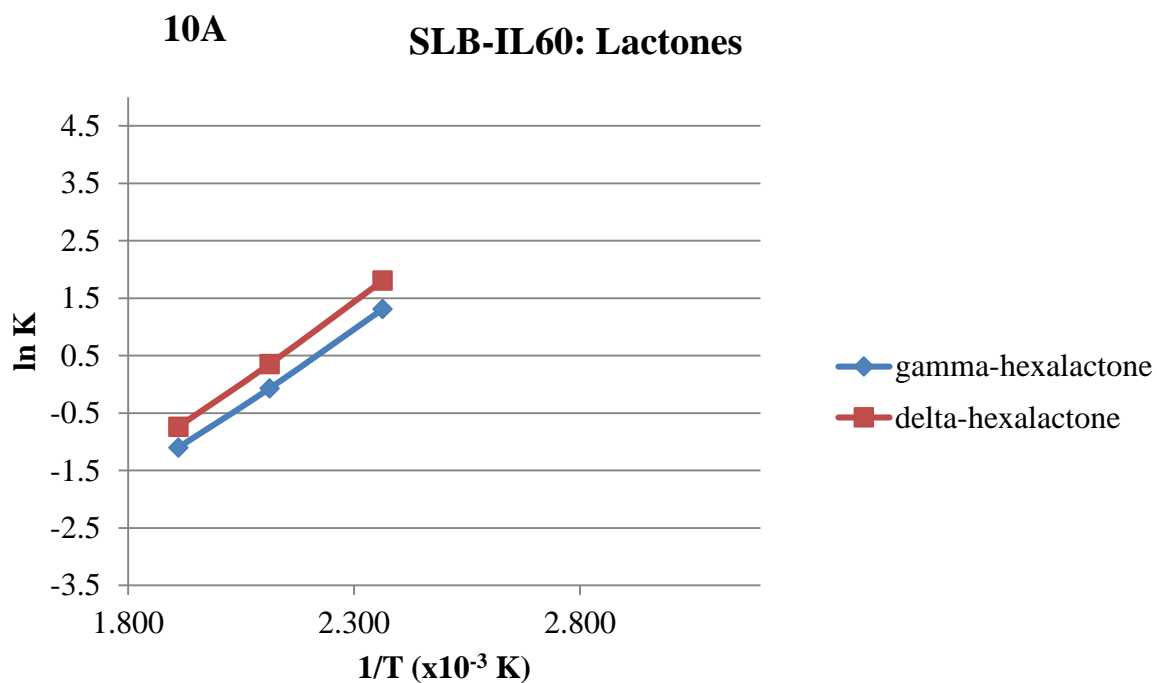


Figure 10: van't Hoff plots of different polarity lactones with a common hexane backbone on SLB-IL60 (A) and HP-20M (B) columns.

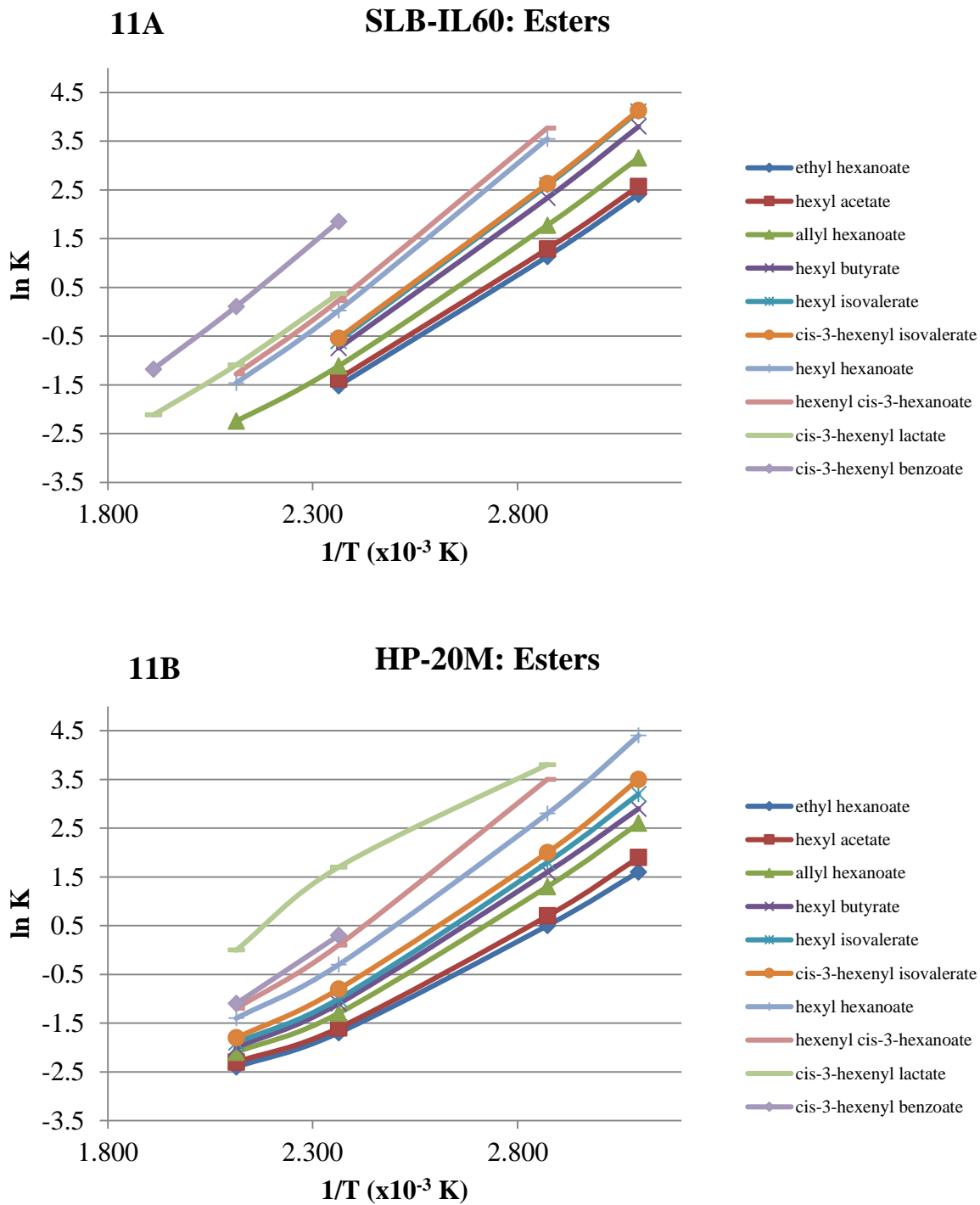
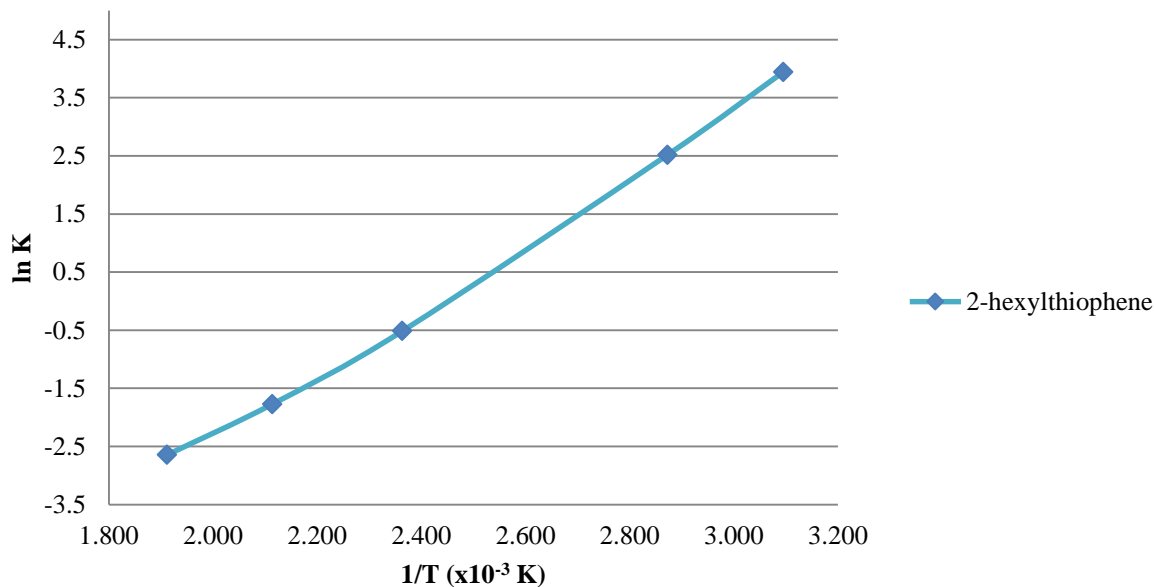


Figure 11: van't Hoff plots of different polarity esters with a common hexane backbone on SLB-IL60 (A) and HP-20M (B) columns.

12A

SLB-IL60: Thiophene



12B

HP20M: Thiophene

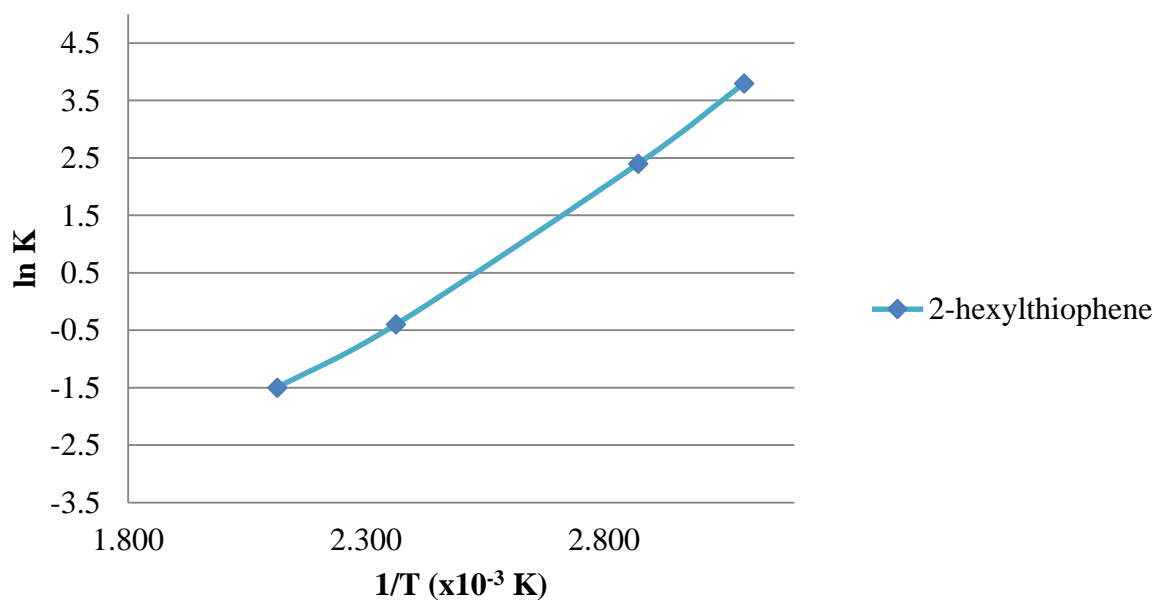


Figure 12: van't Hoff plots for 2-hexylthiophene on SLB-IL60 (A) and HP-20M (B) columns.

Peak Pair	SLB-IL60, α	HP-20M, α
Selectivities at 75 °C		
Cis-3-hexenal/ethyl hexanoate	2.21	1.81
Trans-2-hexenal/3-hexanone	7.26	2.09
3,hexanone/hexanal	1.11*	1.2
3,4-hexanedione/cis-3-hexenal	1.06*	1.06
Cis-3-hexenol/trans-2-hexenol	1.13	1.16
Hexanol/allyl hexanoate	2.01	1.12
Selectivities at 150 °C		
Gamma-hexalactone/ hexenyl cis-3-hexanoate	2.93*	0.98
Delta-hexalactone/cis-3-hexenyl benzoate	1.05	3.36
Hexenyl cis-3-hexanoate/delta-hexalactone	4.81	1.43
Hexyl acetate/hexanol	1.17*	1.66
Allyl hexanoate/cis-3-hexenol	0.71*	1.07
Cis-3-hexenyl isovalerate/2-hexylthiophene (75° C)	1.04	1.45

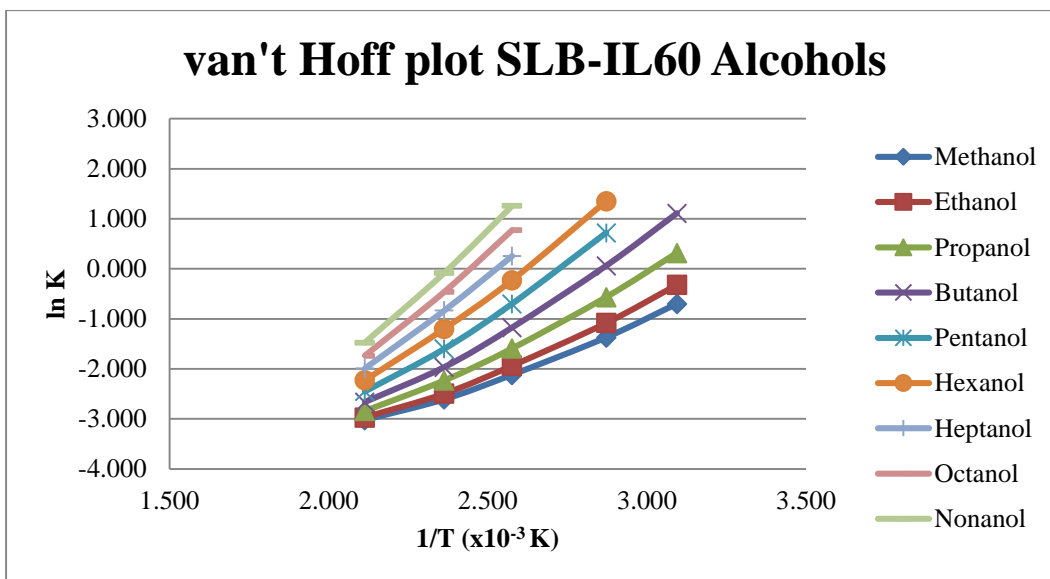
Table 6: Calculated selectivities for peak pairs on the SLB-IL60 and HP-20M column phases. * indicates that the elution order switched for the peak pair.

3.2 Homologous Series Study

Homologous series of primary alcohols, alkyl aldehydes, alkyl carboxylic acids, ethyl esters, and alkanes were analyzed on the SLB-IL60 and HP-20M columns at various temperatures, as described in section 3.1 with the addition of 115 °C. In general, whenever possible at least four temperatures per analyte were used for analysis. For each homologous series, van't Hoff plots ($\ln K$ vs $\frac{1}{T}$) on both column phases were generated. Furthermore, the Gibbs Free Energy change was calculated for each analyte at each temperature such that plots of ΔG° vs T and ΔG° vs the number of carbon atoms could be obtained for each column phase. Based on Equation 8, a linear relationship exists between ΔG° , ΔH° , and ΔS° . In order to generate the most accurate values, the most linear range of the ΔG° vs T must be employed. At higher temperatures, retention mechanisms become less dominant, and mobile phase transport (column flow) becomes the main factor affecting retention. This becomes apparent when looking at the van't Hoff plots, as the data begins to converge towards the same $\ln k$ value at higher temperatures, and in the ΔG° vs T graphs the data begins to plateau at higher elution temperatures. ΔS° and ΔH° values are therefore presented based on the most linear range of the curve, where ΔS° is the calculated slope and ΔH° is the calculated y-intercept. Tables showing ΔG° values for each homologous series have values with bold font – these are the values with the most linear relationship, and R^2 values are provided to show their linearity.

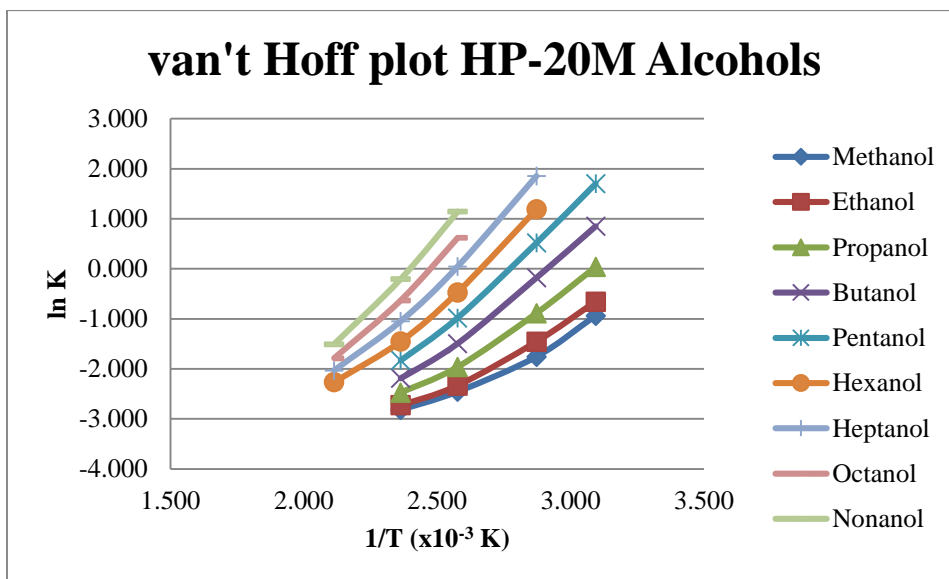
3.3 Alcohols

The van't Hoff plots for the homologous series of primary alcohols (methanol through nonanol) on the SLB-IL60 and HP-20M columns shown in Figures 13 and 14 revealed very similar graphs. Visually, the data is oriented in similar spatial regions on the van't Hoff plots. When looking at the ΔG° vs T plots, there is a slightly larger visual differential between the higher molecular weight alcohols on the HP-20M, shown in Figures 15 and 16. Looking at the values presented, one can see that the ΔG° values for a given analyte at a certain temperature on both column phases are generally within +/- 1.00 kJ/mol. Therefore, one would expect to see similar slopes, which is visually evident from the graphs in Figures 15 and 16, but is also confirmed by the ΔS° values presented in Table 11.



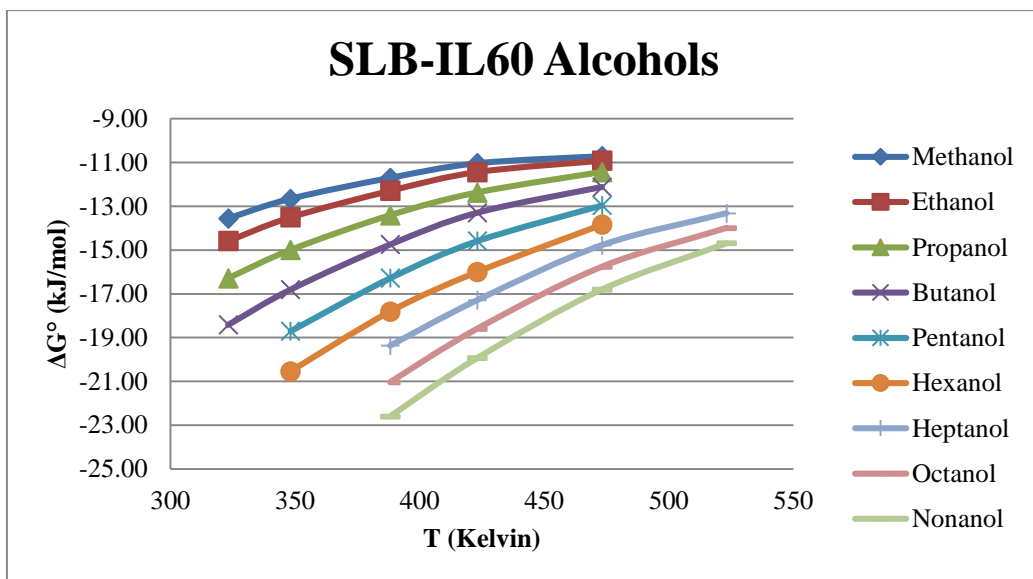
$1/T \text{ (x}10^{-3}\text{)}$	ln K								
	Methanol	Ethanol	Propanol	Butanol	Pentanol	Hexanol	Heptanol	Octanol	Nonanol
3.095	-0.699	-0.318	0.317	1.110					
2.872	-1.372	-1.081	-0.564	0.062	0.719	1.353			
2.576	-2.119	-1.937	-1.590	-1.175	-0.699	-0.226	0.257	0.776	1.260
2.363	-2.610	-2.495	-2.229	-1.966	-1.598	-1.198	-0.831	-0.459	-0.080
2.113	-3.023	-2.971	-2.839	-2.664	-2.450	-2.227	-1.988	-1.737	-1.474

Figure 13: van't Hoff plot of a homologous series of primary alcohols on the SLB-IL60 column. The corresponding table shows the ln k values at various temperatures for a homologous series of primary alcohols on the SLB-IL60 column.



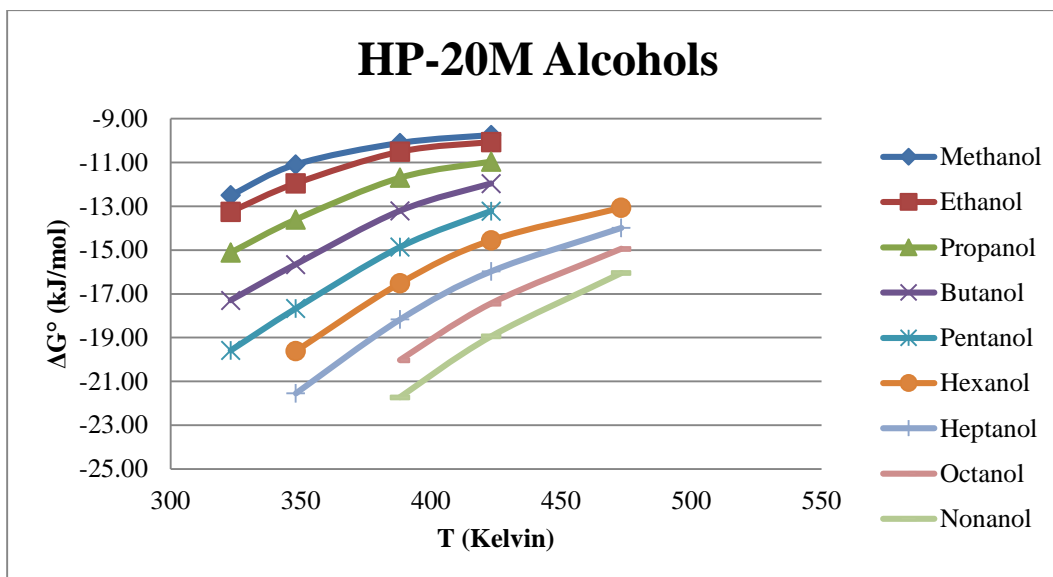
1/T (x10⁻³)	ln K								
	Methanol	Ethanol	Propanol	Butanol	Pentanol	Hexanol	Heptanol	Octanol	Nonanol
3.095	-0.936	-0.655	0.039	0.853	1.703				
2.872	-1.757	-1.456	-0.887	-0.177	0.517	1.189	1.856		
2.576	-2.457	-2.332	-1.964	-1.493	-0.980	-0.470	0.044	0.620	1.146
2.363	-2.818	-2.724	-2.472	-2.186	-1.830	-1.451	-1.046	-0.629	-0.201
2.113						-2.265	-2.030	-1.787	-1.506

Figure 14: van't Hoff plot of a homologous series of primary alcohols on the HP-20M column. The corresponding table shows the ln k values at various temperatures for a homologous series of primary alcohols on the HP-20M column.



		ΔG° (kJ/mol)							
T (Kelvin)	Methanol	Ethanol	Propanol	Butanol	Pentanol	Hexanol	Heptanol	Octanol	Nonanol
323.15	-13.55	-14.58	-16.29	-18.42					
348.15	-12.66	-13.50	-14.99	-16.81	-18.71	-20.54			
388.15	-11.70	-12.29	-13.41	-14.75	-16.28	-17.81	-19.37	-21.04	-22.60
423.15	-11.03	-11.43	-12.37	-13.29	-14.59	-16.00	-17.29	-18.60	-19.93
473.15	-10.71	-10.91	-11.43	-12.12	-12.96	-13.84	-14.78	-15.77	-16.80
523.15							-13.32	-13.99	-14.69
R^2	0.996	0.996	0.993	0.996	0.996	0.994	0.998	0.996	0.997

Figure 15: A plot of ΔG° vs T for a homologous series of primary alcohols on the SLB-IL60 column. The corresponding table shows the ΔG° values at various temperatures for a homologous series of primary alcohols on the SLB-IL60 column.



		ΔG° (kJ/mol)							
	Methanol	Ethanol	Propanol	Butanol	Pentanol	Hexanol	Heptanol	Octanol	Nonanol
T (Kelvin)									
323.15	-12.49	-13.25	-15.11	-17.30	-19.58				
348.15	-11.08	-11.95	-13.60	-15.66	-17.67	-19.61	-21.54		
388.15	-10.10	-10.50	-11.69	-13.21	-14.86	-16.51	-18.17	-20.03	-21.72
423.15	-9.74	-10.07	-10.96	-11.96	-13.21	-14.55	-15.97	-17.44	-18.94
473.15						-13.06	-13.99	-14.94	-16.05
523.15									
R^2	0.946	0.990	0.996	1.000	0.999	0.992	0.993	0.987	0.992

Figure 16: A plot of ΔG° vs T for a homologous series of primary alcohols on the HP-20M column. The corresponding table shows the ΔG° values at various temperatures for a homologous series of primary alcohols on the HP-20M column.

A simple plot of the ΔS° and ΔH° values versus the number of carbon atoms (shown in Figure 17) makes for an excellent visual representation of the thermodynamic trends. Both column phases follow a similar trend for both entropy and enthalpy values, with the SLB-IL60 consistently having less negative values. Methanol through pentanol (C1-C5) have values trending linearly downward, with a consistent difference between the two column values. The trend seems to fail at hexanol through nonanol (C6-C9), suggesting a change in the thermodynamic retention parameters. There was difficulty analyzing these particular analytes at lower column temperatures (50 °C and 75 °C) which could also account for the inconsistency in the trend. While most of the retention factor, k , values were less than 1, the linearity of the data suggests that this is still a decent method to assess the retention thermodynamics. The plots of ΔG° vs number of carbon atoms, shown in Figure 18, also show very similar graphs with consistent linearity between the homologs at various temperatures.

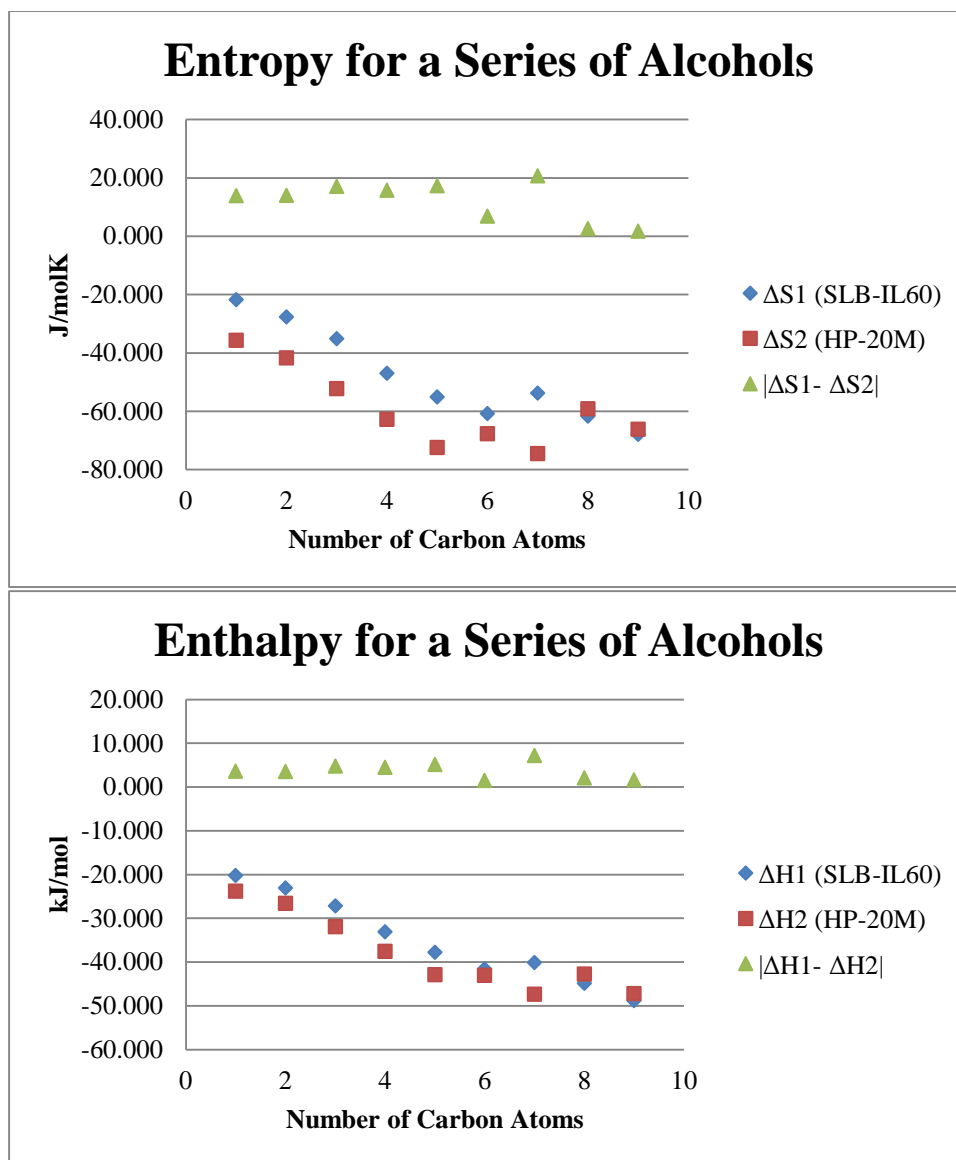


Figure 17: A plot of the ΔS° and ΔH° values and their absolute differential values on the SLB-IL60 and HP-20M columns for a homologous series of primary alcohols.

	Methanol	Ethanol	Propanol	Butanol	Pentanol	Hexanol	Heptanol	Octanol	Nonanol
ΔS°_1 (J/molK)	-21.775	-27.642	-35.142	-46.953	-55.094	-60.814	-53.747	-61.690	-67.883
ΔS°_2 (J/molK)	-35.703	-41.694	-52.213	-62.752	-72.380	-67.746	-74.513	-59.126	-66.173
$ \Delta S^{\circ}_1 - \Delta S^{\circ}_2 $ (J/molK)	13.927	14.052	17.071	15.799	17.285	6.933	20.766	2.564	1.710
ΔH°_1 (kJ/mol)	-20.211	-23.090	-27.171	-33.096	-37.819	-41.620	-40.156	-44.881	-48.842
ΔH°_2 (kJ/mol)	-23.833	-26.626	-31.906	-37.549	-42.932	-43.072	-47.359	-42.785	-47.237
$ \Delta H^{\circ}_1 - \Delta H^{\circ}_2 $ (kJ/mol)	3.622	3.536	4.735	4.454	5.113	1.452	7.202	2.096	1.604

Table 7: ΔH° and ΔS° values for a homologous series of primary alcohols on the SLB-IL60 and HP-20M columns; ΔH°_1 and ΔS°_1 refer to SLB-IL60, ΔH°_2 and ΔS°_2 refer to HP-20M. The absolute differential values between the entropy and enthalpy on both column phases for each analyte were calculated.

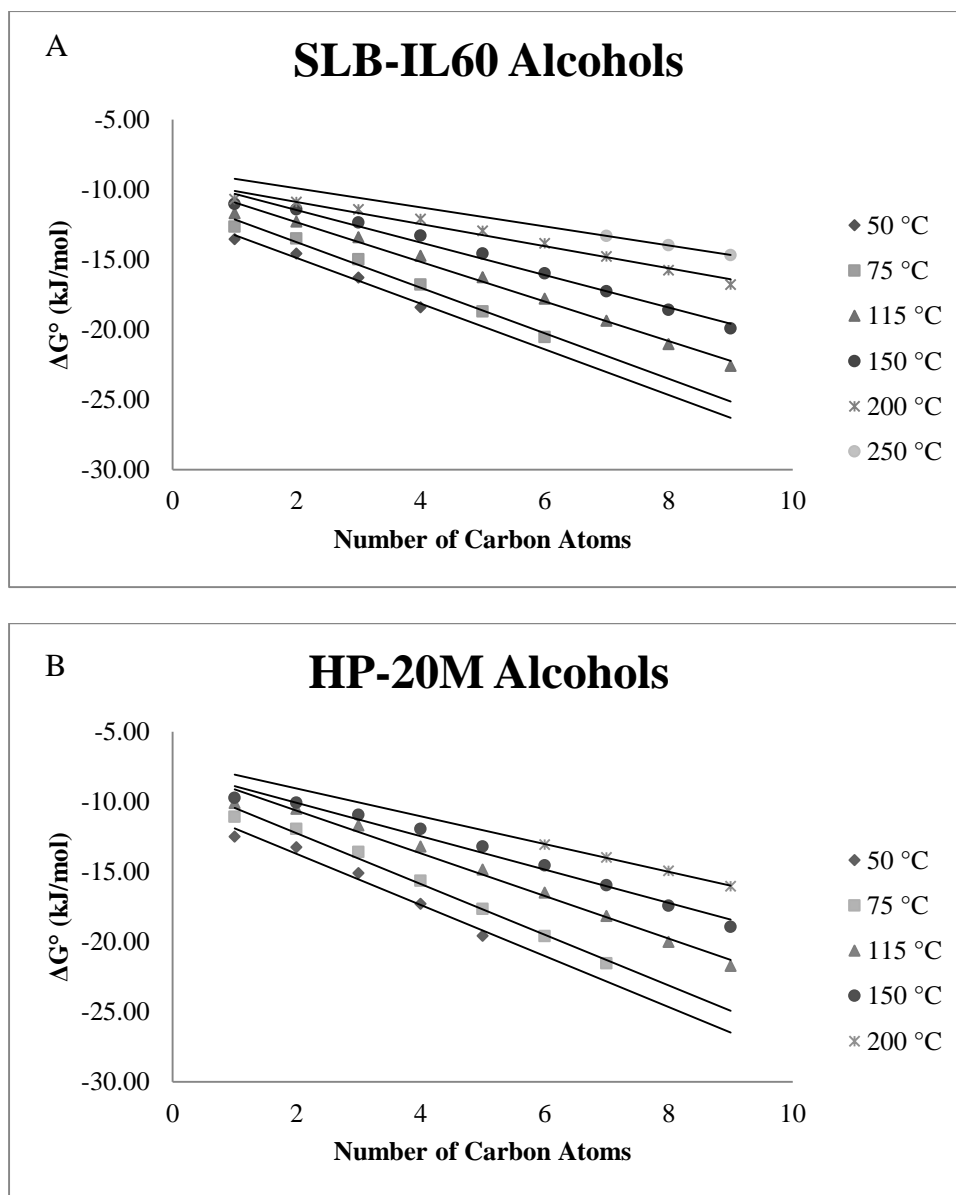
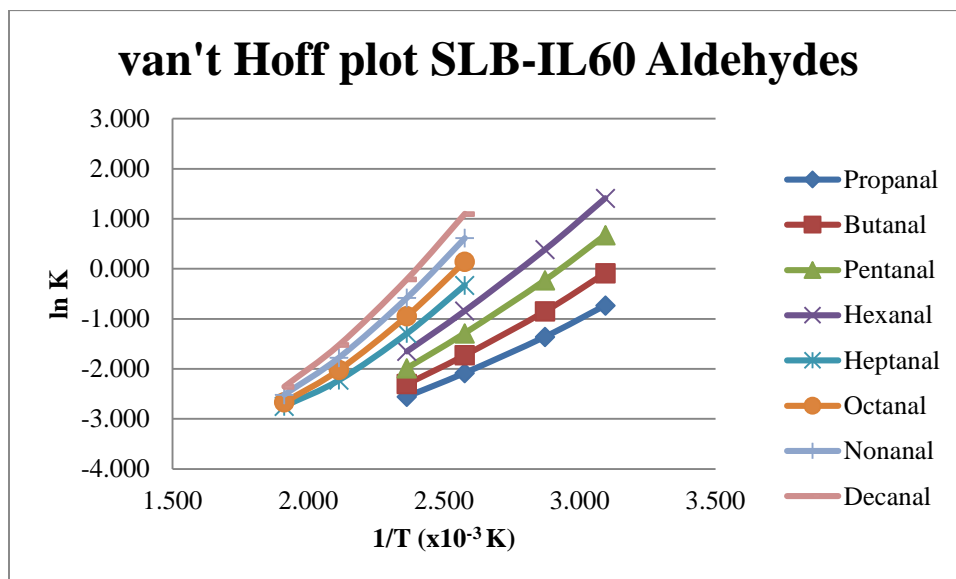


Figure 18: A plot of ΔG° vs the number of carbon atoms for a homologous series of primary alcohols at various temperatures on the (A) SLB-IL60 column and the (B) HP-20M column.

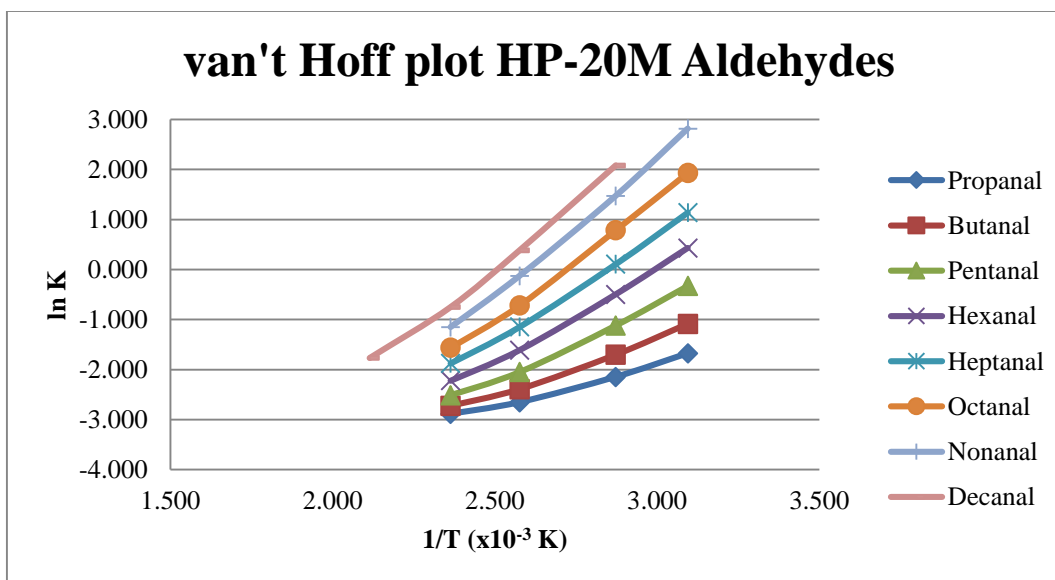
3.4 Aldehydes

The van't Hoff plots for the homologous series of alkyl aldehydes (propanal through decanal) on the SLB-IL60 and HP-20M columns, shown in Figures 19 and 20, revealed some interesting differences. Visually, the analytes occupy different regions of space on the van't Hoff plots. The aldehydes seem to “stack” more closely together on the SLB-IL60 than the HP-20M, suggesting there are smaller differences in the ΔG° values from one temperature to the next for the homologs. This trend is also reflected in the ΔG° vs T plots, shown in Figures 21 and 22. The entire homologous series is shifted vertically up the y-axis on the HP-20M graph.



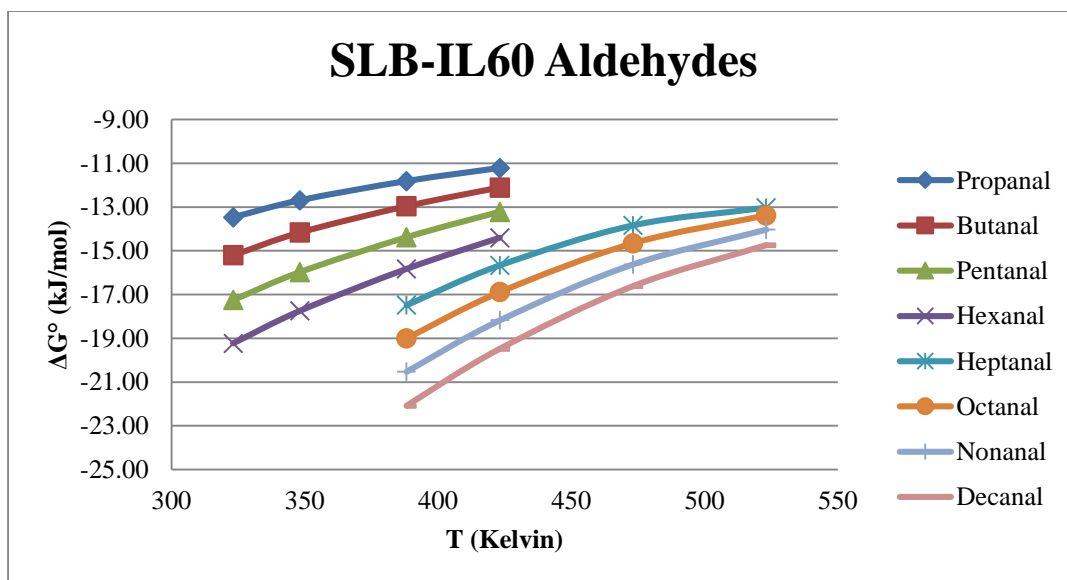
1/T (x10 ⁻³)	ln K							
	Propanal	Butanal	Pentanal	Hexanal	Heptanal	Octanal	Nonanal	Decanal
3.095	-0.732	-0.085	0.677	1.413				
2.872	-1.359	-0.850	-0.226	0.387				
2.576	-2.083	-1.728	-1.288	-0.839	-0.327	0.144	0.616	1.098
2.363	-2.556	-2.304	-1.986	-1.650	-1.293	-0.945	-0.579	-0.209
2.113					-2.227	-2.019	-1.775	-1.521
1.911					-2.749	-2.668	-2.519	-2.356

Figure 19: van't Hoff plot of a homologous series of alkyl aldehydes on the SLB-IL60 column. The corresponding table shows the ln k values at various temperatures for a homologous series of alkyl aldehydes on the SLB-IL60 column.



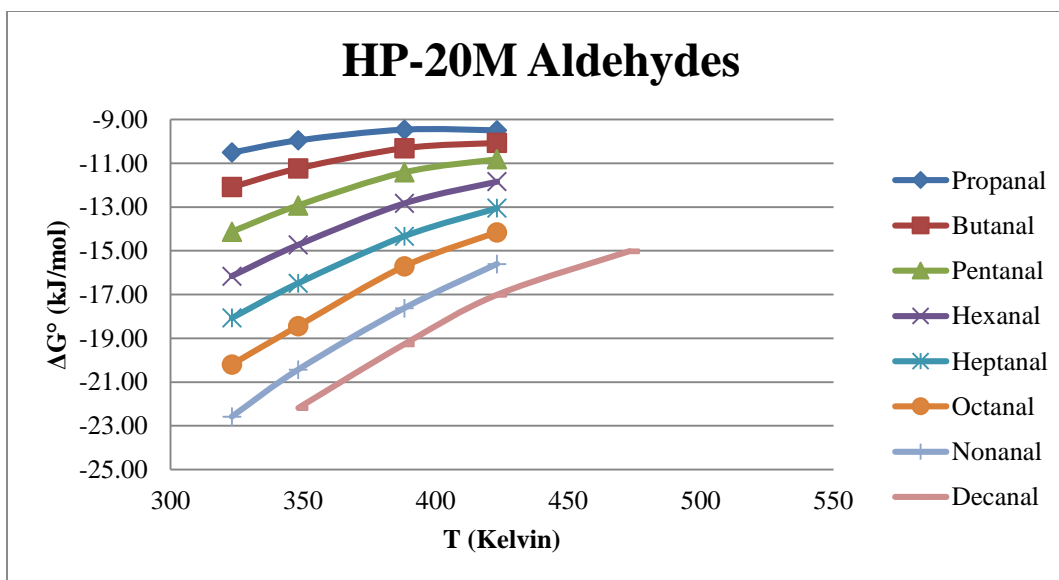
	ln K							
$1/T$ ($\times 10^{-3}$)	Propanal	Butanal	Pentanal	Hexanal	Heptanal	Octanal	Nonanal	Decanal
3.095	-1.675	-1.086	-0.328	0.430	1.139	1.933	2.818	
2.872	-2.147	-1.705	-1.119	-0.497	0.107	0.786	1.472	2.080
2.576	-2.652	-2.392	-2.049	-1.609	-1.145	-0.717	-0.126	0.386
2.363	-2.885	-2.724	-2.511	-2.222	-1.876	-1.562	-1.151	-0.749
2.113								-1.767

Figure 20: van't Hoff plot of a homologous series of alkyl aldehydes on the HP-20M column. The corresponding table shows the ln k values at various temperatures for a homologous series of alkyl aldehydes on the HP-20M column.



T (Kelvin)	ΔG° (kJ/mol)							
	Propanal	Butanal	Pentanal	Hexanal	Heptanal	Octanal	Nonanal	Decanal
323.15	-13.47	-15.21	-17.25	-19.23				
348.15	-12.69	-14.17	-15.97	-17.75				
388.15	-11.82	-12.96	-14.38	-15.83	-17.48	-19.00	-20.53	-22.08
423.15	-11.22	-12.11	-13.22	-14.41	-15.66	-16.89	-18.17	-19.48
473.15					-13.84	-14.66	-15.62	-16.62
523.15					-13.03	-13.38	-14.03	-14.74
R^2	0.991	0.992	0.993	0.995	0.990	0.992	0.994	0.994

Figure 21: A plot of ΔG° vs T for a homologous series of alkyl aldehydes on the SLB-IL60 column. The corresponding table shows the ΔG° values at various temperatures for a homologous series of alkyl aldehydes on the SLB-IL60 column.



T (Kelvin)	ΔG° (kJ/mol)							
	Propanal	Butanal	Pentanal	Hexanal	Heptanal	Octanal	Nonanal	Decanal
323.15	-10.51	-12.09	-14.13	-16.16	-18.07	-20.20	-22.58	
348.15	-9.96	-11.23	-12.93	-14.73	-16.48	-18.44	-20.43	-22.19
388.15	-9.47	-10.31	-11.41	-12.83	-14.33	-15.71	-17.62	-19.27
423.15	-9.50	-10.07	-10.82	-11.84	-13.05	-14.16	-15.60	-17.02
473.15								-15.02
523.15								
R^2	0.972	0.988	0.996	0.997	0.998	1.000	0.997	0.999

Figure 22: A plot of ΔG° vs T for a homologous series of alkyl aldehydes on the HP-20M column. The corresponding table shows the ΔG° values at various temperatures for a homologous series of alkyl aldehydes on the HP-20M column.

The plot of the ΔS° and ΔH° values versus the number of carbon atoms (Figure 23) revealed some interesting trends. On the HP-20M column, the entropy and enthalpy values consistently trend downward across the homologous series. On the SLB-IL60, propanal through hexanal (C1-C6) follow one linear downward trend, while heptanal through decanal (C7-C10) follow a different downward linear trend. These analytes were not analyzed at lower column temperatures (50 °C and 75 °C) on the SLB-IL60, while they were successfully analyzed at these lower temperatures on the HP-20M column. This could account for the apparent switch that happens at C7 in the data. Again, many of the retention factor, k , values were less than 1, but the linearity of the data suggests that this was still a reasonable method for analyzing thermodynamic trends. In addition, good linearity was obtained for the homologous series of aldehydes at varying temperatures which can be seen in the ΔG° vs number of carbon atom plots in Figures 24. At higher temperatures, the lines seem to converge, supporting the theory that carrier gas transport is the main variable affecting retention, specifically at higher elution temperatures.

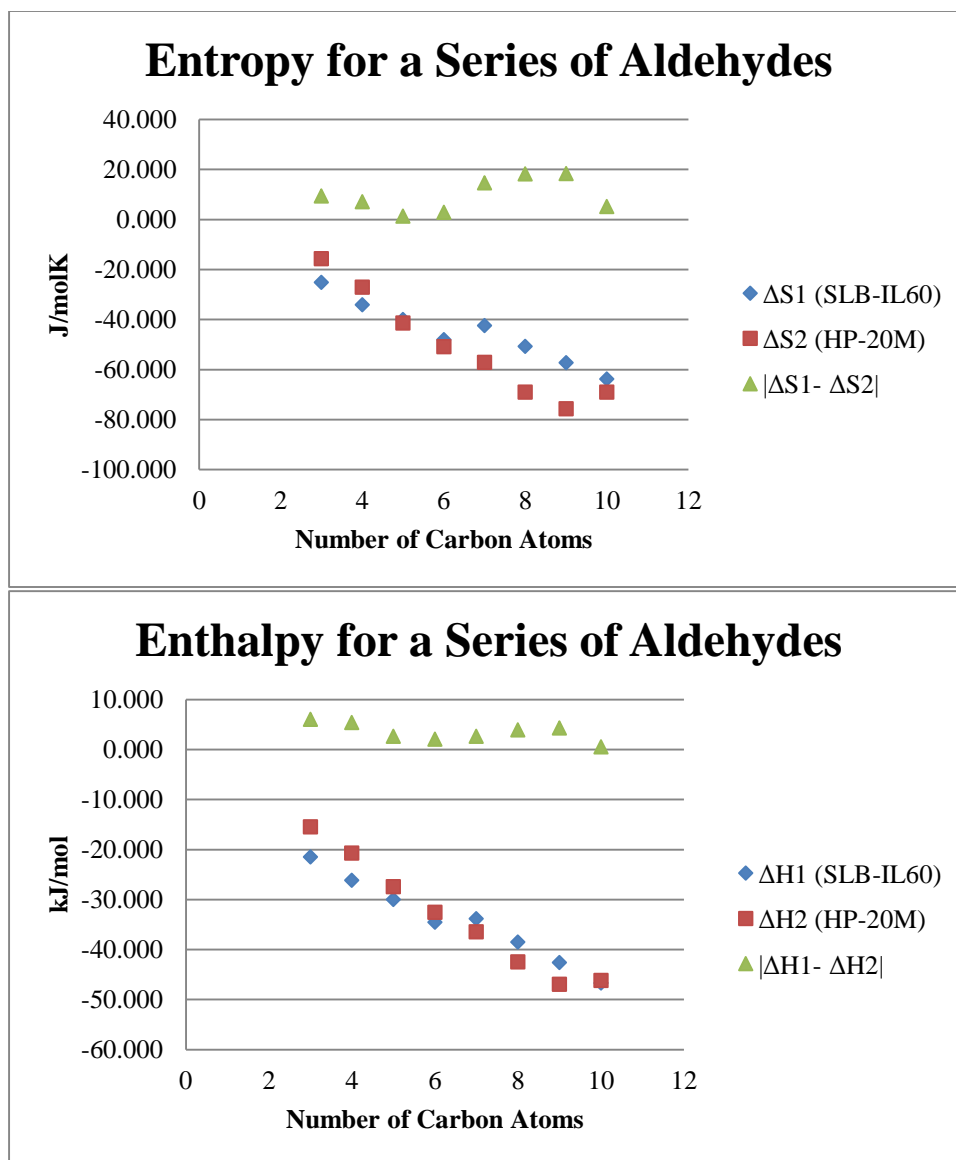


Figure 23: A plot of the ΔS° and ΔH° values and their absolute differential values on the SLB-IL60 and HP-20M columns for a series of alkyl aldehydes.

	Propanal	Butanal	Pentanal	Hexanal	Heptanal	Octanal	Nonanal	Decanal
ΔS°_1 (J/molK)	-25.099	-34.115	-40.015	-47.960	-42.413	-50.672	-57.294	-63.818
ΔS°_2 (J/molK)	-15.676	-27.039	-41.378	-50.877	-57.138	-68.955	-75.698	-69.064
$ \Delta S^{\circ}_1 - \Delta S^{\circ}_2 $ (J/molK)	9.423	7.076	1.363	2.917	14.725	18.284	18.403	5.246
ΔH°_1 (kJ/mol)	-21.523	-26.159	-30.039	-34.579	-33.820	-38.543	-42.636	-46.715
ΔH°_2 (kJ/mol)	-15.513	-20.759	-27.437	-32.542	-36.470	-42.470	-46.942	-46.185
$ \Delta H^{\circ}_1 - \Delta H^{\circ}_2 $ (kJ/mol)	6.010	5.400	2.603	2.037	2.650	3.927	4.306	0.530

Table 8: ΔH° and ΔS° values for a homologous series of alkyl aldehydes on the SLB-IL60 and HP-20M columns; ΔH°_1 and ΔS°_1 refer to SLB-IL60, ΔH°_2 and ΔS°_2 refer to HP-20M. The absolute differential values between the entropy and enthalpy on both column phases for each analyte were calculated.

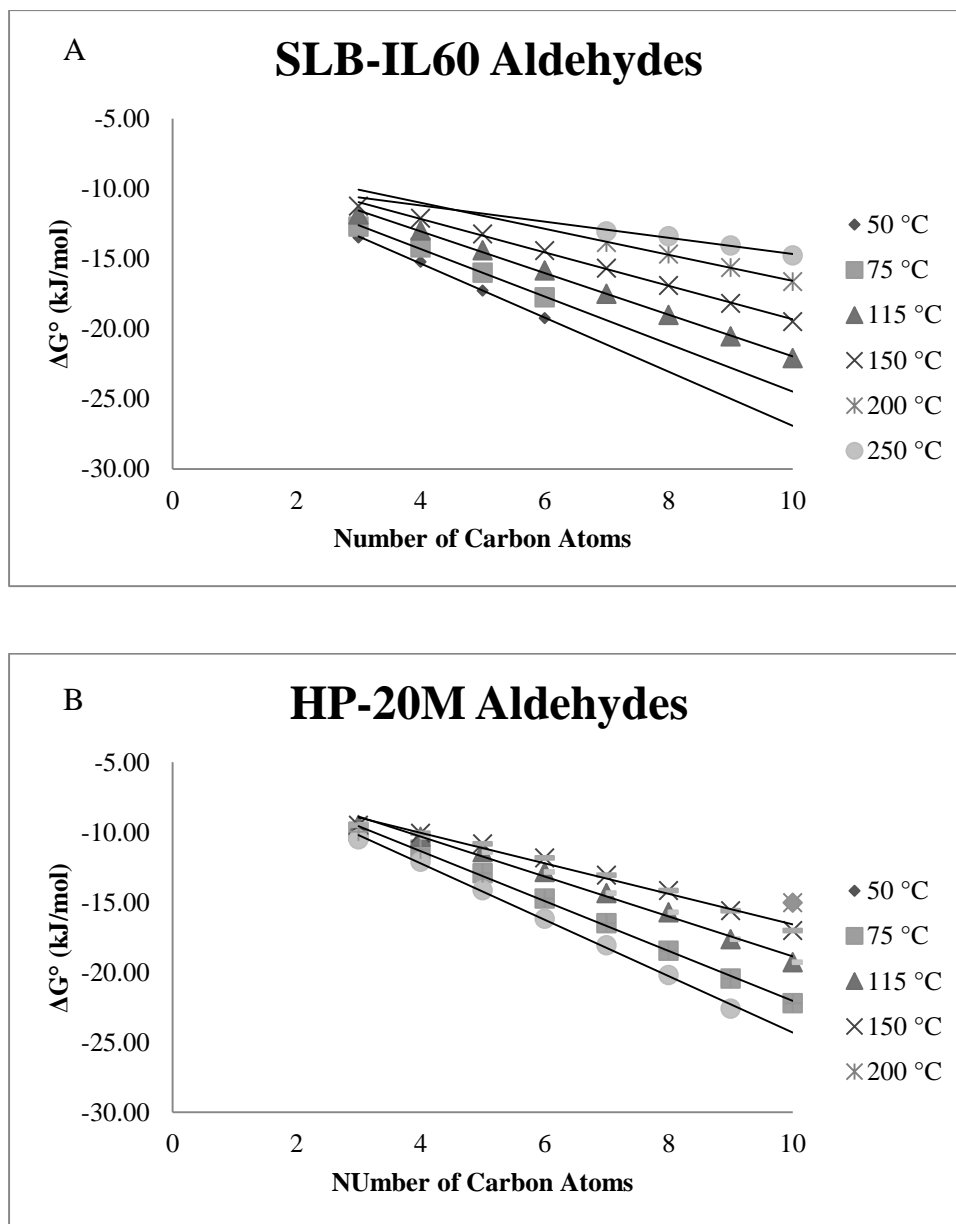
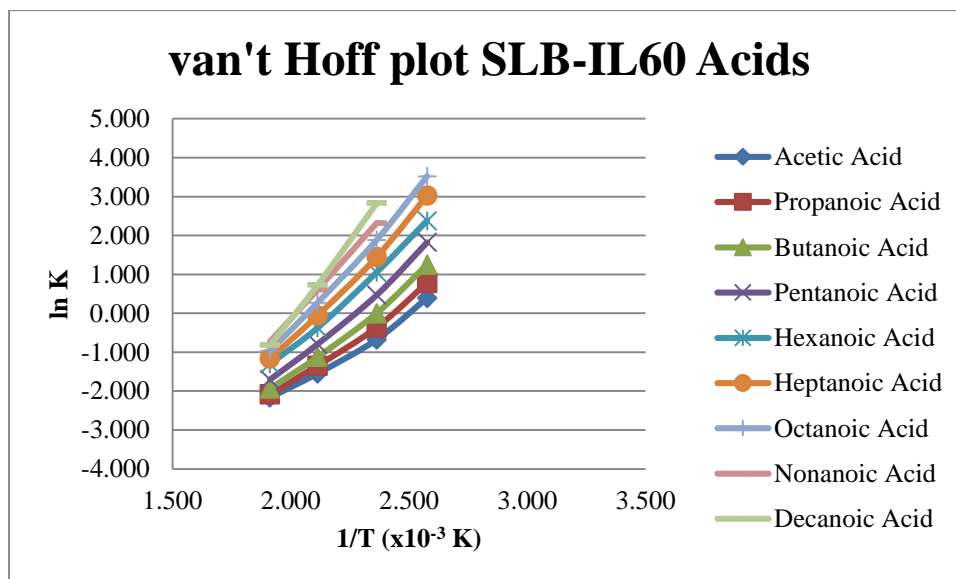


Figure 24: A plot of ΔG° vs the number of carbon atoms for a homologous series of alkyl aldehydes at various temperatures on the (A) SLB-IL60 column and (B) HP-20M column.

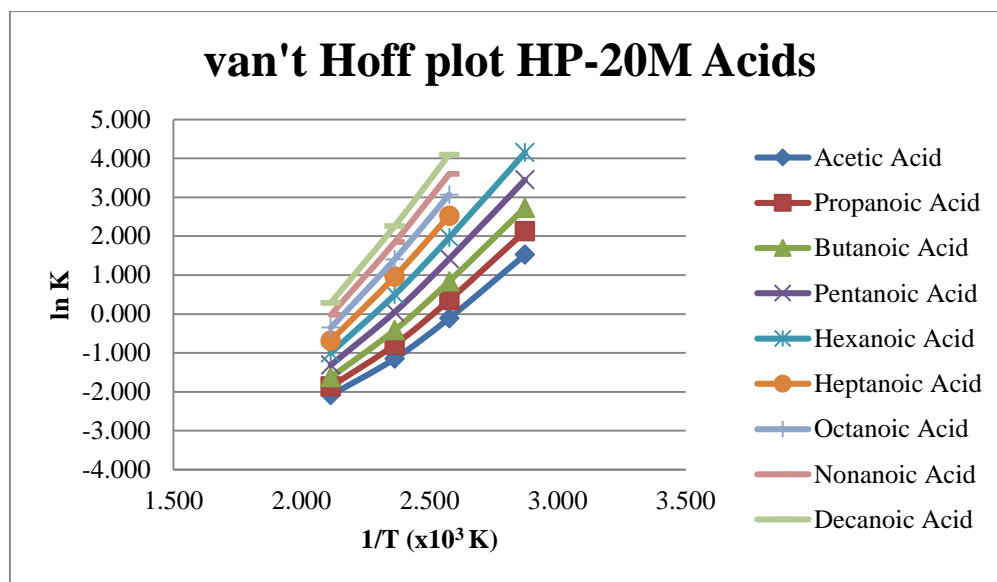
3.5 Acids

The homologous series of alkyl carboxylic acids were an interesting class of compounds to analyze on the two column phases. Analysis on the SLB-IL60 proved to be rather challenging. While 1% dilutions were easily analyzed on the HP-20M, the SLB-IL60 had poor peak shapes and low area counts. In order to account for this, the analytes were injected neat at 0.2 μL with the highest split possible on the SLB-IL60 column. Even still, the acid peaks seemed to “bleed” into the baseline and were far from being Gaussian, showing dramatic peak tailing. Even the smaller acids showed retention factors, k , at or greater than 1 suggesting that solute-solvent interactions were taking place here. The van’t Hoff plots (Figures 25 and 26) show steeper curves for the acids on the HP-20M column. The ΔG° vs T , plots show evenly spaced lines for each analyte of the homologous series on the HP-20M while they are more closely stacked on the SLB-IL60, as seen in Figures 27 and 28, respectively. These trends suggest that there are different thermodynamic retention mechanisms for both column phases.



1/T (x10 ⁻³)	ln K								
	Acetic Acid	Propanoic Acid	Butanoic Acid	Pentanoic Acid	Hexanoic Acid	Heptanoic Acid	Octanoic Acid	Nonanoic Acid	Decanoic Acid
3.095									
2.872									
2.576	0.400	0.787	1.256	1.826	2.384	3.030	3.527		
2.363	-0.673	-0.364	0.005	0.472	1.057	1.448	1.889	2.323	2.837
2.113	-1.542	-1.348	-1.120	-0.787	-0.367	-0.053	0.275	0.614	0.736
1.911	-2.162	-2.078	-1.934	-1.702	-1.300	-1.161	-0.963	-0.729	-0.814

Figure 25: van't Hoff plot of a homologous series of alkyl carboxylic acids on the SLB-IL60 column. The corresponding table shows the ln k values at various temperatures for a homologous series of alkyl carboxylic acids on the SLB-IL60 column.



1/T (x10 ⁻³)	ln K								
	Acetic Acid	Propanoic Acid	Butanoic Acid	Pentanoic Acid	Hexanoic Acid	Heptanoic Acid	Octanoic Acid	Nonanoic Acid	Decanoic Acid
3.095									
2.872	1.523	2.124	2.728	3.448	4.148				
2.576	-0.107	0.359	0.838	1.417	1.966	2.524	3.066	3.597	4.095
2.363	-1.149	-0.791	-0.416	0.048	0.497	0.957	1.403	1.846	2.257
2.113	-2.088	-1.866	-1.625	-1.315	-1.002	-0.683	-0.351	-0.023	0.285

Figure 26: van't Hoff plot of a homologous series of alkyl carboxylic acids on the HP-20M column. The corresponding table shows the ln k values at various temperatures for a homologous series of alkyl carboxylic acids on the HP-20M column.

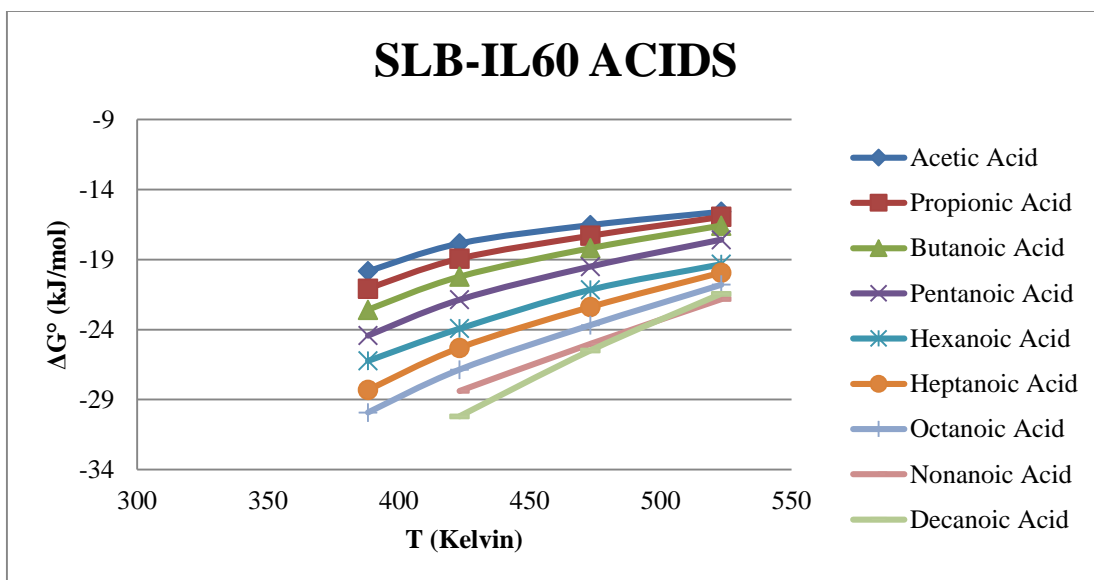
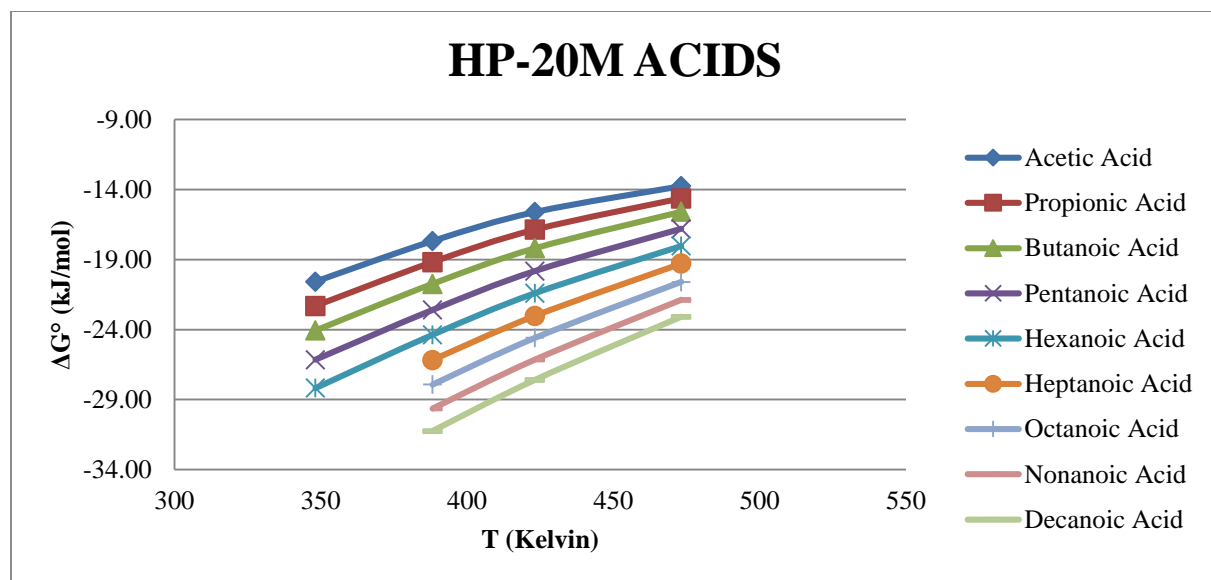


Figure 27: A plot of ΔG° vs T for a homologous series of alkyl carboxylic acids on the SLB-IL60 column. The corresponding table shows the ΔG° values at various temperatures for a homologous series of alkyl carboxylic acids on the SLB-IL60 column.



T (Kelvin)	ΔG° (kJ/mol)								
	Acetic Acid	Propionic Acid	Butanoic Acid	Pentanoic Acid	Hexanoic Acid	Heptanoic Acid	Octanoic Acid	Nonanoic Acid	Decanoic Acid
323.15									
348.15	-20.58	-22.32	-24.06	-26.15	-28.18				
388.15	-17.68	-19.19	-20.73	-22.60	-24.37	-26.17	-27.92	-29.64	-31.24
423.15	-15.61	-16.87	-18.19	-19.82	-21.40	-23.02	-24.59	-26.14	-27.59
473.15	-13.76	-14.63	-15.58	-16.80	-18.03	-19.29	-20.59	-21.88	-23.09
523.15									
R^2	0.997	0.998	0.998	0.991	0.993	0.997	0.998	0.998	0.998

Figure 28: A plot of ΔG° vs T for a homologous series of alkyl carboxylic acids on the HP-20M column. The corresponding table shows the ΔG° values at various temperatures for a homologous series of alkyl carboxylic acids on the HP-20M column.

The slopes and y-intercept values, ΔS° and ΔH° , respectively, reported in Table 21 were consistently more negative for the HP-20M, and the differentials between the two column phases were significant. In fact, a plot of the entropy and enthalpy values versus the number of carbon atoms, shown in Figure 29, shows that the absolute differences on both column phases do not appear to be consistent over the range of the homologous series. Also, there is an overall consistent trend downward, but with more “bounce” from one homolog to the next. Interestingly, the difference between the intercepts for decanoic acid was not very large, suggesting comparable interactions for higher molecular weight molecules in the homologous series. The ΔG° values were linear and nearly parallel for the HP-20M plot of ΔG° vs number of carbon atoms as shown in Figure 30. The SLB-IL60 graph was less consistent and the lines started to converge at acetic acid, suggesting that the retention was not attributed to solute-solvent interactions.

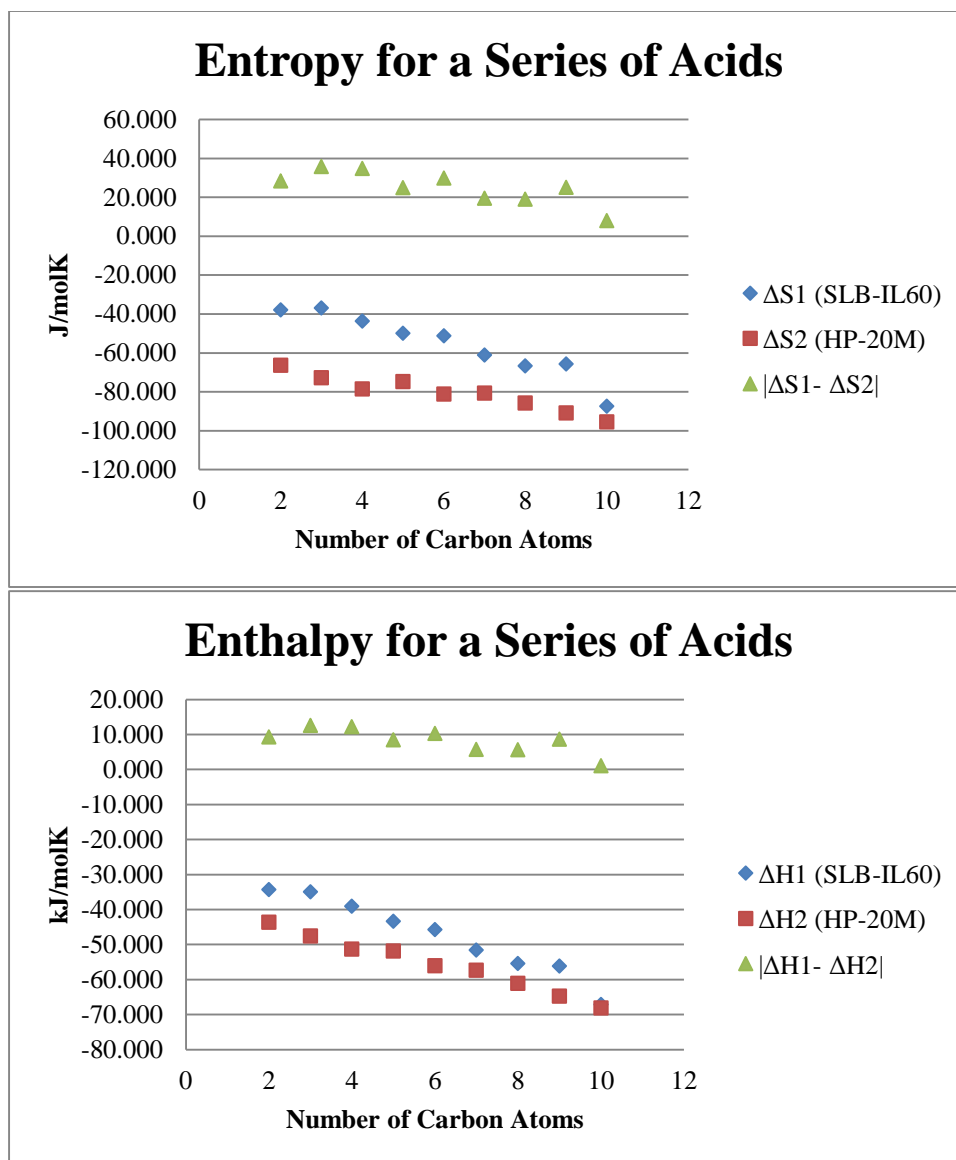


Figure 29: A plot of the ΔS° and ΔH° values and their absolute differential values on the SLB-IL60 and HP-20M columns for a homologous series of alkyl carboxylic acids.

	Acetic Acid	Propionic Acid	Butanoic Acid	Pentanoic Acid	Hexanoic Acid	Heptanoic Acid	Octanoic Acid	Nonanoic Acid	Decanoic Acid
ΔS°_1 (J/molK)	-37.937	-36.884	-43.610	-49.811	-51.196	-61.076	-66.671	-65.666	-87.465
ΔS°_2 (J/molK)	-66.392	-72.778	-78.454	-74.730	-81.056	-80.574	-85.780	-90.792	-95.456
$ \Delta S^{\circ}_1 - \Delta S^{\circ}_2 $ (J/molK)	28.454	35.895	34.844	24.918	29.860	19.498	19.108	25.126	7.992
ΔH°_1 (kJ/mol)	-34.311	-34.981	-39.103	-43.357	-45.796	-51.587	-55.442	-56.140	-67.093
ΔH°_2 (kJ/mol)	-43.615	-47.584	-51.315	-51.844	-56.077	-57.324	-61.094	-64.761	-68.180
$ \Delta H^{\circ}_1 - \Delta H^{\circ}_2 $ (kJ/mol)	9.304	12.603	12.212	8.488	10.282	5.736	5.652	8.620	1.087

Table 9: ΔH° and ΔS° values for a homologous series of alkyl carboxylic acids on the SLB-IL60 and HP-20M columns; ΔH°_1 and ΔS°_1 refer to SLB-IL60, ΔH°_2 and ΔS°_2 refer to HP-20M. The absolute differential values between the entropy and enthalpy on both column phases for each analyte were calculated.

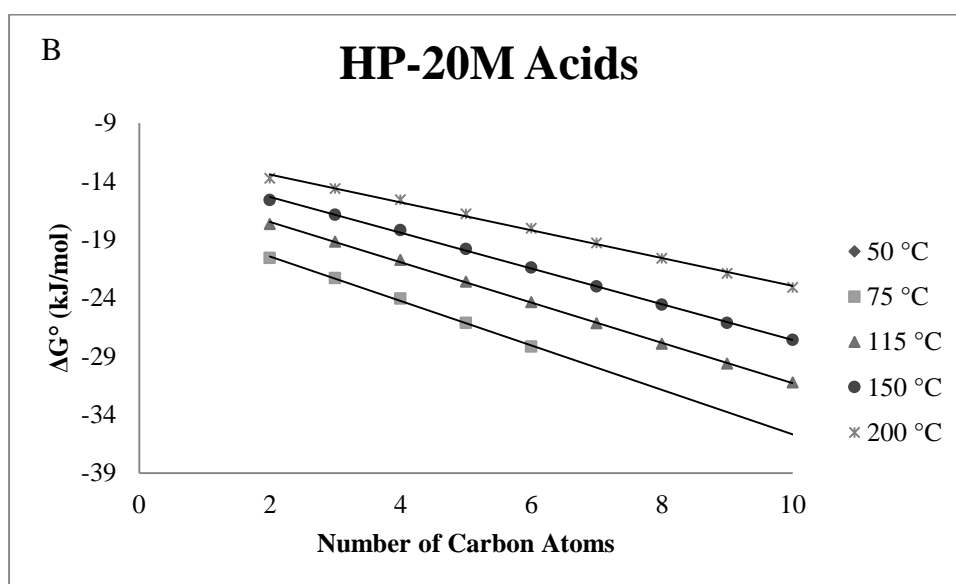
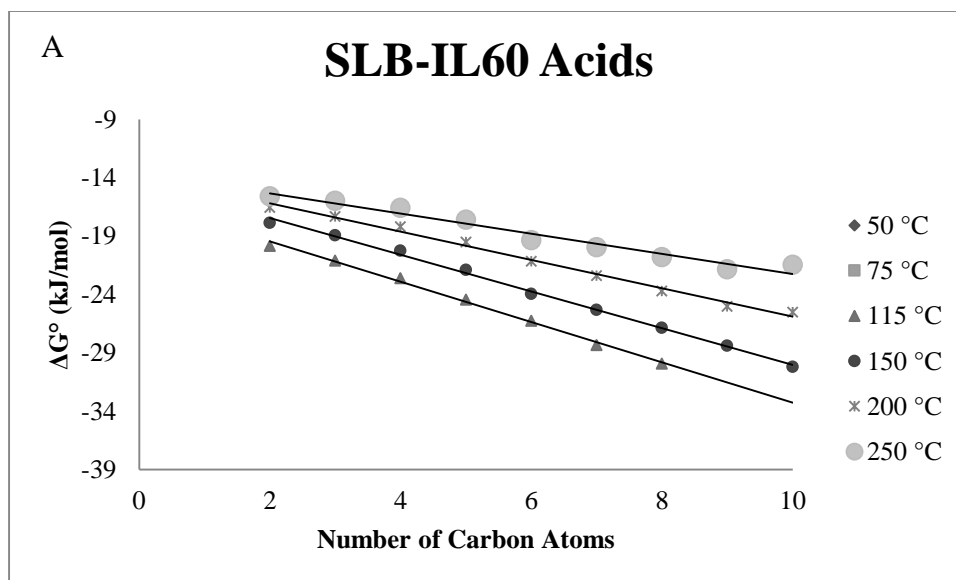
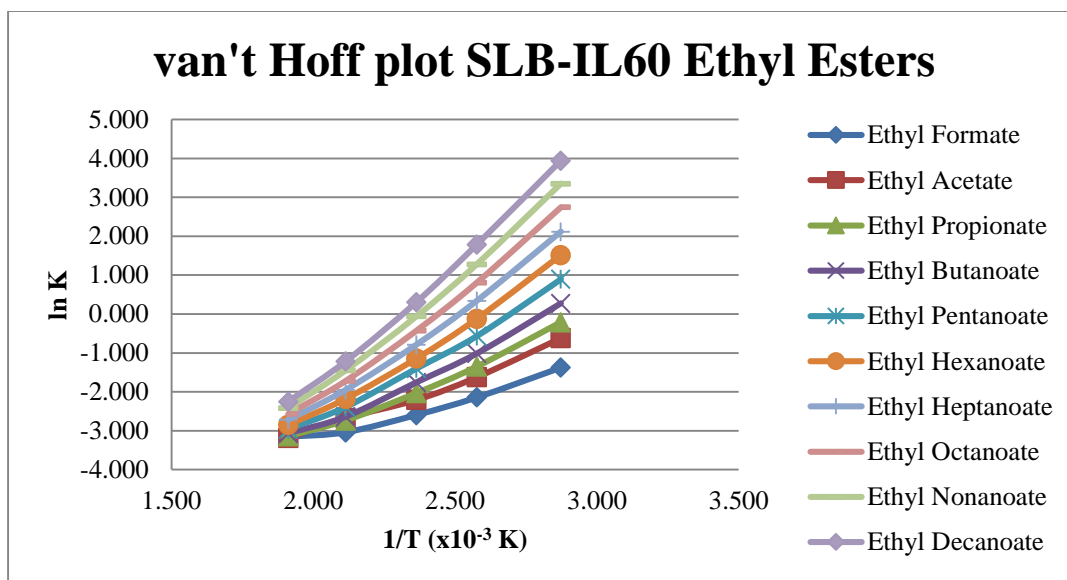


Figure 30: A plot of ΔG° vs the number of carbon atoms for a homologous series of alkyl carboxylic acids at various temperatures on the (A) SLB-IL60 column and (B) HP-20M column.

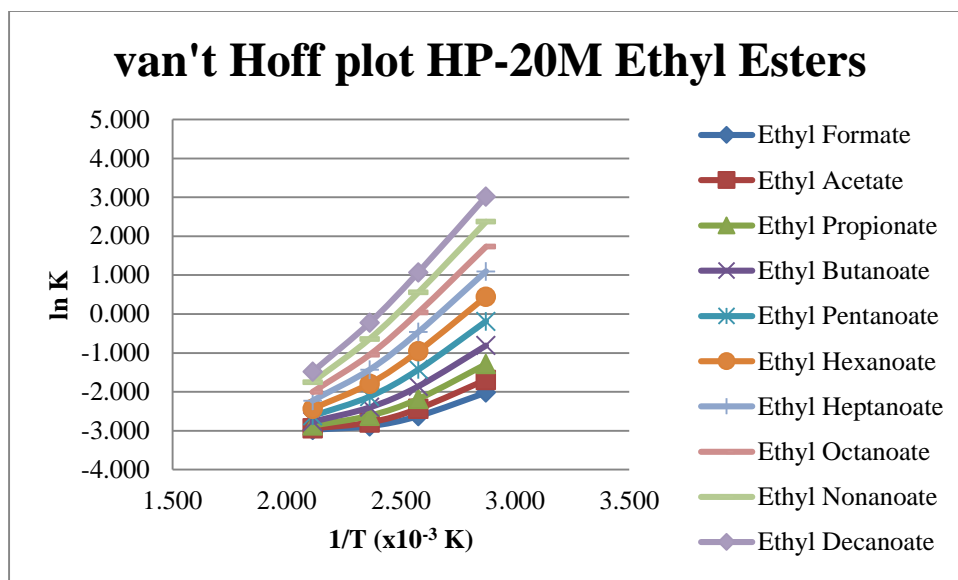
3.6 Ethyl Esters

van't Hoff plots for the homologous series of ethyl esters (ethyl formate through ethyl decanoate) on the SLB-IL60 and HP-20M produced nearly identical graphs, as seen in Figures 31 and 32, with the exception of ethyl formate and ethyl acetate. The entire homologous series is shifted slightly up the y-axis on the HP-20M graph, but the overall shapes of the curves appear to be consistent for each analyte on each column phase. The differences become more apparent when examining the ΔG° vs T graphs in Figures 33 and 34. In fact, the ethyl esters were successfully analyzed over five different temperatures on the SLB-IL60 with much greater ease than the carboxylic acids, as discussed previously. The nearly consistent ΔG° values for ethyl formate and ethyl acetate on the HP-20M column suggest that there was little solute-solvent interaction. Ethyl formate through ethyl hexanoate, although measured at 5 different temperatures, had k values less than 1 for a majority of the analytes, and as stated previously is not an ideal situation in GC data analysis. However, ethyl heptanoate through ethyl decanoate had k values greater than 1 for a number of the temperature points, making them sufficient for retention thermodynamic analysis.



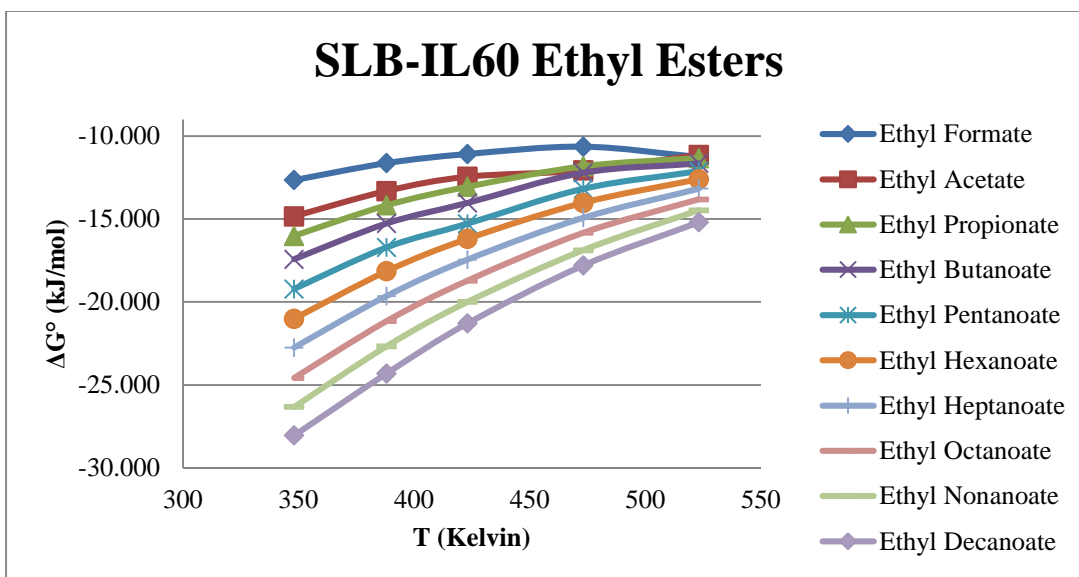
1/T (x10 ⁻³)	ln K									
	Ethyl Formate	Ethyl Acetate	Ethyl Propionate	Ethyl Butanoate	Ethyl Pentanoate	Ethyl Hexanoate	Ethyl Heptanoate	Ethyl Octanoate	Ethyl Nonanoate	Ethyl Decanoate
3.095										
2.872	-1.376	-0.619	-0.214	0.274	0.894	1.515	2.115	2.746	3.351	3.944
2.576	-2.143	-1.620	-1.353	-1.016	-0.567	-0.121	0.341	0.809	1.279	1.787
2.363	-2.596	-2.205	-2.033	-1.759	-1.402	-1.141	-0.786	-0.426	-0.060	0.305
2.113	-3.041	-2.676	-2.739	-2.643	-2.394	-2.179	-1.950	-1.719	-1.452	-1.220
1.911	-3.157	-3.185	-3.141	-3.068	-2.959	-2.848	-2.716	-2.569	-2.417	-2.251

Figure 31: van't Hoff plot of a homologous series of ethyl esters on the SLB-IL60 column. The corresponding table shows the ln k values at various temperatures for a homologous series of ethyl esters on the SLB-IL60 column.



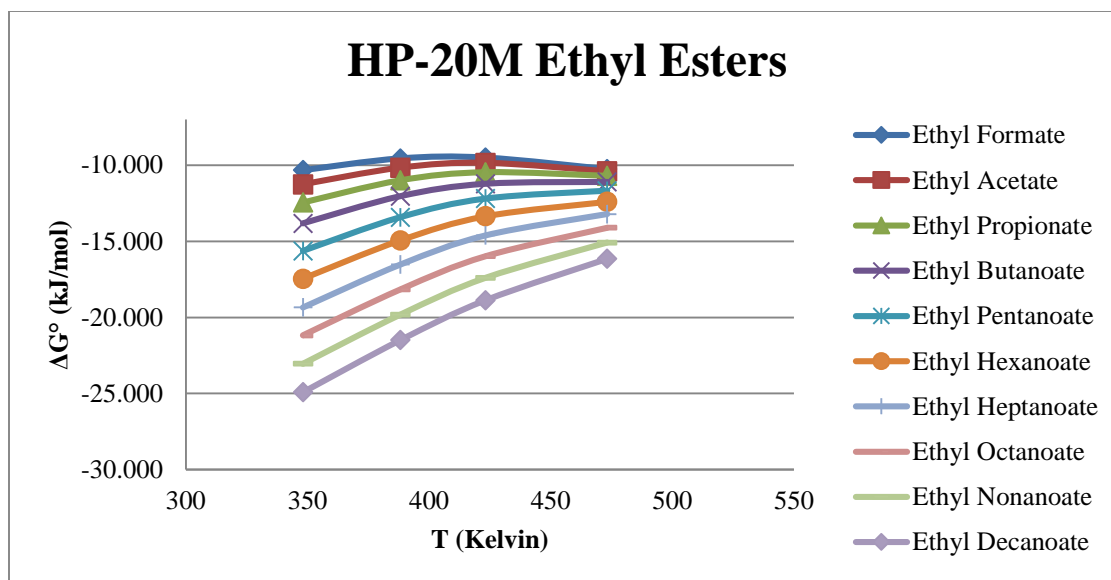
$1/T \text{ (x}10^{-3}\text{)}$	ln K									
	Ethyl Formate	Ethyl Acetate	Ethyl Propionate	Ethyl Butanoate	Ethyl Pentanoate	Ethyl Hexanoate	Ethyl Heptanoate	Ethyl Octanoate	Ethyl Nonanoate	Ethyl Decanoate
3.095										
2.872	-2.018	-1.695	-1.286	-0.809	-0.186	0.445	1.096	1.732	2.375	3.023
2.576	-2.626	-2.435	-2.180	-1.857	-1.427	-0.957	-0.464	0.043	0.556	1.073
2.363	-2.885	-2.786	-2.612	-2.398	-2.119	-1.790	-1.431	-1.044	-0.640	-0.223
2.113	-2.978	-2.939	-2.866	-2.765	-2.617	-2.433	-2.227	-2.000	-1.752	-1.483

Figure 32: van't Hoff plot of a homologous series of ethyl esters on the HP-20M column. The corresponding table shows the ln k values at various temperatures for a homologous series of ethyl esters on the HP-20M column.



		ΔG° (kJ/mol)								
T (Kelvin)	Ethyl Formate	Ethyl Acetate	Ethyl Propionate	Ethyl Butanoate	Ethyl Pentanoate	Ethyl Hexanoate	Ethyl Heptanoate	Ethyl Octanoate	Ethyl Nonanoate	Ethyl Decanoate
323.15										
348.15	-12.646	-14.837	-16.010	-17.421	-19.214	-21.014	-22.749	-24.576	-26.326	-28.044
388.15	-11.622	-13.309	-14.173	-15.261	-16.708	-18.148	-19.637	-21.150	-22.665	-24.304
423.15	-11.077	-12.452	-13.057	-14.022	-15.279	-16.194	-17.444	-18.711	-19.998	-21.285
473.15	-10.634	-12.071	-11.822	-12.202	-13.181	-14.026	-14.926	-15.834	-16.886	-17.800
523.15	-11.253	-11.132	-11.324	-11.641	-12.116	-12.597	-13.171	-13.812	-14.474	-15.196
R²	0.982	0.985	0.990	0.989	0.986	0.995	0.996	0.997	0.997	0.999

Figure 33: A plot of ΔG° vs T for a homologous series of ethyl esters on the SLB-IL60 column. The corresponding table shows the ΔG° values at various temperatures for a homologous series of ethyl esters on the SLB-IL60 column.



T (Kelvin)	ΔG° (kJ/mol)									
	Ethyl Formate	Ethyl Acetate	Ethyl Propionate	Ethyl Butanoate	Ethyl Pentanoate	Ethyl Hexanoate	Ethyl Heptanoate	Ethyl Octanoate	Ethyl Nonanoate	Ethyl Decanoate
323.15										
348.15	-10.329	-11.264	-12.45	-13.83	-15.63	-17.46	-19.34	-21.18	-23.04	-24.92
388.15	-9.553	-10.169	-10.99	-12.03	-13.42	-14.94	-16.53	-18.16	-19.82	-21.49
423.15	-9.502	-9.852	-10.46	-11.22	-12.20	-13.35	-14.62	-15.98	-17.40	-18.87
473.15	-10.260	-10.412	-10.70	-11.10	-11.68	-12.40	-13.21	-14.11	-15.08	-16.14
523.15										
R^2	0.826	0.929	0.950	0.970	0.984	0.992	0.995	0.997	0.998	0.999

Figure 34: A plot of ΔG° vs T for a homologous series of ethyl esters on the HP-20M column. The corresponding table shows the ΔG° values at various temperatures for a homologous series of ethyl esters on the HP-20M column.

The ΔS° and ΔH° (slope and intercept, respectively) values were consistently more negative on the SLB-IL60 column. The linearity of this data across the entire homologous series on both column phases is remarkable, as can be seen in Figure 35. Both column phases follow the same downward trend with consistent absolute differential values between all data points, whereas in previous series the higher molecular weight molecules seemed to converge towards the same y-intercept values (with smaller differentials). The retention factor, k , values for almost all temperatures were less than 1 from ethyl formate through ethyl hexanoate. While this is not ideal for GC analysis, the linearity of the data suggests that this method still provides sufficient data for analysis of retention thermodynamics. Lastly, the ethyl esters seemed to perform more linearly on the SLB-IL60 than the HP-20M, particularly at higher temperatures, as can be seen in Figure 36. At lower molecular weights, the lines seemed to converge even more so for the HP-20M than the SLB-IL60.

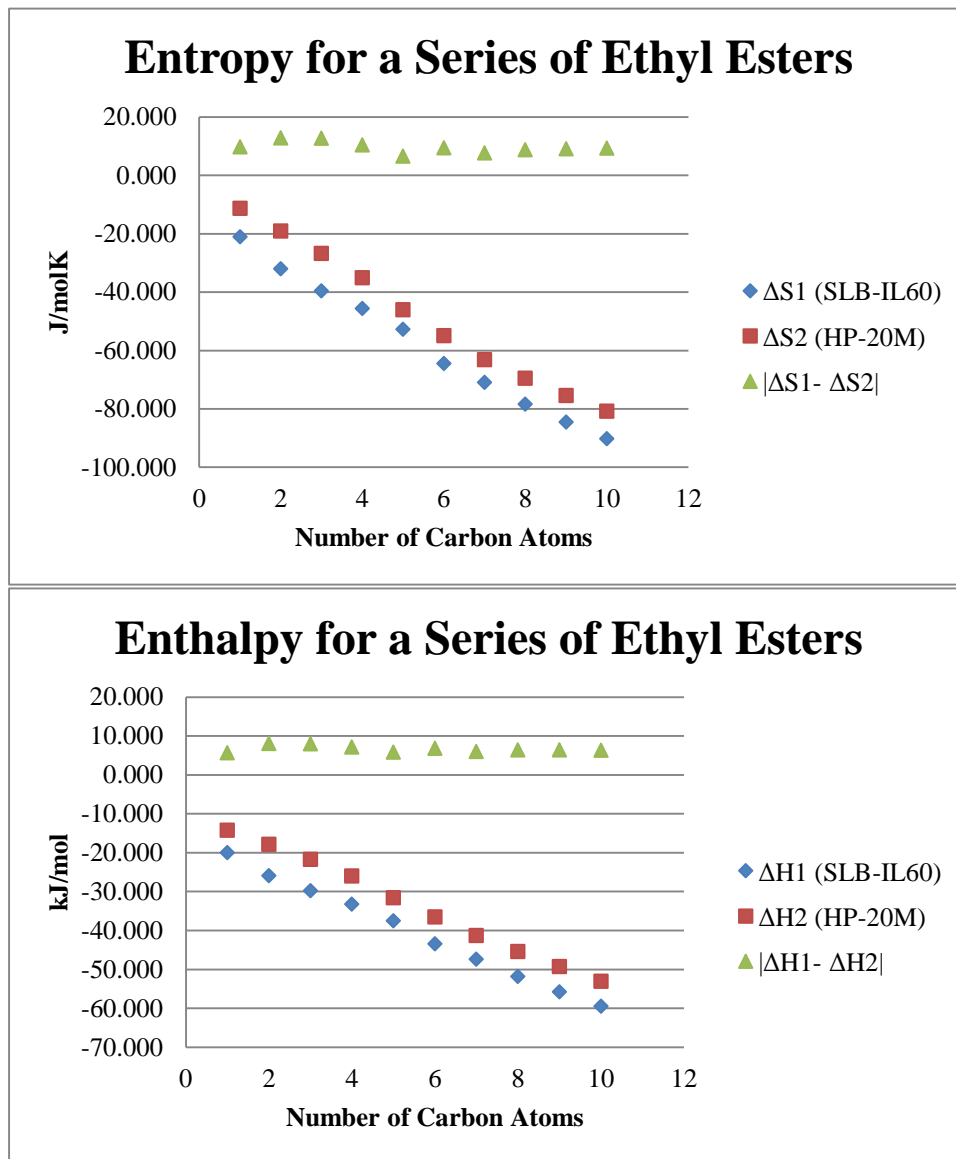


Figure 35: A plot of the ΔS° and ΔH° values and their absolute differential values on the SLB-IL60 and HP-20M columns for a homologous series of ethyl esters.

	Ethyl Formate	Ethyl Acetate	Ethyl Propionate	Ethyl Butanoate	Ethyl Pentanoate	Ethyl Hexanoate	Ethyl Heptanoate	Ethyl Octanoate	Ethyl Nonanoate	Ethyl Decanoate
ΔS°_1 (J/molK)	-21.031	-31.949	-39.532	-45.523	-52.710	-64.445	-70.901	-78.377	-84.551	-90.212
ΔS°_2 (J/molK)	-11.224	-19.028	-26.701	-35.049	-46.022	-54.908	-63.165	-69.533	-75.387	-80.804
$ \Delta S^{\circ}_1 - \Delta S^{\circ}_2 $ (J/molK)	9.808	12.921	12.831	10.474	6.688	9.537	7.736	8.844	9.164	9.408
ΔH°_1 (kJ/mol)	-19.910	-25.880	-29.691	-33.162	-37.439	-43.359	-47.345	-51.771	-55.674	-59.410
ΔH°_2 (kJ/mol)	-14.132	-17.782	-21.619	-25.905	-31.536	-36.471	-41.240	-45.315	-49.224	-52.987
$ \Delta H^{\circ}_1 - \Delta H^{\circ}_2 $ (kJ/mol)	5.778	8.098	8.072	7.257	5.902	6.889	6.105	6.456	6.450	6.422

Table 10: ΔH° and ΔS° values for a homologous series of ethyl esters on the SLB-IL60 and HP-20M columns; ΔH°_1 and ΔS°_1 refer to SLB-IL60, ΔH°_2 and ΔS°_2 refer to HP-20M. The absolute differential values between the entropy and enthalpy on both column phases for each analyte were calculated.

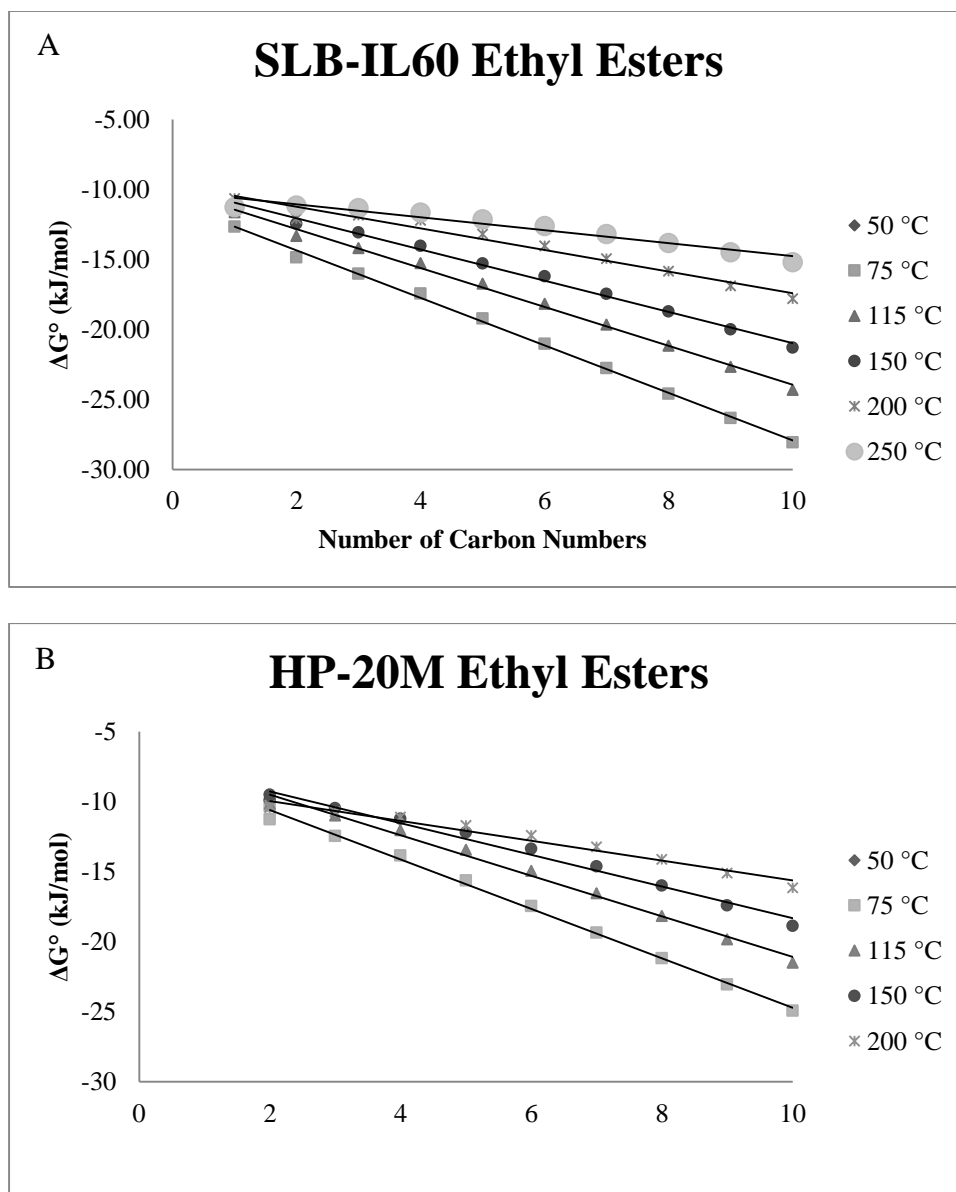
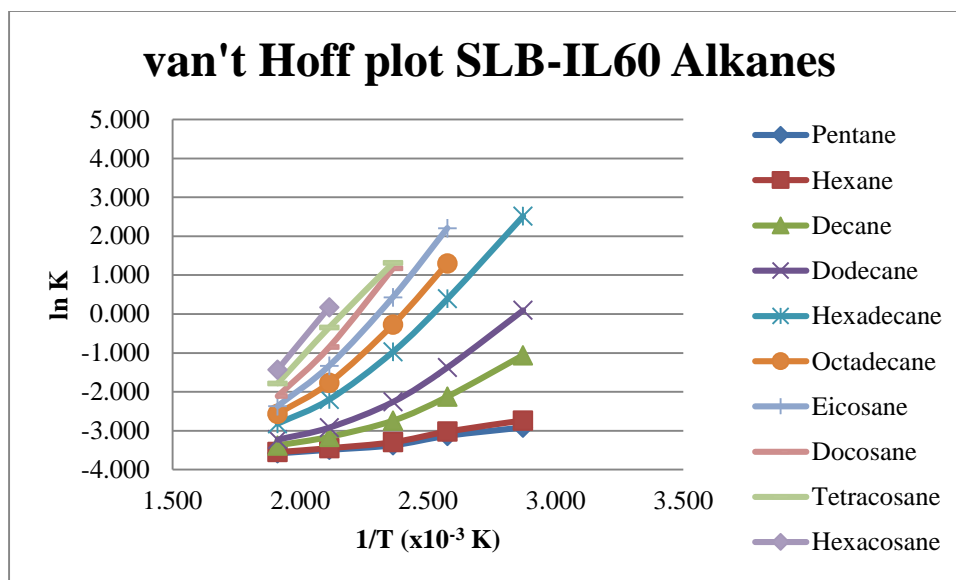


Figure 36: A plot of ΔG° vs the number of carbon atoms for a homologous series of ethyl esters at various temperatures on the (A) SLB-IL60 and (B) HP-20M column.

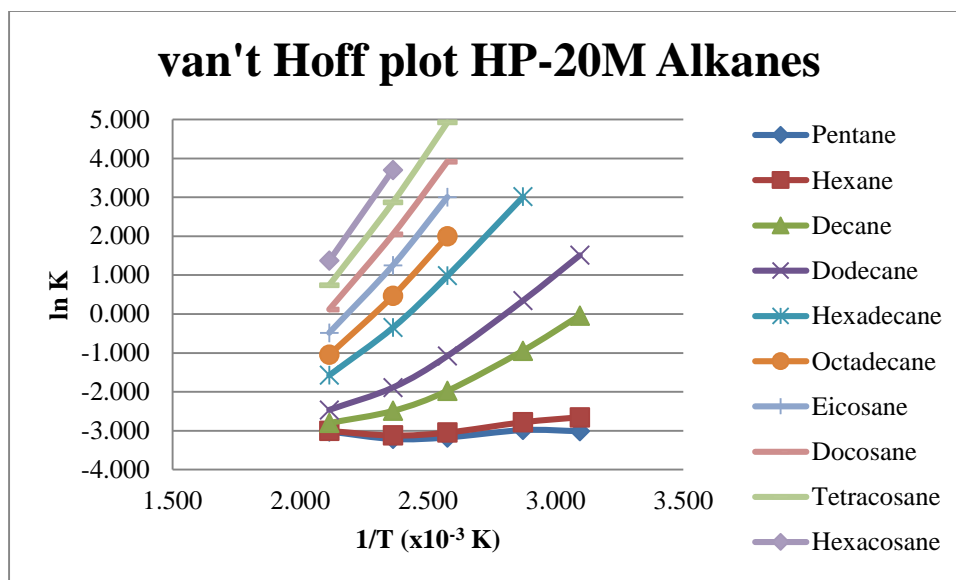
3.7 Alkanes

The van't Hoff plots for the homologous series of alkanes on the SLB-IL60 and HP-20M produced very different graphs suggesting very different selectivity on both column phases, as seen in Figures 37 and 38. Visually, the plots are more consistently spread out over the HP-20M graph, while they are more clustered together on the SLB-IL60. The two graphs have in common the overlapping plots for heptane and hexane, with very little differences in the $\ln k$ values over the temperature range. This alludes to the fact that small molecular weight alkanes are not retained but rather elute within or near the dead volume of the column (also supported by extremely small, hundredth decimal place k values.) This is further supported by the ΔG° vs T graphs in Figures 39 and 40. The SLB-IL60 data points are more clustered together, while the HP-20M data is more consistently spread out. It is important to note that this series included all even numbered alkanes up to hexacosane (C26), with the exception of pentane, and C8 and C14 missing due to availability. The trends described herein would be even more apparent if the odd carbon number alkanes were also analyzed. It is also important to note that the higher molecular weight alkanes were exceptionally difficult to analyze on both columns at temperatures lower than 150 °C (HP-20M) and 200 °C (SLB-IL60), and even after 2 hours with 1 uL injections split 100:1 peaks were not detected.



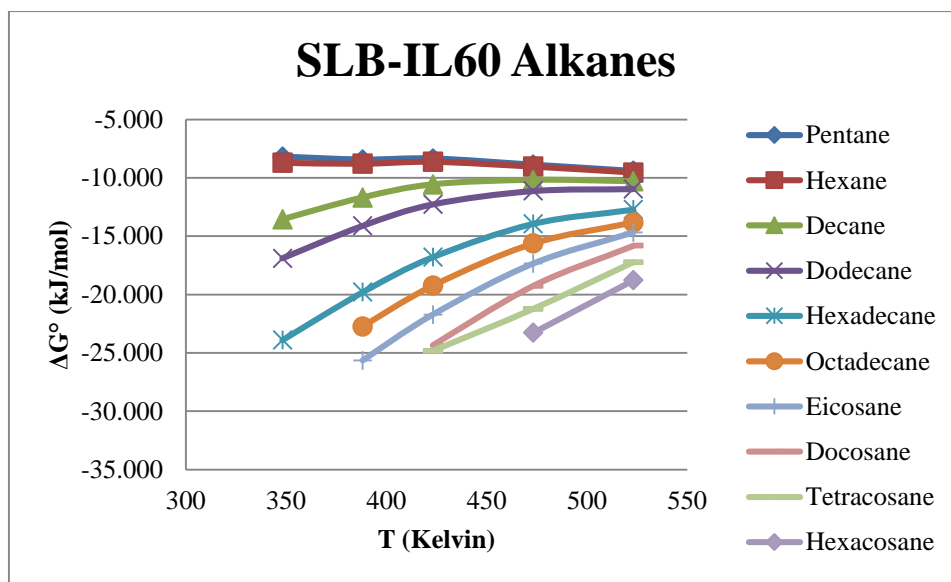
$1/T \text{ (}\times 10^{-3}\text{)}$	ln K									
	Pentane	Hexane	Decane	Dodecane	Hexadecane	Octadecane	Eicosane	Docosane	Tetracosane	Hexacosane
3.095										
2.872	-2.920	-2.737	-1.061	0.095	2.513					
2.576	-3.132	-3.021	-2.124	-1.371	0.391	1.302	2.205			
2.363	-3.374	-3.295	-2.742	-2.256	-0.971	-0.275	0.431	1.176	1.313	
2.113	-3.490	-3.448	-3.158	-2.917	-2.201	-1.771	-1.332	-0.849	-0.343	0.174
1.911	-3.582	-3.549	-3.378	-3.226	-2.821	-2.566	-2.368	-2.107	-1.782	-1.428

Figure 37: van't Hoff plot of a homologous series of alkanes on the SLB-IL60 column. The corresponding table shows the ln k values at various temperatures for a homologous series of alkanes on the SLB-IL60 column.



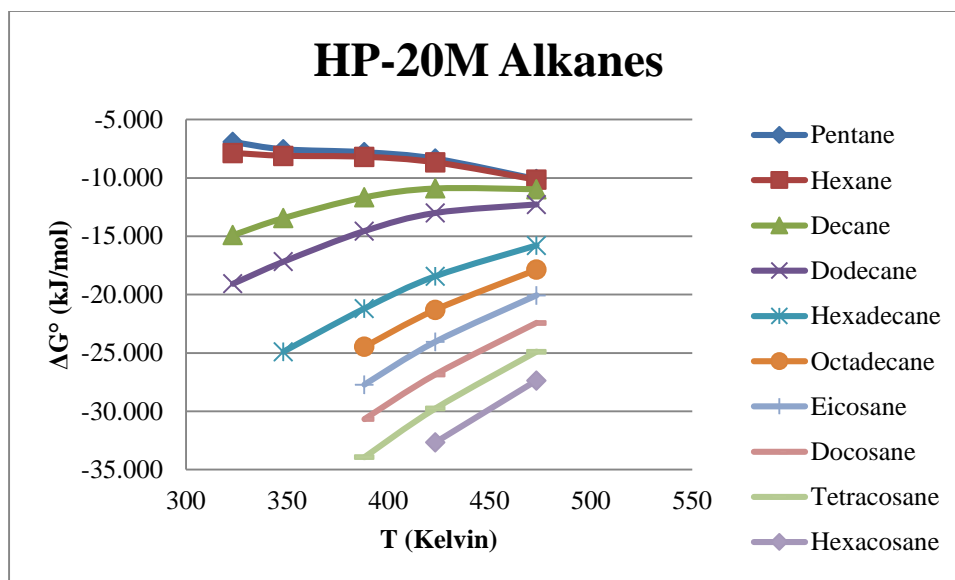
$1/T \text{ (x}10^{-3}\text{)}$	ln K									
	Pentane	Hexane	Decane	Dodecane	Hexadecane	Octadecane	Eicosane	Docosane	Tetracosane	Hexacosane
3.095	-3.011	-2.655	-0.041	1.511						
2.872	-2.982	-2.783	-0.943	0.348	3.016					
2.576	-3.172	-3.045	-1.973	-1.076	0.984	1.996	3.005	3.919	4.927	
2.363	-3.212	-3.120	-2.488	-1.888	-0.346	0.468	1.253	2.046	2.873	3.702
2.113	-3.018	-3.004	-2.798	-2.464	-1.572	-1.045	-0.483	0.115	0.742	1.372

Figure 38: van't Hoff plot of a homologous series of alkanes on the HP-20M column. The corresponding table shows the ln k values at various temperatures for a homologous series of alkanes on the HP-20M column.



T (Kelvin)	ΔG° (kJ/mol)									
	Pentane	Hexane	Decane	Dodecane	Hexadecane	Octadecane	Eicosane	Docosane	Tetracosane	Hexacosane
323.15										
348.15	-8.176	-8.707	-13.557	-16.904	-23.902					
388.15	-8.430	-8.790	-11.685	-14.115	-19.799	-22.739	-25.652			
423.15	-8.339	-8.619	-10.563	-12.273	-16.792	-19.242	-21.726	-24.347	-24.829	
473.15	-8.869	-9.035	-10.177	-11.125	-13.942	-15.633	-17.359	-19.260	-21.247	-23.283
523.15	-9.408	-9.551	-10.296	-10.957	-12.718	-13.825	-14.685	-15.823	-17.236	-18.774
R^2	1.000	0.996	0.989	0.994	0.997	0.991	0.995	0.988	0.999	1.000

Figure 39: A plot of ΔG° vs T for a homologous series of alkanes on the SLB-IL60 column. The corresponding table shows the ΔG° values at various temperatures for a homologous series of alkanes on the SLB-IL60 column.



ΔG° (kJ/mol)										
T (Kelvin)	Pentane	Hexane	Decane	Dodecane	Hexadecane	Octadecane	Eicosane	Docosane	Tetracosane	Hexacosane
323.15	-6.919	-7.874	-14.90	-19.07						
348.15	-7.538	-8.113	-13.44	-17.17	-24.90					
388.15	-7.789	-8.202	-11.66	-14.55	-21.20	-24.47	-27.72	-30.67	-33.93	
423.15	-8.350	-8.675	-10.90	-13.01	-18.44	-21.30	-24.06	-26.85	-29.76	-32.68
473.15	-10.102	-10.155	-10.97	-12.28	-15.79	-17.86	-20.07	-22.43	-24.89	-27.370
523.15										
R ²	0.965	0.965	0.994	0.998	0.998	0.994	0.994	0.996	0.997	1.000

Figure 40: A plot of ΔG° vs T for a homologous series of alkanes on the HP-20M column. The corresponding table shows the ΔG° values at various temperatures for a homologous series of alkanes on the HP-20M column.

The thermodynamic values ΔS° and ΔH° for both column phases are even more telling about the alkane interactions. Looking at the graphs in Figure 41, a plot of the entropy and enthalpy values vs the number of carbon atoms reveals some very interesting data. The positive ΔS° values and nearly positive ΔH° values for heptane and hexane confirm that retention is solely due to column flow, not solute-solvent interactions. The entropy values don't seem to follow any consistent trend on both column phases and neither phase is consistently more negative than the other. The enthalpy values for the HP-20M column seem to follow that consistent downward linear trend seen previously in the other homologous series, but the SLB-IL60 values seem to be less consistent after docosane (C20). Data seems to follow a more consistent trend at C16 and higher, as indicated by the linearity of the ΔG° vs number of carbon atom graphs shown in Figure 42. Values converge for lower molecular weight alkanes around C10 on both column phases.

It is important to remember that alkanes are used for Kovats retention index value calculations, I , and ultimately McReynolds constants, ΔI , which are used to assess intermolecular interactions in comparison to a non-polar stationary phase, squalane. These values are used to measure and describe a column phase's polarity. The inconsistency and lack of trending data alludes to the fact that alkane retention on these column phases is anything but indicative of column phase polarity. Not being able to successfully measure retention thermodynamics below hexadecane makes it very difficult to calculate accurate I values for any analyte eluting between alkanes C1 through C15, particularly on the SLB-IL60 column; again, failing to provide an accurate means to measure column polarity.

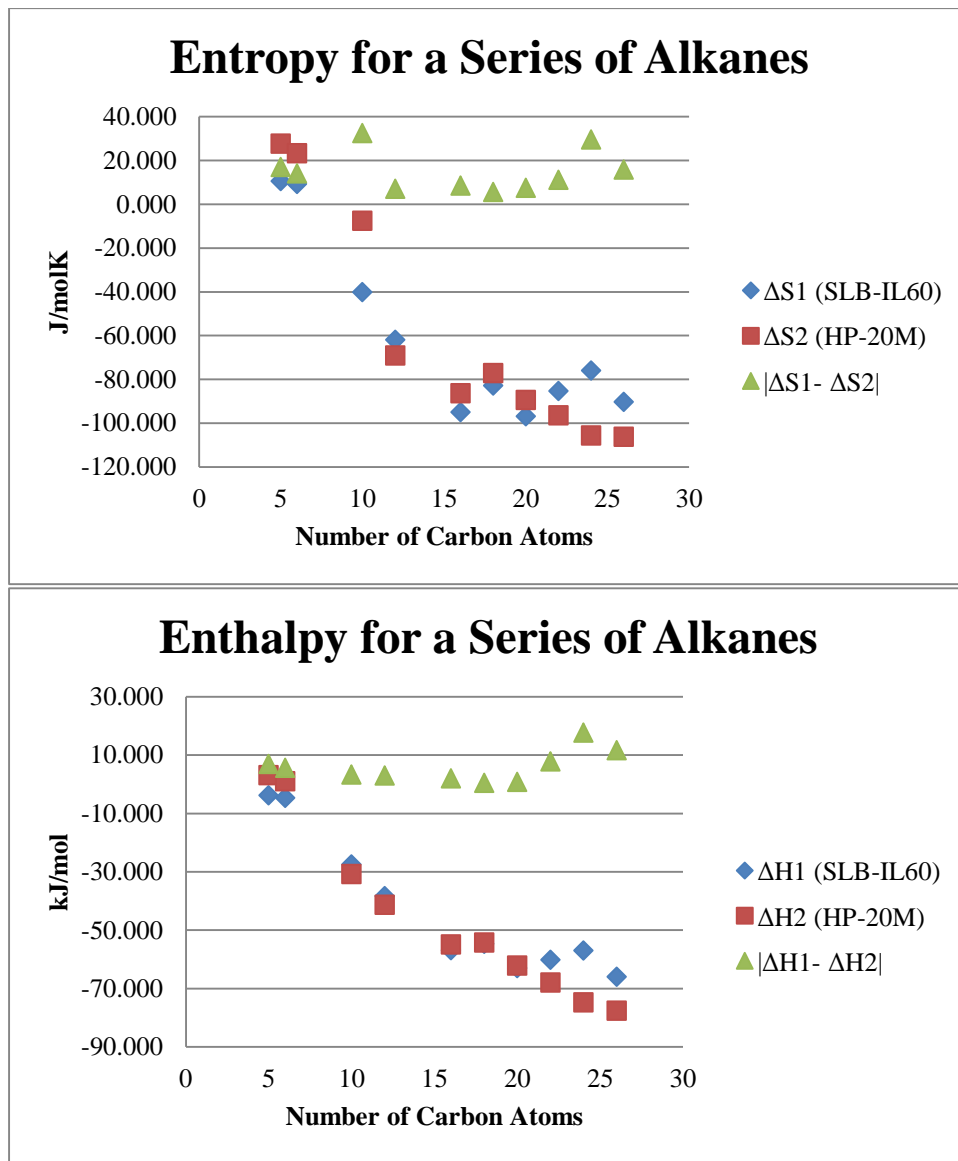


Figure 41: A plot of the ΔS° and ΔH° values and their absolute differential values on the SLB-IL60 and HP-20M columns for a homologous series of alkanes.

	Pentane	Hexane	Decane	Dodecane	Hexadecane	Octadecane	Eicosane	Docosane	Tetracosane	Hexacosane
ΔS°_1 (J/molK)	10.687	9.322	-40.085	-61.932	-94.980	-82.824	-96.866	-85.232	-75.934	-90.176
ΔS°_2 (J/molK)	27.742	23.436	-7.480	-69.082	-86.324	-77.095	-89.305	-96.439	-105.642	-106.119
$ \Delta S^{\circ}_1 - \Delta S^{\circ}_2 $ (J/molK)	17.055	14.114	32.605	7.149	8.656	5.728	7.561	11.206	29.708	15.943
ΔH°_1 (kJ/mol)	-3.815	-4.658	-27.427	-38.366	-56.873	-54.666	-63.052	-60.138	-57.032	-65.950
ΔH°_2 (kJ/mol)	3.131	1.023	-30.750	-41.329	-54.875	-54.218	-62.189	-67.940	-74.758	-77.581
$ \Delta H^{\circ}_1 - \Delta H^{\circ}_2 $ (kJ/mol)	6.946	5.681	3.322	2.962	1.998	0.447	0.864	7.803	17.725	11.631

Table 11: ΔH° and ΔS° values for a homologous series of alkanes on the SLB-IL60 and HP-20M columns; ΔH°_1 and ΔS°_1 refer to SLB-IL60, ΔH°_2 and ΔS°_2 refer to HP-20M. The absolute differential values between the entropy and enthalpy on both column phases for each analyte were calculated.

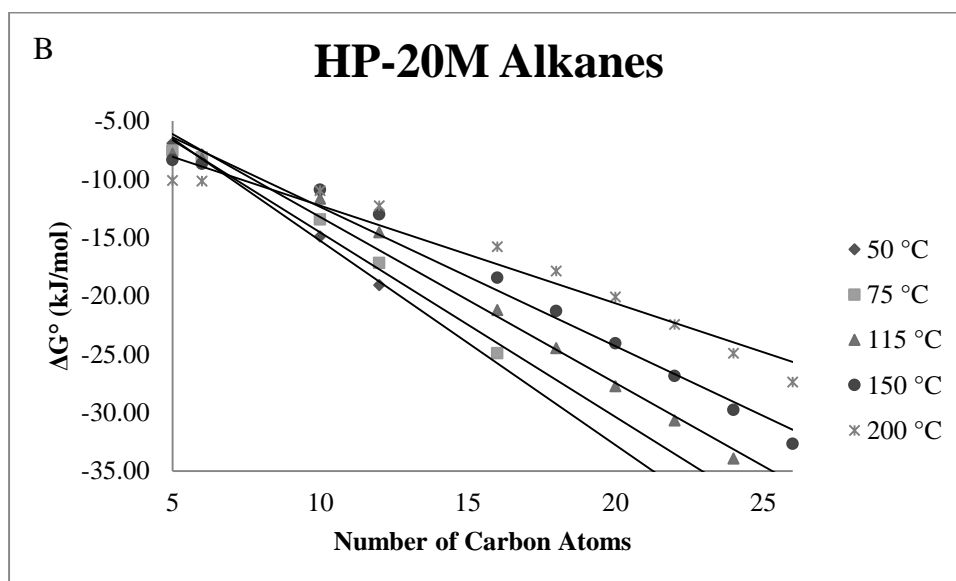
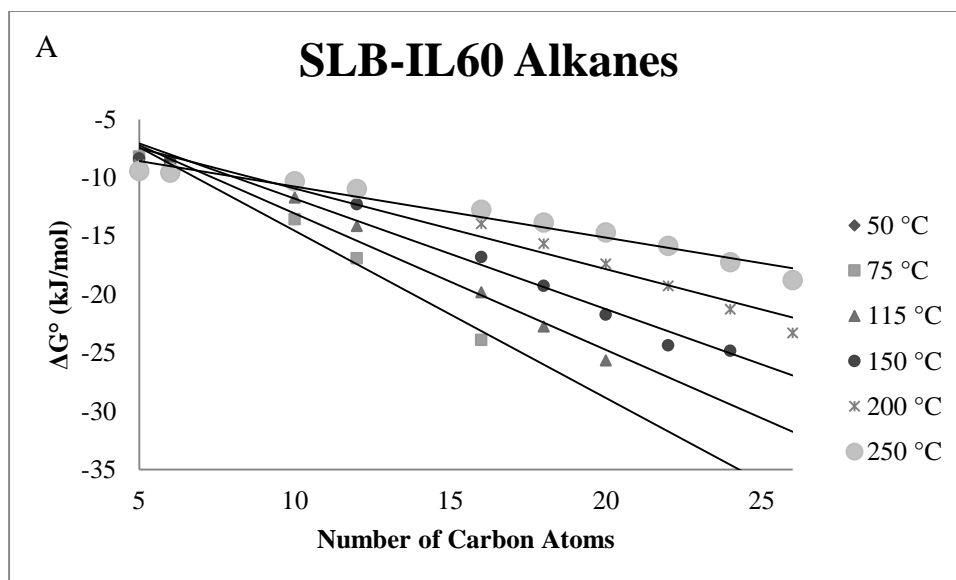


Figure 42: A plot of ΔG° vs the number of carbon atoms for a homologous series of alkanes at various temperatures on the (A) SLB-IL60 column and (B) HP-20M column.

3.8 Polyol-Induced Extraction

Flavor and fragrance materials can be extracted using a multitude of techniques depending on the matrix, the sample size, and the application. Typical extraction techniques include steam distillation, solid-phase microextraction (SPME), solid phase extraction (SPE), stir bar sorptive extraction, QuEChERS (Quick, Easy, Cheap, Effective, Rugged, Safe), and liquid/liquid extraction. Liquid/liquid extraction is generally the most common and typically employs the use of toxic solvents, such as pentane/ether or dichloromethane (DCM). DCM is effective at extracting both polar and non-polar analytes and generally gives a profile characteristic of the original product.

Extraction of alcoholic beverages tends to be very challenging. While they are mostly aqueous and range from 5-15% ABV (alcohol by volume), the flavor components are generally low in concentration and tend to co-elute with the alcohol peaks, making it difficult to get a complete picture of the flavor profile. Since the extraction of water from acetonitrile using sorbitol was previously shown to be effective³¹ and the extraction of flavor molecules using water, acetonitrile, and polyols was also shown to be successful³², it was chosen to study the extraction of an alcoholic beverage using the polyol-induced extraction method.

Mead, which is crafted from the fermentation of honey and water, was chosen as the drink of alcoholic beverage of choice for this extraction technique. There is little in the scientific literature about mead, making it an interesting and unique sample of choice.

3.8.1 Organoleptics

Two flavor experts were asked to blindly evaluate the extracts by blotter. The dichloromethane extract was described as having a strong honey note with sweet, floral, fermented, and light beer

characters. The acetonitrile extract was described as being more complex with a more upfront fermented note. Odor descriptors included honey, yeast, chocolate, beer, syrup, brown, dried fruit (cherry, prune), sour, and acidic. The extracts were compared to the neat mead on blotters. In this case, the DCM extract was said to be more comparable.

3.8.2 GC-FID Analysis

The extracts were analyzed on both the SLB-IL60 and HP-20M columns. The intent was to analyze the extracts using mass spectrometry to identify the major components in each extract. However, analysis on the SLB-IL60 column failed to produce any chromatographic profile for either of the extracts. In fact, the ramp rate was increased to 10 °C/min to determine if temperature was playing a role in analyte retention but produced chromatograms similar to those seen in Figure 43. The HP-20M produced chromatograms with an acceptable chromatographic profile, as shown in Figure 44. The extracts produced fairly different peak profiles, and even though the acetonitrile extract was not as concentrated as the dichloromethane extract it still had significantly large peaks. The acetonitrile extract also had more back end peaks, suggesting more matrix interferences were extracted.

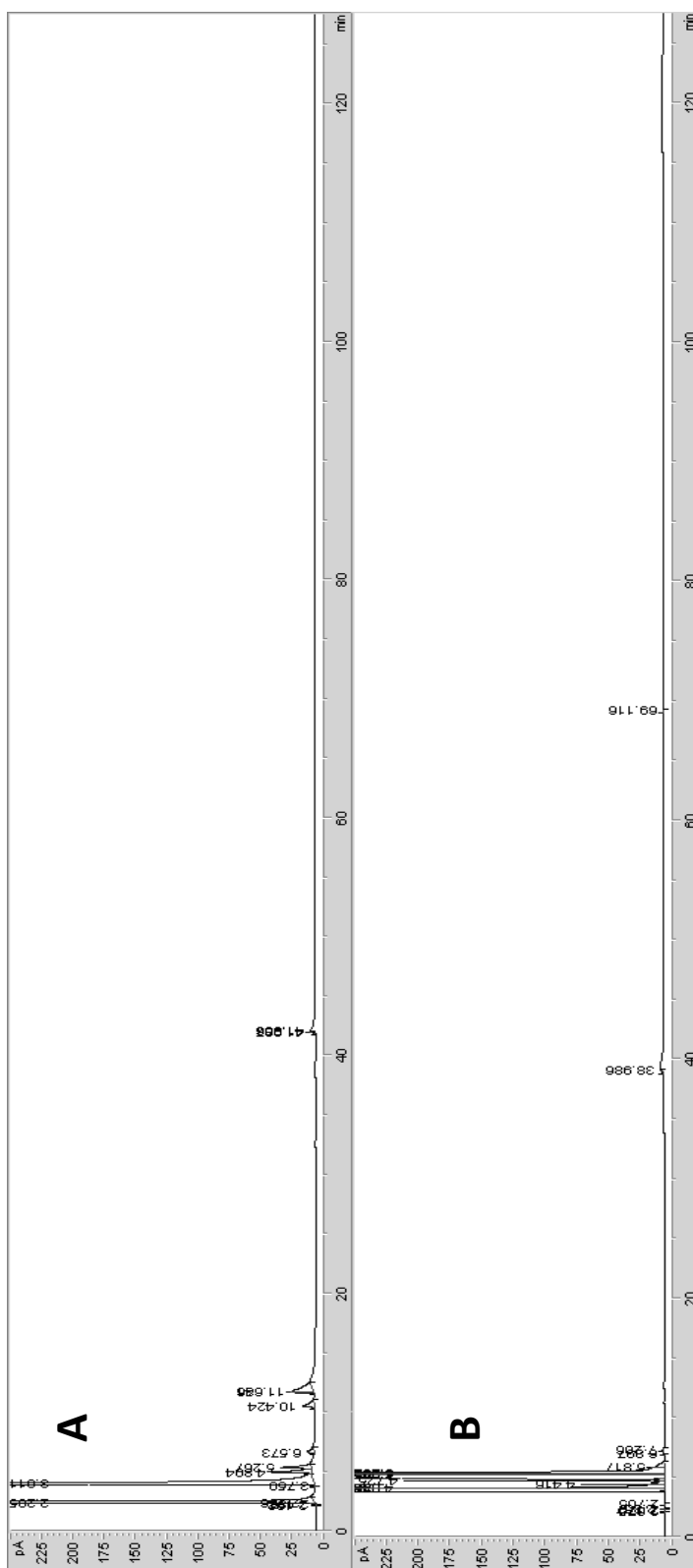


Figure 43: Chromatograms of the mead extracts on the SLB-IL60 column. Chromatogram A is the dichloromethane extract and chromatogram B is the acetonitrile extract.

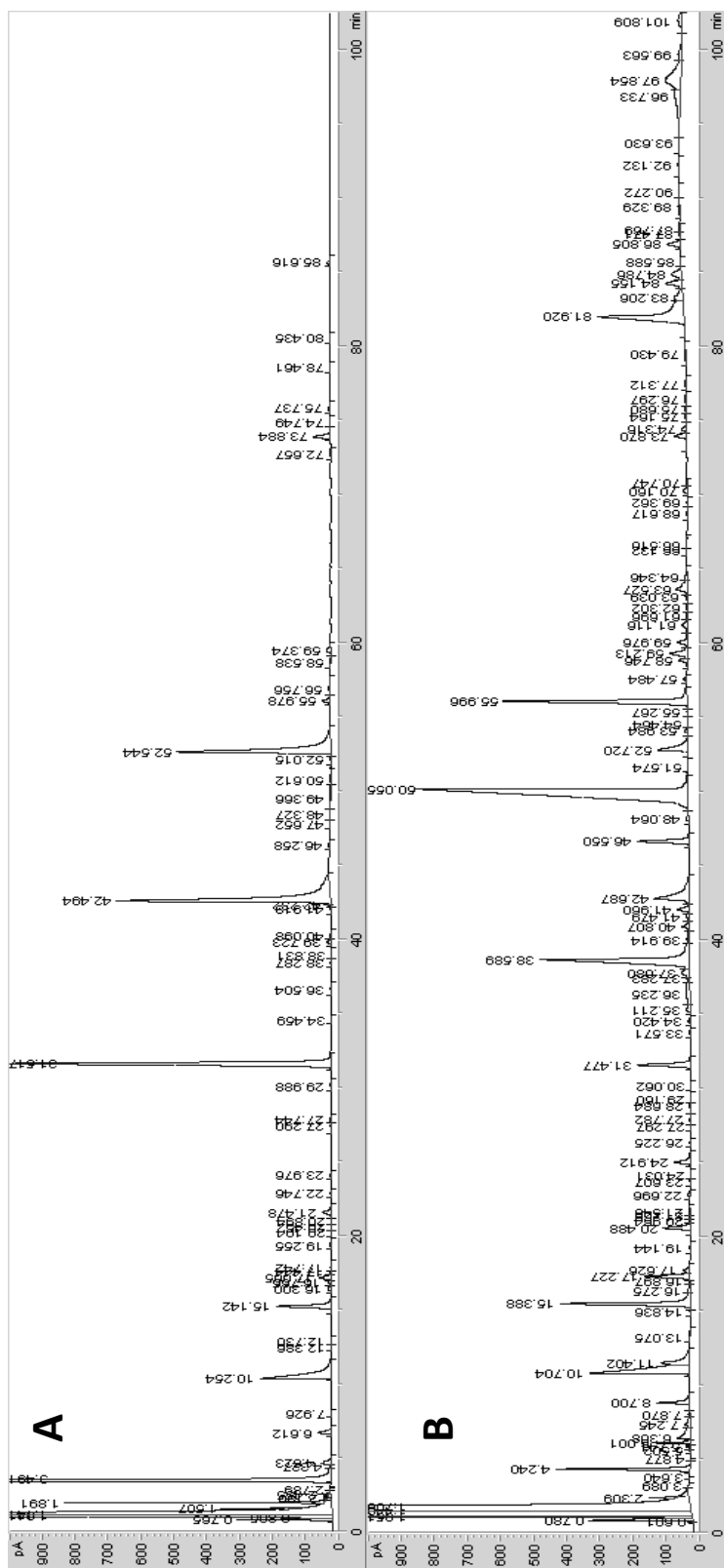


Figure 44: Chromatograms of the mead extracts on the HP-20M column. Chromatogram A is the dichloromethane extract and chromatogram B is the acetonitrile extract.

4 Conclusions and Future Work

In total, 61 flavor/fragrance ingredients were evaluated on the SLB-IL60 and HP-20M columns. An in-depth analysis of the thermodynamic retention properties allowed for a comparative study of homologous series on two column phases with supposedly similar polarity. While many of the retention factor, k , values were less than 1 which is generally not ideal for GC analysis (due to column flow being the main variable affecting retention rather than partitioning), the data consistently followed expected trends suggesting the method was still acceptable for analysis. Due to the vast number of analytes being analyzed (in triplicate, at five different temperatures) it essentially became impractical to have long GC method times. However, future analyses should focus on obtaining k values greater than one to eliminate the potential impact of column flow versus retention mechanisms.

It was found that alcohols behaved similarly on both column phases, following similar trends for enthalpy and entropy values across the homologous series. Aldehydes were found to be retained differently; the HP-20M thermodynamic data followed a consistent downward trend, while the SLB-IL-60 did not seem to follow the same trend. Acids were difficult to analyze on the SLB-IL60 and peak shapes are potentially more telling than the thermodynamics. More work should be done to assess the symmetry/asymmetry, peak heights, and area counts to determine what is driving retention and affecting peak shape. The homologous series of ethyl esters appeared to produce the most comparable thermodynamic results on both column phases. This is perhaps a more appropriate series to determine Kovats values (and has previously been shown to be useful¹⁸), McReynolds constants, and ultimately polarity values, but the series should also be studied on a methyl siloxane stationary phase for a more complete picture. The series of alkanes produced the most interesting and least consistent thermodynamic results. Therefore, it would be

appropriate to study the thermodynamic retention mechanism of alkanes on methyl siloxane phases to get a full understanding of thermodynamic retention mechanisms and retention indices. That being said, it is evident through this data that alkanes are not an acceptable series to calculate these values and ultimately describe column phase polarity.

Future work studying thermodynamic retention parameters of the SLB-IL60 column phase should include analysis of additional homologous series such as ketones, terpenoids, hydrocarbons, and branched alcohols/aldehydes/acids/alkanes. Since a majority of this work included oxygenated species, selectivity of sulfur and nitrogen containing molecules should also be evaluated, especially because these molecules are instrumental in flavor and fragrance formulations.

Polyol-induced extraction of mead using acetonitrile and sorbitol was successful and produced a more complex extract than the dichloromethane extract. This method has strong potential in the application of flavor and fragrance ingredients, and is particularly interesting due to its “green chemistry” properties. However, due to the high boiling point (82 °C) of acetonitrile, it is likely not ideal for extraction of large volumes that need further concentration, particularly for novel molecule discovery. Unfortunately, The SLB-IL60 was not an appropriate column phase for the analysis of either of the mead extracts, and an in-depth analysis via GC/MS of the analytes extracted should be done to determine if there are any trends that indicate why this column phase failed to produce decent chromatograms.

In conclusion, a wide range of flavor and fragrance ingredients were analyzed to study the thermodynamic retention mechanisms of an IL stationary phase and a PEG stationary phase. The thermodynamics of homologous series suggested that the calculated values used to describe

polarity are insufficient. Therefore, it is incorrect to describe the polarity of these columns as similar.

5 References

1. Sigma-Aldrich. Supelco Ionic Liquid GC Columns: Introduction to the Technology. http://www.sigmaaldrich.com/content/dam/sigma-aldrich/docs/Supelco/Posters/1/ionic_liquid_gc_columns.pdf (accessed February 28, 2014).
2. Ho, T.D.; Zhang, C.; Hantao, L.W., Anderson, J.L. Ionic liquids in analytical chemistry: Fundamentals, advances, and perspectives. *Anal. Chem.* **2014**, *86*, 262-285.
3. Armstrong, D.W.; Payagala T.; Sidisky, L.M. The advent and potential impact of ionic liquid stationary phases in GC and GCxGC. *LC GC Europe.* **2009**, *22*, 459-460, 462, 464, 466-467.
4. Yao, C.; Anderson, J.L. Retention characteristics of organic compounds on molten salt and ionic liquid-based gas chromatography stationary phases. *J. Chromatogr. A.* **2009**, *1216*, 1658-1712.
5. Poole, C.F.; Poole, S.K. Ionic liquid stationary phases for gas chromatography. *J. Sep. Sci.* **2011**, *34*, 888-900.
6. Poole, C.F.; Lenca, N. Gas chromatography on wall-coated open tubular columns with ionic liquid stationary phases. *J. Chromatogr. A.* **2014**, *1357*, 87-109.
7. Armstrong, D.W.; He, L.; Liu, Y.S. Examination of ionic liquids and their interactions with molecules, when used as stationary phases in gas chromatography. *Anal. Chem.* **1999**, *71*, 3873-3876.
8. Cagliero, C.; Bicchi, C.; Cordero, C.; Liberto, E.; Sgorbini, B.; Rubiolo, P. Room temperature ionic liquids: New GC stationary phases with a novel selectivity for flavor and fragrance analyses. *J. Chromatogr. A.* **2012**, *1268*, 130-138.

9. Ragonese, C.; Sciarrone, D.; Tranchida, P. Q.; Dugo, P.; Dugo, G.; Mondello, L. Evaluation of a medium-polarity ionic liquid stationary phase in the analysis of flavor and fragrance compounds. *Anal. Chem.* **2011**, *83*, 7947-7954.
10. Poole, C.F.; Poole, S.K. Characterization of solvent properties of gas chromatographic liquid phases. *Chem. Rev.* **1989**, *89*, 377-395.
11. Abraham, M.H.; Poole, C.F.; Poole, S.K. Classification of stationary phases and other materials by gas chromatography. *J. Chromatogr. A.* **1999**, *842*, 79-114.
12. Grob, R.L.; Barry, E.F. *Modern Practice of Gas Chromatography*. 4th Ed. John Wiley and Sons, Inc.: New Jersey, 2004.
13. Anderson, J.L.; Ding, J.; Welton, T.; Armstrong, D.W. Characterizing ionic liquids on the basis of multiple solvation interactions. *J. Am. Chem. Soc.* **2002**, *124*, 14247-14254.
14. Anderson, J.L. Ionic liquids as stationary phases in gas chromatography. in *Ionic Liquids in Chemical Analysis*; Koala, M., Ed.; Taylor and Francis Publishing Group: 2009.
15. Anderson, J.L.; Armstrong, D.W. High-stability ionic liquids. A new class of stationary phases for gas chromatography. *Anal. Chem.* **2003**, *75*, 4851-4858.
16. Poole, S.K.; Kersten, B.R.; Poole, C.F. Comparison of solvent models for characterizing stationary phase selectivity in gas chromatography. *J. Chromatogr.* **1989**, *471*, 91-103.
17. McNair, H.M.; Miller, J.M. *Basic Gas Chromatography*. 2nd Ed. John Wiley and Sons, Inc.: New Jersey, 2009.
18. Van Den Dool, H.; Kratz, P.D. A generalization of the retention index system including linear temperature programmed gas-liquid partition chromatography. *J. Chromatogr.* **1963**, *11*, 463-471.

19. McReynolds, W.O. Characterization of some liquid phases. *J. Chromatog. Sci.* **1970**, *8*, 685-691.
20. Poole, C.F.; Poole, S.K.; Pomaville, R.M.; Kersten, B.R. Importance of the retention index standards in determining the magnitude of McReynolds phase constants. *J. High Resolut. Chromatogr. Chromatogr. Commun.* **1987**, *10*, 670-671.
21. Morales, R.; Blanco, C.; Furton, K.G. The gas-liquid chromatographic stationary phase properties of liquid organic salts: anomalous selectivity variation when employing the Rohrschneider/McReynolds System. *Talanta.* **1993**, *40*, 1541-1549.
22. Kersten, B.R.; Poole, C.F.; Furton, K.G. Ambiguities in the determination of McReynolds stationary phase constants. *J. Chromatog.* **1987**, *411*, 43-59.
23. Conder, J.R. *Physicochemical Measurements: Gas Chromatography*. Associated Press.: 2000.
24. Poole, C.F.; Poole, S.K. Column selectivity from the perspective of the solvation parameter model. *J. Chromatogr. A.* **2002**, *965*, 263-299.
25. Anderson, J.L.; Armstrong, D.W. Immobilized ionic liquids as high-selectivity/high-temperature/high-stability gas chromatography stationary phases. *Anal. Chem.* **2005**, *77*, 6453-6462.
26. Rodriguez-Sanchez, S.; Galindo-Iranzo, P., Soria, A.C.; Sanz, M.L.; Quintanilla-Lopez, J.E.; Lebron-Aguilar, R. Characterization by the solvation parameter model of the retention properties of commercial ionic liquid columns for gas chromatography. *J.Chromatogr A.* **2014**, *1326*, 96-102.
27. Sprunger, L.M.; Gibbs, J.; Baltazar, Q.Q.; Acree Jr., W.E., Abraham, M.H.; Anderson, J.L. Charaterisation of room temperature ionic liquid chromatographic stationary phases

by combining experimental retention factor and partition coefficient data into a single model. *Phys. Chem. Liq.* **2009**, *47*, 74-83.

28. Kazakevich, Y.; LoBrutto, R. *HPLC for Pharmaceutical Students*; John Wiley & Sons: Hoboken, N.J., 2007.
29. Dose, E.V. Simulation of gas chromatographic retention and peak width using thermodynamic retention indexes. *Anal. Chem.* **1987**, *59*, 2414-2419.
30. Snow, N.H. Determination of free-energy relationships using gas chromatography. *J. Chem. Ed.* **1996**, *73*, 592-597.
31. Sowa Jr, J.R.; Murphy, W.R.; Deshpande, M. Polyol-induced extraction of water from organic liquids. U.S. Patent US 20140263050 A1, Sep 18, 2014.
32. DelMastro, T.; Sowa Jr, J.R.; Murphy, W.R.; Snow, N.H. Polyol-induced partitioning of essential oils in water/acetonitrile solvent mixtures. Submitted to *Chem. Cent. J.*. 2016.

6 Appendix

6.1 Raw Data from Polarity Study

6.1.1 SLB-IL60 data

Table 12: SLB-IL60 data from increasing polarity study.

SLB-IL60					
<u>ALDEHYDES</u>					
TRANS-2-HEXENAL					
T (°C)	T (Kelvin)	methane(t ₀)	RT ₁	k	ln k
50	323.15	2.133	3.122	0.463	-0.769
75	348.15	2.020	2.411	0.193	-1.643
150	423.15	1.741	1.822	0.046	-3.072
200	473.15	1.621	-	-	-
250	523.15	1.523	-	-	-
HEXANAL					
T (°C)	T (Kelvin)	methane(t ₀)	RT ₁	k	ln k
50	323.15	2.133	9.975	3.676	1.302
75	348.15	2.020	4.573	1.263	0.234
150	423.15	1.741	1.996	0.146	-1.922
200	473.15	1.621	-	-	-
250	523.15	1.523	-	-	-
CIS-3-HEXENAL					
T (°C)	T (Kelvin)	methane(t ₀)	RT ₁	k	ln k
50	323.15	2.133	10.996	4.154	1.424
75	348.15	2.020	4.861	1.406	0.341
150	423.15	1.741	2.007	0.153	-1.880
200	473.15	1.621	-	-	-
250	523.15	1.523	-	-	-

KETONES**3-HEXANONE**

T (°C)	T (Kelvin)	methane(to)	RT ₁	k	ln k
50	323.15	2.133	10.882	4.101	1.411
75	348.15	2.020	4.856	1.404	0.339
150	423.15	1.741	2.008	0.153	-1.876
200	473.15	1.621	-	-	-
250	523.15	1.523	-	-	-

3,4-HEXANEDIONE

T (°C)	T (Kelvin)	methane(to)	RT ₁	k	ln k
50	323.15	2.133	12.047	4.647	1.536
75	348.15	2.020	5.026	1.488	0.397
150	423.15	1.741	1.993	0.145	-1.934
200	473.15	1.621	-	-	-
250	523.15	1.523	-	-	-

ESTERS**ETHYL HEXANOATE**

T (°C)	T (Kelvin)	methane(to)	RT ₁	k	ln k
50	323.15	2.133	25.914	11.147	2.411
75	348.15	2.020	8.302	3.109	1.134
150	423.15	1.741	2.123	0.219	-1.518
200	473.15	1.621	-	-	-
250	523.15	1.523	-	-	-

HEXYL ACETATE

T (°C)	T (Kelvin)	methane(to)	RT ₁	k	ln k
50	323.15	2.133	30.101	13.110	2.573
75	348.15	2.020	9.358	3.632	1.290
150	423.15	1.741	2.18	0.252	-1.379
200	473.15	1.621	-	-	-
250	523.15	1.523	-	-	-

ALLYL HEXANOATE					
T (°C)	T (Kelvin)	methane(t ₀)	RT ₁	k	ln k
50	323.15	2.133	52.254	23.494	3.157
75	348.15	2.020	13.933	5.896	1.774
150	423.15	1.741	2.314	0.329	-1.112
200	473.15	1.621	1.793	0.106	-2.243
250	523.15	1.523	-	-	-
HEXYL BUTYRATE					
T (°C)	T (Kelvin)	methane(t ₀)	RT ₁	k	ln k
50	323.15	2.133	97.649	44.773	3.802
75	348.15	2.020	22.949	10.359	2.338
150	423.15	1.741	2.568	0.475	-0.745
200	473.15	1.621	-	-	-
250	523.15	1.523	-	-	-
HEXYL ISOVALERATE					
T (°C)	T (Kelvin)	methane(t ₀)	RT ₁	k	ln k
50	323.15	2.133	132.257	60.995	4.111
75	348.15	2.020	29.101	13.404	2.596
150	423.15	1.741	2.699	0.550	-0.598
200	473.15	1.621	-	-	-
250	523.15	1.523	-	-	-
CIS-3-HEXENYL ISOVALERATE					
T (°C)	T (Kelvin)	methane(t ₀)	RT ₁	k	ln k
50	323.15	2.133	135.18	62.366	4.133
75	348.15	2.020	30.127	13.912	2.633
150	423.15	1.741	2.755	0.582	-0.541
200	473.15	1.621	-	-	-
250	523.15	1.523	-	-	-
HEXYL HEXANOATE					
T (°C)	T (Kelvin)	methane(t ₀)	RT ₁	k	ln k
50	323.15	2.133	-	-	-
75	348.15	2.020	72.082	34.678	3.546
150	423.15	1.741	3.525	1.024	0.024
200	473.15	1.621	1.997	0.232	-1.461
250	523.15	1.523	-	-	-

HEXENYL CIS-3-HEXANOATE					
T (°C)	T (Kelvin)	methane(t ₀)	RT ₁	k	ln k
50	323.15	2.133	-	-	-
75	348.15	2.020	89.795	43.446	3.772
150	423.15	1.741	3.941	1.263	0.234
200	473.15	1.621	2.074	0.279	-1.275
250	523.15	1.523	-	-	-
CIS-3-HEXENYL LACTATE					
T (°C)	T (Kelvin)	methane(t ₀)	RT ₁	k	ln k
50	323.15	2.133	-	-	-
75	348.15	2.020	-	-	-
150	423.15	1.741	4.263	1.448	0.370
200	473.15	1.621	2.165	0.336	-1.092
250	523.15	1.523	1.706	0.120	-2.117
CIS-3-HEXENYL BENZOATE					
T (°C)	T (Kelvin)	methane(t ₀)	RT ₁	k	ln k
50	323.15	2.133	-	-	-
75	348.15	2.020	-	-	-
150	423.15	1.741	12.840	6.374	1.852
200	473.15	1.621	3.428	1.115	0.109
250	523.15	1.523	1.992	0.308	-1.177
<u>LACTONES</u>					
GAMMA-HEXALACTONE					
T (°C)	T (Kelvin)	methane(t ₀)	RT ₁	k	ln k
50	323.15	2.133	-	-	-
75	348.15	2.020	-	-	-
150	423.15	1.741	8.177	3.696	1.307
200	473.15	1.621	3.130	0.931	-0.072
250	523.15	1.523	2.029	0.333	-1.101

DELTA-HEXALACTONE					
T (°C)	T (Kelvin)	methane(to)	RT ₁	k	ln k
50	323.15	2.133	-	-	-
75	348.15	2.020	-	-	-
150	423.15	1.741	12.315	6.072	1.804
200	473.15	1.621	3.924	1.421	0.351
250	523.15	1.523	2.249	0.477	-0.740
<u>ALCOHOLS</u>					
CIS-3-HEXENOL					
T (°C)	T (Kelvin)	methane(to)	RT ₁	k	ln k
50	323.15	2.133	23.622	10.073	2.310
75	348.15	2.020	7.992	2.956	1.084
150	423.15	1.741	2.148	0.234	-1.454
200	473.15	1.621	-	-	-
250	523.15	1.523	-	-	-
CIS-4-HEXENOL					
T (°C)	T (Kelvin)	methane(to)	RT ₁	k	ln k
50	323.15	2.133	30.615	13.351	2.592
75	348.15	2.020	9.622	3.763	1.325
150	423.15	1.741	2.211	0.270	-1.310
200	473.15	1.621	-	-	-
250	523.15	1.523	-	-	-
HEXANOL					
T (°C)	T (Kelvin)	methane(to)	RT ₁	k	ln k
50	323.15	2.133	24.215	10.351	2.337
75	348.15	2.020	7.933	2.927	1.074
150	423.15	1.741	2.115	0.215	-1.539
200	473.15	1.621	-	-	-
250	523.15	1.523	-	-	-

TRANS-2-HEXENOL					
T (°C)	T (Kelvin)	methane(t ₀)	RT ₁	k	ln k
50	323.15	2.133	26.991	11.652	2.455
75	348.15	2.020	8.786	3.349	1.209
150	423.15	1.741	2.182	0.253	-1.374
200	473.15	1.621	1.764	0.088	-2.428
250	523.15	1.523	-	-	-
<u>THIOPHENES</u>					
2-HEXYLTHIOPHENE					
T (°C)	T (Kelvin)	methane(t ₀)	RT ₁	k	ln k
50	323.15	2.133	111.8	51.406	3.940
75	348.15	2.020	27.014	12.371	2.515
150	423.15	1.741	2.783	0.598	-0.514
200	473.15	1.621	1.897	0.170	-1.770
250	523.15	1.523	1.631	0.071	-2.643

Table 13: HP-20M data from increasing polarity study.

HP-20M					
<u>ALDEHYDES</u>					
TRANS-2-HEXENAL					
T (°C)	T (Kelvin)	methane(t ₀)	RT ₁	k	ln k
50	323.15	0.542	1.388	1.559	0.444
75	348.15	0.529	0.859	0.623	-0.474
150	423.15	0.506	0.588	0.161	-1.825
200	473.15	0.494	-	-	-
250	523.15	-	-	-	-
HEXANAL					
T (°C)	T (Kelvin)	methane(t ₀)	RT ₁	k	ln k
50	323.15	0.542	1.79	2.301	0.833
75	348.15	0.529	0.988	0.866	-0.143
150	423.15	0.506	0.581	0.147	-1.914
200	473.15	0.494	-	-	-
250	523.15	-	-	-	-
CIS-3-HEXENAL					
T (°C)	T (Kelvin)	methane(t ₀)	RT ₁	k	ln k
50	323.15	0.542	0.833	0.536	-0.624
75	348.15	0.529	0.661	0.249	-1.391
150	423.15	0.506	0.59	0.165	-1.800
200	473.15	0.494	-	-	-
250	523.15	-	-	-	-
<u>KETONES</u>					
3-HEXANONE					
T (°C)	T (Kelvin)	methane(t ₀)	RT ₁	k	ln k
50	323.15	0.542	1.789	2.299	0.832
75	348.15	0.529	0.963	0.819	-0.199
150	423.15	0.506	0.58	0.145	-1.928
200	473.15	0.494	-	-	-
250	523.15	-	-	-	-

3,4-HEXANEDIONE					
T (°C)	T (Kelvin)	methane(to)	RT ₁	k	ln k
50	323.15	0.542	1.222	1.253	0.226
75	348.15	0.529	0.805	0.521	-0.652
150	423.15	0.506	0.563	0.112	-2.190
200	473.15	0.494	-	-	-
250	523.15	-	-	-	-
<u>ESTERS</u>					
ETHYL HEXANOATE					
T (°C)	T (Kelvin)	methane(to)	RT ₁	k	ln k
50	323.15	0.542	3.166	4.838	1.576
75	348.15	0.529	1.36	1.569	0.451
150	423.15	0.506	0.598	0.181	-1.709
200	473.15	0.494	0.541	0.095	-2.352
250	523.15	-	-	-	-
HEXYL ACETATE					
T (°C)	T (Kelvin)	methane(to)	RT ₁	k	ln k
50	323.15	0.542	4.02	6.412	1.858
75	348.15	0.529	1.584	1.992	0.689
150	423.15	0.506	0.609	0.203	-1.596
200	473.15	0.494	0.544	0.101	-2.291
250	523.15	-	-	-	-
ALLYL HEXANOATE					
T (°C)	T (Kelvin)	methane(to)	RT ₁	k	ln k
50	323.15	0.542	7.677	13.156	2.577
75	348.15	0.529	2.479	3.683	1.304
150	423.15	0.506	0.651	0.286	-1.253
200	473.15	0.494	0.554	0.121	-2.108
250	523.15	-	-	-	-

HEXYL BUTYRATE					
T (°C)	T (Kelvin)	methane(t ₀)	RT ₁	k	ln k
50	323.15	0.542	10.617	18.577	2.922
75	348.15	0.529	3.177	5.002	1.610
150	423.15	0.506	0.681	0.345	-1.064
200	473.15	0.494	0.562	0.138	-1.983
250	523.15	-	-	-	-
HEXYL ISOVALERATE					
T (°C)	T (Kelvin)	methane(t ₀)	RT ₁	k	ln k
50	323.15	0.542	13.406	23.719	3.166
75	348.15	0.529	3.738	6.062	1.802
150	423.15	0.506	0.791	0.562	-0.576
200	473.15	0.494	0.566	0.146	-1.926
250	523.15	-	-	-	-
CIS-3-HEXENYL ISOVALERATE					
T (°C)	T (Kelvin)	methane(t ₀)	RT ₁	k	ln k
50	323.15	0.542	17.971	32.136	3.470
75	348.15	0.529	4.64	7.766	2.050
150	423.15	0.506	0.736	0.454	-0.791
200	473.15	0.494	0.574	0.162	-1.821
250	523.15	-	-	-	-
HEXYL HEXANOATE					
T (°C)	T (Kelvin)	methane(t ₀)	RT ₁	k	ln k
50	323.15	0.542	43.236	78.722	4.366
75	348.15	0.529	9.565	17.070	2.837
150	423.15	0.506	0.878	0.734	-0.309
200	473.15	0.494	0.61	0.235	-1.449
250	523.15	-	-	-	-
HEXENYL CIS-3-HEXANOATE					
T (°C)	T (Kelvin)	methane(t ₀)	RT ₁	k	ln k
50	323.15	0.542	-	-	-
75	348.15	0.529	17.547	32.149	3.470
150	423.15	0.506	1.076	1.125	0.118
200	473.15	0.494	0.639	0.294	-1.226
250	523.15	-	-	-	-

CIS-3-HEXENYL LACTATE					
T (°C)	T (Kelvin)	methane(t ₀)	RT ₁	k	ln k
50	323.15	0.542	-	-	-
75	348.15	0.529	23.594	43.573	3.774
150	423.15	0.506	3.252	5.423	1.691
200	473.15	0.494	0.994	1.012	0.012
250	523.15	-	-	-	-
CIS-3-HEXENYL BENZOATE					
T (°C)	T (Kelvin)	methane(t ₀)	RT ₁	k	ln k
50	323.15	0.542	-	-	-
75	348.15	0.529	-	-	-
150	423.15	0.506	1.195	1.360	0.308
200	473.15	0.494	0.661	0.338	-1.085
250	523.15	-	-	-	-
<u>LACTONES</u>					
GAMMA-HEXALACTONE					
T (°C)	T (Kelvin)	methane(t ₀)	RT ₁	k	ln k
50	323.15	0.542	-	-	-
75	348.15	0.529	12.363	22.356	3.107
150	423.15	0.506	1.088	1.149	0.139
200	473.15	0.494	0.659	0.334	-1.097
250	523.15			#DIV/0!	#DIV/0!
DELTA-HEXALACTONE					
T (°C)	T (Kelvin)	methane(t ₀)	RT ₁	k	ln k
50	323.15	0.542	-	-	-
75	348.15	0.529	18.880	34.668	3.546
150	423.15	0.506	1.323	1.613	0.478
200	473.15	0.494	0.711	0.439	-0.823
250	523.15	-	-	-	-

ALCOHOLS**CIS-3-HEXENOL**

T (°C)	T (Kelvin)	methane(to)	RT ₁	k	ln k
50	323.15	0.542	8.286	14.278	2.659
75	348.15	0.529	2.61	3.931	1.369
150	423.15	0.506	0.652	0.288	-1.246
200	473.15	0.494	0.554	0.121	-2.108
250	523.15	-	-	-	-

CIS-4-HEXENOL

T (°C)	T (Kelvin)	methane(to)	RT ₁	k	ln k
50	323.15	0.542	11.618	20.422	3.017
75	348.15	0.529	3.341	5.312	1.670
150	423.15	0.506	0.683	0.349	-1.053
200	473.15	0.494	0.567	0.148	-1.912
250	523.15	-	-	-	-

HEXANOL

T (°C)	T (Kelvin)	methane(to)	RT ₁	k	ln k
50	323.15	0.542	9.85	17.162	2.843
75	348.15	0.529	2.935	4.545	1.514
150	423.15	0.506	0.660	0.303	-1.192
200	473.15	0.494	0.556	0.126	-2.075
250	523.15	-	-	-	-

TRANS-2-HEXENOL

T (°C)	T (Kelvin)	methane(to)	RT ₁	k	ln k
50	323.15	0.542	8.286	14.278	2.659
75	348.15	0.529	2.61	3.931	1.369
150	423.15	0.506	0.652	0.288	-1.246
200	473.15	0.494	0.554	0.121	-2.108
250	523.15	-	-	-	-

<u>THIOPHENES</u>					
2-HEXYLTHIOPHENE					
T (°C)	T (Kelvin)	methane(to)	RT ₁	k	ln k
50	323.15	0.542	25.042	45.175	3.811
75	348.15	0.529	6.482	11.246	2.420
150	423.15	0.506	0.837	0.653	-0.426
200	473.15	0.494	0.601	0.217	-1.530
250	523.15	-	-	-	-

6.2 Raw Data for Alcohols

6.2.1 SLB-IL60: Alcohols

Table 14: Raw data for a homologous series of primary alcohols on the SLB-IL60 column. RT is the retention time measured in triplicate, β is the column phase volume ratio calculated according to equation 11, and ΔG° , the Gibbs Free Energy, was calculated according to equation 7.

C1 <u>METHANOL</u>											
T (°C)	T (Kelvin)	methane(to)	RT ₁	RT ₂	RT ₃	stdev	avg RT	k	K (=k β)	ln K	ΔG° (kJ/mol)
50	323.15	2.026	3.036	3.031	3.029	0.004	3.032	0.497	155.286	5.045	-13.555
75	348.15	1.904	2.389	2.385	2.386	0.002	2.387	0.254	79.288	4.373	-12.658
115	388.15	1.747	1.957	1.956	1.956	0.001	1.956	0.120	37.545	3.626	-11.700
150	423.15	1.645	1.766	1.766	1.766	0.000	1.766	0.074	22.986	3.135	-11.029
200	473.15	1.5245	1.599	1.598	1.599	0.001	1.599	0.049	15.203	2.721	-10.706
250	523.15	1.428	-	-	-	-	-	-	-	-	-
C2 <u>ETHANOL</u>											
T (°C)	T (Kelvin)	methane(to)	RT ₁	RT ₂	RT ₃	stdev	avg RT	k	K (=k β)	ln K	ΔG° (kJ/mol)
50	323.15	2.026	3.501	3.498	3.499	0.002	3.499	0.728	227.387	5.427	-14.580
75	348.15	1.904	2.551	2.549	2.549	0.001	2.550	0.339	106.045	4.664	-13.500
115	388.15	1.747	1.999	1.998	1.998	0.001	1.998	0.144	45.060	3.808	-12.289
150	423.15	1.645	1.781	1.781	1.78	0.001	1.781	0.082	25.773	3.249	-11.431
200	473.15	1.5245	1.603	1.603	1.602	0.001	1.603	0.051	16.023	2.774	-10.912
250	523.15	1.428	-	-	-	-	-	-	-	-	-
C3 <u>PROPANOL</u>											
T (°C)	T (Kelvin)	methane(to)	RT ₁	RT ₂	RT ₃	stdev	avg RT	k	K (=k β)	ln K	ΔG° (kJ/mol)
50	323.15	2.026	4.806	4.808	4.806	0.001	4.807	1.373	429.086	6.062	-16.286

75	348.15	1.904	2.983	2.984	2.992	0.005	2.986	0.569	177.727	5.180	-14.994
115	388.15	1.747	2.101	2.103	2.104	0.002	2.103	0.204	63.729	4.155	-13.407
150	423.15	1.645	1.817	1.819	1.83	0.007	1.822	0.108	33.625	3.515	-12.367
200	473.15	1.5245	1.614	1.614	1.613	0.001	1.614	0.058	18.278	2.906	-11.430
250	523.15	1.428	-	-	-	-	-	-	-	-	-

C4 BUTANOL											
T (°C)	T (Kelvin)	methane(t ₀)	RT ₁	RT ₂	RT ₃	stdev	avg RT	k	K (=kβ)	ln K	ΔG° (kJ/mol)
50	323.15	2.026	8.179	8.171	8.171	0.005	8.174	3.035	948.557	6.855	-18.417
75	348.15	1.904	3.926	3.93	3.93	0.002	3.929	1.064	332.418	5.806	-16.807
115	388.15	1.747	2.286	2.286	2.286	0.000	2.286	0.309	96.532	4.570	-14.747
150	423.15	1.645	1.885	1.886	1.855	0.018	1.875	0.140	43.756	3.779	-13.294
200	473.15	1.5245	1.63	1.631	1.631	0.001	1.631	0.070	21.763	3.080	-12.117
250	523.15	1.428	-	-	-	-	-	-	-	-	-
C5 PENTANOL											
T (°C)	T (Kelvin)	methane(t ₀)	RT ₁	RT ₂	RT ₃	stdev	avg RT	k	K (=kβ)	ln K	ΔG° (kJ/mol)
50	323.15	2.026									
75	348.15	1.904	5.812	5.81	5.809	0.002	5.810	2.052	641.306	6.464	-18.709
115	388.15	1.747	2.614	2.615	2.615	0.001	2.615	0.497	155.340	5.046	-16.283
150	423.15	1.645	1.978	1.978	1.977	0.001	1.978	0.202	63.197	4.146	-14.587
200	473.15	1.5245	1.656	1.656	1.656	0.000	1.656	0.086	26.956	3.294	-12.959
250	523.15	1.428	-	-	-	-	-	-	-	-	-
C6 HEXANOL											
T (°C)	T (Kelvin)	methane(t ₀)	RT ₁	RT ₂	RT ₃	stdev	avg RT	k	K (=kβ)	ln K	ΔG° (kJ/mol)
50	323.15	2.026									
75	348.15	1.904	9.265	9.273	9.268	0.004	9.269	3.869	1209.015	7.098	-20.544
115	388.15	1.747	3.14	3.14	3.139	0.001	3.140	0.798	249.278	5.519	-17.809
150	423.15	1.645	2.142	2.141	2.142	0.001	2.142	0.302	94.352	4.547	-15.997
200	473.15	1.5245	1.689	1.689	1.689	0.000	1.689	0.108	33.720	3.518	-13.839
250	523.15	1.428	-	-	-	-	-	-	-	-	-
C7 HEPTANOL											
T (°C)	T (Kelvin)	methane(t ₀)	RT ₁	RT ₂	RT ₃	stdev	avg RT	k	K (=kβ)	ln K	ΔG° (kJ/mol)
50	323.15	2.026	-	-	-	-	-	-	-	-	-
75	348.15	1.904	-	-	-	-	-	-	-	-	-
115	388.15	1.747	4.005	4.007	4.005	0.001	4.006	1.294	404.231	6.002	-19.369
150	423.15	1.645	2.362	2.361	2.362	0.001	2.362	0.436	136.145	4.914	-17.287
200	473.15	1.5245	1.734	1.733	1.733	0.001	1.733	0.137	42.808	3.757	-14.778
250	523.15	1.428	1.526	1.526	1.526	0.000	1.526	0.068	21.388	3.063	-13.322

C8 OCTANOL											
T (°C)	T (Kelvin)	methane(t ₀)	RT ₁	RT ₂	RT ₃	stdev	avg RT	k	K (=kβ)	ln K	ΔG° (kJ/mol)
50	323.15	2.026	-	-	-	-	-	-	-	-	-
75	348.15	1.904	-	-	-	-	-	-	-	-	-
115	388.15	1.747	5.54	5.541	5.542	0.001	5.541	2.173	678.947	6.521	-21.042
150	423.15	1.645	2.684	2.686	2.684	0.001	2.685	0.632	197.505	5.286	-18.596
200	473.15	1.5245	1.793	1.793	1.793	0.000	1.793	0.176	55.039	4.008	-15.767
250	523.15	1.428	1.543	1.542	1.542	0.001	1.542	0.080	24.961	3.217	-13.994
C9 NONANOL											
T (°C)	T (Kelvin)	methane(t ₀)	RT ₁	RT ₂	RT ₃	stdev	avg RT	k	K (=kβ)	ln K	ΔG° (kJ/mol)
50	323.15	2.026	-	-	-	-	-	-	-	-	-
75	348.15	1.904	-	-	-	-	-	-	-	-	-
115	388.15	1.747	7.896	7.902	7.906	0.005	7.901	3.524	1101.280	7.004	-22.603
150	423.15	1.645	3.164	3.164	3.164	0.000	3.164	0.923	288.564	5.665	-19.930
200	473.15	1.5245	1.873	1.874	1.874	0.001	1.874	0.229	71.574	4.271	-16.800
250	523.15	1.428	1.562	1.562	1.562	0.000	1.562	0.094	29.264	3.376	-14.685

6.2.2 HP-20M: Alcohols

Table 15: Raw data for a homologous series of primary alcohols on the HP-20M column. RT is the retention time measured in triplicate, β is the column phase volume ratio calculated according to equation 11, and ΔG° , the Gibbs Free Energy, was calculated according to equation 7.

C1 METHANOL											
T (°C)	T (Kelvin)	methane(t ₀)	RT ₁	RT ₂	RT ₃	stdev	avg RT	k	K (=k β)	ln K	ΔG° (kJ/mol)
50	323.15	0.555	0.772	0.773	0.773	0.001	0.773	0.392	104.585	4.650	-12.493
75	348.15	0.539	0.614	0.641	0.641	0.016	0.632	0.173	46.011	3.829	-11.083
115	388.15	0.525	0.57	0.57	0.57	0.000	0.570	0.086	22.857	3.129	-10.098
150	423.15	0.513	0.544	0.544	0.544	0.000	0.544	0.060	15.931	2.768	-9.739
200	473.15	0.498	-	-	-	-	-	-	-	-	-
C2 ETHANOL											
T (°C)	T (Kelvin)	methane(t ₀)	RT ₁	RT ₂	RT ₃	stdev	avg RT	k	K (=k β)	ln K	ΔG° (kJ/mol)
50	323.15	0.555	0.843	0.844	0.843	0.001	0.843	0.520	138.539	4.931	-13.248
75	348.15	0.539	0.664	0.665	0.665	0.001	0.665	0.233	62.173	4.130	-11.954
115	388.15	0.525	0.576	0.576	0.576	0.000	0.576	0.097	25.905	3.254	-10.502
150	423.15	0.513	0.547	0.547	0.547	0.000	0.547	0.066	17.489	2.862	-10.067
200	473.15	0.498	-	-	-	-	-	-	-	-	-
C3 PROPANOL											
T (°C)	T (Kelvin)	methane(t ₀)	RT ₁	RT ₂	RT ₃	stdev	avg RT	k	K (=k β)	ln K	ΔG° (kJ/mol)
50	323.15	0.555	1.132	1.132	1.132	0.000	1.132	1.040	277.237	5.625	-15.112
75	348.15	0.539	0.761	0.761	0.761	0.000	0.761	0.412	109.833	4.699	-13.601
115	388.15	0.525	0.6	0.598	0.598	0.001	0.599	0.140	37.418	3.622	-11.689
150	423.15	0.513	0.557	0.557	0.556	0.001	0.557	0.084	22.511	3.114	-10.955
200	473.15	0.498	-	-	-	-	-	-	-	-	-
C4 BUTANOL											
T (°C)	T (Kelvin)	methane(t ₀)	RT ₁	RT ₂	RT ₃	stdev	avg RT	k	K (=k β)	ln K	ΔG° (kJ/mol)
50	323.15	0.555	1.899	1.84	1.832	0.037	1.857	2.346	625.586	6.439	-17.299
75	348.15	0.539	0.988	0.993	0.991	0.003	0.991	0.838	223.459	5.409	-15.657
115	388.15	0.525	0.645	0.642	0.642	0.002	0.643	0.225	59.937	4.093	-13.209
150	423.15	0.513	0.571	0.571	0.571	0.000	0.571	0.112	29.957	3.400	-11.961
200	473.15	0.498	-	-	-	-	-	-	-	-	-

C5 PENTANOL											
T (°C)	T (Kelvin)	methane(t ₀)	RT ₁	RT ₂	RT ₃	stdev	avg RT	k	K (=kβ)	ln K	ΔG° (kJ/mol)
50	323.15	0.555	3.606	3.602	3.599	0.004	3.602	5.491	1464.184	7.289	-19.583
75	348.15	0.539	1.444	1.444	1.442	0.001	1.443	1.678	447.413	6.103	-17.667
115	388.15	0.525	0.724	0.721	0.721	0.002	0.722	0.375	100.063	4.606	-14.863
150	423.15	0.513	0.596	0.596	0.595	0.001	0.596	0.160	42.771	3.756	-13.213
200	473.15	0.498	-	-	-	-	-	-	-	-	-
C6 HEXANOL											
T (°C)	T (Kelvin)	methane(t ₀)	RT ₁	RT ₂	RT ₃	stdev	avg RT	k	K (=kβ)	ln K	ΔG° (kJ/mol)
50	323.15	0.555	-	-	-	-	-	-	-	-	-
75	348.15	0.539	2.311	2.31	2.308	0.002	2.310	3.285	876.026	6.775	-19.612
115	388.15	0.525	0.863	0.848	0.848	0.009	0.853	0.625	166.603	5.116	-16.508
150	423.15	0.513	0.634	0.633	0.634	0.001	0.634	0.234	62.511	4.135	-14.548
200	473.15	0.498	0.549	0.55	0.549	0.001	0.549	0.104	27.685	3.321	-13.064
C7 HEPTANOL											
T (°C)	T (Kelvin)	methane(t ₀)	RT ₁	RT ₂	RT ₃	stdev	avg RT	k	K (=kβ)	ln K	ΔG° (kJ/mol)
50	323.15	0.555	-	-	-	-	-	-	-	-	-
75	348.15	0.539	3.991	3.99	3.986	0.003	3.989	6.401	1706.865	7.442	-21.542
115	388.15	0.525	1.066	1.083	1.072	0.009	1.074	1.045	278.688	5.630	-18.169
150	423.15	0.513	0.694	0.694	0.693	0.001	0.694	0.351	93.680	4.540	-15.972
200	473.15	0.498	0.563	0.563	0.563	0.000	0.563	0.131	35.008	3.556	-13.987
C8 OCTANOL											
T (°C)	T (Kelvin)	methane(t ₀)	RT ₁	RT ₂	RT ₃	stdev	avg RT	k	K (=kβ)	ln K	ΔG° (kJ/mol)
50	323.15	0.555	-	-	-	-	-	-	-	-	-
75	348.15	0.539	-	-	-	-	-	-	-	-	-
115	388.15	0.525	1.502	1.501	1.5	0.001	1.501	1.859	495.746	6.206	-20.027
150	423.15	0.513	0.787	0.787	0.787	0.000	0.787	0.533	142.165	4.957	-17.439
200	473.15	0.498	0.581	0.581	0.581	0.000	0.581	0.167	44.653	3.799	-14.944
C9 NONANOL											
T (°C)	T (Kelvin)	methane(t ₀)	RT ₁	RT ₂	RT ₃	stdev	avg RT	k	K (=kβ)	ln K	ΔG° (kJ/mol)
50	323.15	0.555	-	-	-	-	-	-	-	-	-
75	348.15	0.539	-	-	-	-	-	-	-	-	-
115	388.15	0.525	2.163	2.183	2.183	0.012	2.176	3.145	838.772	6.732	-21.725
150	423.15	0.513	0.933	0.933	0.933	0.000	0.933	0.818	218.009	5.385	-18.943
200	473.15	0.498	0.608	0.608	0.608	0.000	0.608	0.222	59.120	4.080	-16.048

6.3 Raw Data for Aldehydes

6.3.1 SLB-IL60: Aldehydes

Table 16: Raw data for a homologous series of alkyl aldehydes on the SLB-IL60 column. RT is the retention time measured in triplicate, β is the column phase volume ratio calculated according to equation 11, and ΔG° , the Gibbs Free Energy, was calculated according to equation 7.

C3 PROPANAL											
T (°C)	T (Kelvin)	methane(t_0)	RT ₁	RT ₂	RT ₃	stdev	avg RT	k	K (=k β)	ln K	ΔG° (kJ/mol)
50	323.15	2.026	3.004	3.000	2.996	0.004	3.000	0.481	150.349	5.013	-13.468
75	348.15	1.904	2.390	2.392	2.396	0.003	2.393	0.257	80.273	4.385	-12.694
115	388.15	1.747	1.964	1.964	1.964	0.000	1.964	0.125	38.917	3.661	-11.816
150	423.15	1.645	1.773	1.773	1.772	0.001	1.773	0.078	24.253	3.189	-11.217
200	473.15	1.5245	-	-	-	-	-	-	-	-	-
250	523.15	1.428	-	-	-	-	-	-	-	-	-
C4 BUTANAL											
T (°C)	T (Kelvin)	methane(t_0)	RT ₁	RT ₂	RT ₃	stdev	avg RT	k	K (=k β)	ln K	ΔG° (kJ/mol)
50	323.15	2.026	3.893	3.885	3.879	0.007	3.886	0.918	286.992	5.659	-15.205
75	348.15	1.904	2.718	2.718	2.715	0.002	2.717	0.427	133.514	4.894	-14.166
115	388.15	1.747	2.057	2.056	2.057	0.001	2.057	0.178	55.498	4.016	-12.961
150	423.15	1.645	1.809	1.809	1.810	0.001	1.809	0.100	31.218	3.441	-12.106
200	473.15	1.5245	-	-	-	-	-	-	-	-	-
250	523.15	1.428	-	-	-	-	-	-	-	-	-
C5 PENTANAL											
T (°C)	T (Kelvin)	methane(t_0)	RT ₁	RT ₂	RT ₃	stdev	avg RT	k	K (=k β)	ln K	ΔG° (kJ/mol)
50	323.15	2.026	6.010	6.012	6.011	0.001	6.011	1.968	614.894	6.421	-17.252
75	348.15	1.904	3.424	3.422	3.422	0.001	3.423	0.798	249.354	5.519	-15.974
115	388.15	1.747	2.228	2.229	2.228	0.001	2.228	0.276	86.214	4.457	-14.383
150	423.15	1.645	1.870	1.871	1.871	0.001	1.871	0.137	42.870	3.758	-13.221
200	473.15	1.5245	-	-	-	-	-	-	-	-	-
250	523.15	1.428	-	-	-	-	-	-	-	-	-

C6 <u>HEXANAL</u>											
T (°C)	T (Kelvin)	methane(t ₀)	RT ₁	RT ₂	RT ₃	stdev	avg RT	k	K (=kβ)	ln K	ΔG° (kJ/mol)
50	323.15	2.026	10.350	10.341	10.340	0.006	10.344	4.107	1283.351	7.157	-19.229
75	348.15	1.904	4.709	4.707	4.703	0.003	4.706	1.472	460.077	6.131	-17.747
115	388.15	1.747	2.501	2.501	2.501	0.000	2.501	0.432	135.002	4.905	-15.830
150	423.15	1.645	1.961	1.961	1.961	0.000	1.961	0.192	60.030	4.095	-14.406
200	473.15	1.5245	-	-	-	-	-	-	-	-	-
250	523.15	1.428	-	-	-	-	-	-	-	-	-
C7 <u>HEPTANAL</u>											
T (°C)	T (Kelvin)	methane(t ₀)	RT ₁	RT ₂	RT ₃	stdev	avg RT	k	K (=kβ)	ln K	ΔG° (kJ/mol)
50	323.15	2.026	-	-	-	-	-	-	-	-	-
75	348.15	1.904	-	-	-	-	-	-	-	-	-
115	388.15	1.747	3.006	3.005	3.005	0.001	3.005	0.721	225.242	5.417	-17.482
150	423.15	1.645	2.097	2.096	2.097	0.001	2.097	0.275	85.803	4.452	-15.663
200	473.15	1.5245	1.689	1.689	1.689	0.000	1.689	0.108	33.720	3.518	-13.839
250	523.15	1.428	1.520	1.520	1.519	0.001	1.520	0.064	20.002	2.996	-13.030
C8 <u>OCTANAL</u>											
T (°C)	T (Kelvin)	methane(t ₀)	RT ₁	RT ₂	RT ₃	stdev	avg RT	k	K (=kβ)	ln K	ΔG° (kJ/mol)
50	323.15	2.026	-	-	-	-	-	-	-	-	-
75	348.15	1.904	-	-	-	-	-	-	-	-	-
115	388.15	1.747	3.762	3.762	3.765	0.002	3.763	1.155	360.811	5.888	-19.002
150	423.15	1.645	2.284	2.284	2.285	0.001	2.284	0.389	121.454	4.800	-16.885
200	473.15	1.5245	1.727	1.726	1.728	0.001	1.727	0.133	41.510	3.726	-14.657
250	523.15	1.428	1.527	1.527	1.528	0.001	1.527	0.069	21.679	3.076	-13.381
C9 <u>NONANAL</u>											
T (°C)	T (Kelvin)	methane(t ₀)	RT ₁	RT ₂	RT ₃	stdev	avg RT	k	K (=kβ)	ln K	ΔG° (kJ/mol)
50	323.15	2.026	-	-	-	-	-	-	-	-	-
75	348.15	1.904	-	-	-	-	-	-	-	-	-
115	388.15	1.747	4.984	4.982	4.974	0.005	4.980	1.851	578.568	6.361	-20.526
150	423.15	1.645	2.567	2.567	2.567	0.000	2.567	0.560	175.152	5.166	-18.173
200	473.15	1.5245	1.783	1.783	1.783	0.000	1.783	0.170	52.989	3.970	-15.617
250	523.15	1.428	1.544	1.543	1.543	0.001	1.543	0.081	25.180	3.226	-14.032

C10 DECANAL											
T (°C)	T (Kelvin)	methane(t ₀)	RT ₁	RT ₂	RT ₃	stdev	avg RT	k	K (=kβ)	ln K	ΔG° (kJ/mol)
50	323.15	2.026	-	-	-	-	-	-	-	-	-
75	348.15	1.904	-	-	-	-	-	-	-	-	-
115	388.15	1.747	6.977	6.983	6.987	0.005	6.982	2.998	936.844	6.843	-22.081
150	423.15	1.645	2.981	2.980	2.980	0.001	2.980	0.812	253.673	5.536	-19.476
200	473.15	1.5245	1.858	1.858	1.857	0.001	1.858	0.219	68.294	4.224	-16.616
250	523.15	1.428	1.564	1.563	1.564	0.001	1.564	0.095	29.629	3.389	-14.739

6.3.2 HP-20M: Aldehydes

Table 17: Raw data for a homologous series of alkyl aldehydes on the HP-20M column. RT is the retention time measured in triplicate, β is the column phase volume ratio calculated according to equation 11, and ΔG° , the Gibbs Free Energy, was calculated according to equation 7.

C3 PROPANAL											
T (°C)	T (Kelvin)	methane(t_0)	RT ₁	RT ₂	RT ₃	stdev	avg RT	k	K (=k β)	ln K	ΔG° (kJ/mol)
50	323.15	0.555	0.659	0.659	0.659	0.000	0.659	0.187	49.970	3.911	-10.509
75	348.15	0.539	0.602	0.602	0.602	0.000	0.602	0.117	31.169	3.439	-9.955
115	388.15	0.525	0.562	0.562	0.562	0.000	0.562	0.070	18.794	2.934	-9.467
150	423.15	0.513	0.542	0.542	0.542	0.000	0.542	0.056	14.892	2.701	-9.502
200	473.15	0.498	-	-	-	-	-	-	-	-	-
C4 BUTANAL											
T (°C)	T (Kelvin)	methane(t_0)	RT ₁	RT ₂	RT ₃	stdev	avg RT	k	K (=k β)	ln K	ΔG° (kJ/mol)
50	323.15	0.555	0.742	0.742	0.743	0.001	0.742	0.338	90.010	4.500	-12.090
75	348.15	0.539	0.637	0.637	0.637	0.000	0.637	0.182	48.485	3.881	-11.234
115	388.15	0.525	0.573	0.573	0.573	0.000	0.573	0.091	24.381	3.194	-10.307
150	423.15	0.513	0.547	0.547	0.547	0.000	0.547	0.066	17.489	2.862	-10.067
200	473.15	0.498	-	-	-	-	-	-	-	-	-
C5 PENTANAL											
T (°C)	T (Kelvin)	methane(t_0)	RT ₁	RT ₂	RT ₃	stdev	avg RT	k	K (=k β)	ln K	ΔG° (kJ/mol)
50	323.15	0.555	0.955	0.955	0.955	0.000	0.955	0.721	192.192	5.258	-14.128
75	348.15	0.539	0.715	0.715	0.715	0.000	0.715	0.327	87.075	4.467	-12.929
115	388.15	0.525	0.593	0.593	0.592	0.001	0.593	0.129	34.370	3.537	-11.415
150	423.15	0.513	0.555	0.555	0.555	0.000	0.555	0.081	21.645	3.075	-10.817
200	473.15	0.498	-	-	-	-	-	-	-	-	-
C6 HEXANAL											
T (°C)	T (Kelvin)	methane(t_0)	RT ₁	RT ₂	RT ₃	stdev	avg RT	k	K (=k β)	ln K	ΔG° (kJ/mol)
50	323.15	0.555	1.407	1.408	1.409	0.001	1.408	1.537	409.850	6.016	-16.162
75	348.15	0.539	0.867	0.867	0.867	0.000	0.867	0.609	162.276	5.089	-14.731
115	388.15	0.525	0.630	0.630	0.630	0.000	0.630	0.200	53.333	3.977	-12.833
150	423.15	0.513	0.569	0.569	0.569	0.000	0.569	0.108	28.918	3.364	-11.836
200	473.15	0.498	-	-	-	-	-	-	-	-	-

C7 HEPTANAL											
T (°C)	T (Kelvin)	methane(t_0)	RT ₁	RT ₂	RT ₃	stdev	avg RT	k	K (=k β)	ln K	ΔG° (kJ/mol)
50	323.15	0.555	2.287	2.287	2.290	0.002	2.288	3.123	832.673	6.725	-18.067
75	348.15	0.539	1.138	1.139	1.140	0.001	1.139	1.113	296.846	5.693	-16.479
115	388.15	0.525	0.692	0.692	0.692	0.000	0.692	0.318	84.825	4.441	-14.330
150	423.15	0.513	0.592	0.592	0.592	0.000	0.592	0.153	40.866	3.710	-13.053
200	473.15	0.498	-	-	-	-	-	-	-	-	-
C8 OCTANAL											
T (°C)	T (Kelvin)	methane(t_0)	RT ₁	RT ₂	RT ₃	stdev	avg RT	k	K (=k β)	ln K	ΔG° (kJ/mol)
50	323.15	0.555	4.390	4.393	4.382	0.006	4.388	6.907	1841.842	7.519	-20.200
75	348.15	0.539	1.720	1.720	1.724	0.002	1.721	2.194	584.952	6.372	-18.443
115	388.15	0.525	0.781	0.781	0.782	0.001	0.781	0.488	130.201	4.869	-15.713
150	423.15	0.513	0.621	0.621	0.621	0.000	0.621	0.210	55.931	4.024	-14.157
200	473.15	0.498	-	-	-	-	-	-	-	-	-
C9 NONANAL											
T (°C)	T (Kelvin)	methane(t_0)	RT ₁	RT ₂	RT ₃	stdev	avg RT	k	K (=k β)	ln K	ΔG° (kJ/mol)
50	323.15	0.555	9.823	9.859	9.850	0.019	9.844	16.737	4463.183	8.404	-22.578
75	348.15	0.539	2.889	2.888	2.888	0.001	2.888	4.359	1162.317	7.058	-20.430
115	388.15	0.525	0.988	0.988	0.988	0.000	0.988	0.882	235.175	5.460	-17.621
150	423.15	0.513	0.676	0.675	0.676	0.001	0.676	0.316	84.329	4.435	-15.602
200	473.15	0.498	-	-	-	-	-	-	-	-	-
C10 DECANAL											
T (°C)	T (Kelvin)	methane(t_0)	RT ₁	RT ₂	RT ₃	stdev	avg RT	k	K (=k β)	ln K	ΔG° (kJ/mol)
50	323.15	0.555	-	-	-	-	-	-	-	-	-
75	348.15	0.539	4.788	4.884	4.886	0.056	4.853	8.003	2134.158	7.666	-22.189
115	388.15	0.525	1.299	1.298	1.296	0.002	1.298	1.472	392.466	5.972	-19.274
150	423.15	0.513	0.756	0.756	0.756	0.000	0.756	0.473	126.061	4.837	-17.016
200	473.15	0.498	0.583	0.582	0.583	0.001	0.583	0.171	45.546	3.819	-15.022

6.4 Raw Data for Acids

6.4.1 SLB-IL60: Acids

Table 18: Raw data for a homologous series of alkyl carboxylic acids on the SLB-IL60 column. RT is the retention time measured in triplicate, β is the column phase volume ratio calculated according to equation 11, and ΔG° , the Gibbs Free Energy, was calculated according to equation 7.

C2 ACETIC ACID											
T (°C)	T (Kelvin)	methane(to)	RT ₁	RT ₂	RT ₃	stdev	avg RT	k	K (=k β)	ln K	ΔG° (kJ/mol)
50	323.15	2.026	-	-	-	-	-	-	-	-	-
75	348.15	1.904	-	-	-	-	-	-	-	-	-
115	388.15	1.747	4.353	4.352	4.353	0.001	4.353	1.492	466.320	6.145	-19.830
150	423.15	1.645	2.485	2.484	2.484	0.001	2.484	0.510	159.448	5.072	-17.843
200	473.15	1.5245	1.851	1.851	1.850	0.001	1.851	0.214	66.859	4.203	-16.532
250	523.15	1.428	1.593	1.591	1.594	0.002	1.593	0.115	35.974	3.583	-15.583
C3 PROPANOIC ACID											
T (°C)	T (Kelvin)	methane(to)	RT ₁	RT ₂	RT ₃	stdev	avg RT	k	K (=k β)	ln K	ΔG° (kJ/mol)
50	323.15	2.026	-	-	-	-	-	-	-	-	-
75	348.15	1.904	-	-	-	-	-	-	-	-	-
115	388.15	1.747	5.583	5.585	5.585	0.001	5.584	2.197	686.701	6.532	-21.079
150	423.15	1.645	2.789	2.788	2.789	0.001	2.789	0.695	217.262	5.381	-18.931
200	473.15	1.5245	1.920	1.921	1.921	0.001	1.921	0.260	81.208	4.397	-17.297
250	523.15	1.428	1.607	1.607	1.607	0.000	1.607	0.125	39.110	3.666	-15.947
C4 BUTANOIC ACID											
T (°C)	T (Kelvin)	methane(to)	RT ₁	RT ₂	RT ₃	stdev	avg RT	k	K (=k β)	ln K	ΔG° (kJ/mol)
50	323.15	2.026	-	-	-	-	-	-	-	-	-
75	348.15	1.904	-	-	-	-	-	-	-	-	-
115	388.15	1.747	7.879	7.880	7.881	0.001	7.880	3.512	1097.463	7.001	-22.592
150	423.15	1.645	3.298	3.299	3.297	0.001	3.298	1.005	314.020	5.749	-20.227
200	473.15	1.5245	2.023	2.021	2.022	0.001	2.022	0.326	101.980	4.625	-18.193
250	523.15	1.428	1.636	1.636	1.632	0.002	1.635	0.145	45.164	3.810	-16.573

C5 PENTANOIC ACID											
T (°C)	T (Kelvin)	methane(t ₀)	RT ₁	RT ₂	RT ₃	stdev	avg RT	k	K (=kβ)	ln K	ΔG° (kJ/mol)
50	323.15	2.026	-	-	-	-	-	-	-	-	-
75	348.15	1.904	-	-	-	-	-	-	-	-	-
115	388.15	1.747	12.590	12.593	12.589	0.002	12.591	6.209	1940.339	7.571	-24.431
150	423.15	1.645	4.281	4.282	4.283	0.001	4.282	1.603	500.950	6.217	-21.870
200	473.15	1.5245	2.219	2.219	2.218	0.001	2.219	0.455	142.294	4.958	-19.503
250	523.15	1.428	1.689	1.687	1.690	0.002	1.689	0.182	56.979	4.043	-17.584
C6 HEXANOIC ACID											
T (°C)	T (Kelvin)	methane(t ₀)	RT ₁	RT ₂	RT ₃	stdev	avg RT	k	K (=kβ)	ln K	ΔG° (kJ/mol)
50	323.15	2.026	-	-	-	-	-	-	-	-	-
75	348.15	1.904	-	-	-	-	-	-	-	-	-
115	388.15	1.747	20.687	20.689	20.688	0.001	20.688	10.845	3389.189	8.128	-26.231
150	423.15	1.645	6.380	6.378	6.377	0.002	6.378	2.877	899.189	6.801	-23.928
200	473.15	1.5245	2.579	2.580	2.582	0.002	2.580	0.693	216.430	5.377	-21.153
250	523.15	1.428	1.818	1.818	1.816	0.001	1.817	0.272	85.131	4.444	-19.330
C7 HEPTANOIC ACID											
T (°C)	T (Kelvin)	methane(t ₀)	RT ₁	RT ₂	RT ₃	stdev	avg RT	k	K (=kβ)	ln K	ΔG° (kJ/mol)
50	323.15	2.026	-	-	-	-	-	-	-	-	-
75	348.15	1.904	-	-	-	-	-	-	-	-	-
115	388.15	1.747	37.894	37.893	37.891	0.002	37.893	20.696	6467.608	8.775	-28.316
150	423.15	1.645	8.646	8.648	8.643	0.003	8.646	4.256	1329.914	7.193	-25.305
200	473.15	1.5245	2.970	2.971	2.971	0.001	2.971	0.949	296.443	5.692	-22.390
250	523.15	1.428	1.876	1.877	1.874	0.002	1.876	0.313	97.894	4.584	-19.937

C8 OCTANOIC ACID											
T (°C)	T (Kelvin)	methane(to)	RT ₁	RT ₂	RT ₃	stdev	avg RT	k	K (=kβ)	ln K	ΔG° (kJ/mol)
50	323.15	2.026	-	-	-	-	-	-	-	-	-
75	348.15	1.904	-	-	-	-	-	-	-	-	-
115	388.15	1.747	61.182	61.181	61.179	0.002	61.181	34.030	10634.513	9.272	-29.921
150	423.15	1.645	12.522	12.523	12.525	0.002	12.523	6.613	2066.553	7.634	-26.856
200	473.15	1.5245	3.532	3.530	3.533	0.002	3.532	1.317	411.440	6.020	-23.680
250	523.15	1.428	1.973	1.974	1.973	0.001	1.973	0.382	119.264	4.781	-20.796
C9 NONANOIC ACID											
T (°C)	T (Kelvin)	methane(to)	RT ₁	RT ₂	RT ₃	stdev	avg RT	k	K (=kβ)	ln K	ΔG° (kJ/mol)
50	323.15	2.026	-	-	-	-	-	-	-	-	-
75	348.15	1.904	-	-	-	-	-	-	-	-	-
115	388.15	1.747	-	-	-	-	-	-	-	-	-
150	423.15	1.645	18.437	18.433	18.435	0.002	18.435	10.207	3189.590	8.068	-28.383
200	473.15	1.5245	4.340	4.342	4.341	0.001	4.341	1.847	577.341	6.358	-25.013
250	523.15	1.428	2.117	2.118	2.117	0.001	2.117	0.482	150.771	5.016	-21.816
C10 DECANOIC ACID											
T (°C)	T (Kelvin)	methane(to)	RT ₁	RT ₂	RT ₃	stdev	avg RT	k	K (=kβ)	ln K	ΔG° (kJ/mol)
50	323.15	2.026				#DIV/0!	#DIV/0!	#DIV/0!	#DIV/0!	#DIV/0!	#DIV/0!
75	348.15	1.904				#DIV/0!	#DIV/0!	#DIV/0!	#DIV/0!	#DIV/0!	#DIV/0!
115	388.15	1.747				#DIV/0!	#DIV/0!	#DIV/0!	#DIV/0!	#DIV/0!	#DIV/0!
150	423.15	1.645	29.722	29.718	29.721	0.002	29.720	17.067	5333.460	8.582	-30.191
200	473.15	1.5245	4.706	4.711	4.704	0.004	4.707	2.088	652.366	6.481	-25.493
250	523.15	1.428	2.531	2.530	2.528	0.002	2.530	0.771	240.989	5.485	-23.856

6.4.2 HP-20M: Acids

Table 19: Raw data for a homologous series of alkyl carboxylic acids on the HP-20M column. RT is the retention time measured in triplicate, β is the column phase volume ratio calculated according to equation 11, and ΔG° , the Gibbs Free Energy, was calculated according to equation 7.

C2 ACETIC ACID											
T (°C)	T (Kelvin)	methane(t_0)	RT ₁	RT ₂	RT ₃	stdev	avg RT	k	K (=k β)	ln K	ΔG° (kJ/mol)
50	323.15	0.555	-	-	-	-	-	-	-	-	-
75	348.15	0.539	3.008	3.012	3.013	0.003	3.011	4.586	1223.006	7.109	-20.577
115	388.15	0.525	0.997	0.998	0.995	0.002	0.997	0.898	239.577	5.479	-17.681
150	423.15	0.513	0.676	0.676	0.676	0.000	0.676	0.317	84.502	4.437	-15.609
200	473.15	0.498	0.559	0.560	0.559	0.001	0.559	0.124	33.043	3.498	-13.760
C3 PROPANOIC ACID											
T (°C)	T (Kelvin)	methane(t_0)	RT ₁	RT ₂	RT ₃	stdev	avg RT	k	K (=k β)	ln K	ΔG° (kJ/mol)
50	323.15	0.555	-	-	-	-	-	-	-	-	-
75	348.15	0.539	5.045	5.050	5.046	0.003	5.047	8.364	2230.303	7.710	-22.316
115	388.15	0.525	1.277	1.277	1.277	0.000	1.277	1.432	381.968	5.945	-19.186
150	423.15	0.513	0.746	0.746	0.746	0.000	0.746	0.453	120.866	4.795	-16.868
200	473.15	0.498	0.575	0.574	0.575	0.001	0.575	0.155	41.259	3.720	-14.633
C4 BUTANOIC ACID											
T (°C)	T (Kelvin)	methane(t_0)	RT ₁	RT ₂	RT ₃	stdev	avg RT	k	K (=k β)	ln K	ΔG° (kJ/mol)
50	323.15	0.555	-	-	-	-	-	-	-	-	-
75	348.15	0.539	8.787	8.776	8.788	0.007	8.784	15.296	4078.994	8.314	-24.064
115	388.15	0.525	1.739	1.739	1.738	0.001	1.739	2.312	616.466	6.424	-20.731
150	423.15	0.513	0.852	0.852	0.852	0.000	0.852	0.660	175.931	5.170	-18.189
200	473.15	0.498	0.595	0.596	0.596	0.001	0.596	0.197	52.512	3.961	-15.582
C5 PENTANOIC ACID											
T (°C)	T (Kelvin)	methane(t_0)	RT ₁	RT ₂	RT ₃	stdev	avg RT	k	K (=k β)	ln K	ΔG° (kJ/mol)
50	323.15	0.555	-	-	-	-	-	-	-	-	-
75	348.15	0.539	17.494	17.476	17.488	0.009	17.486	31.442	8384.416	9.034	-26.149
115	388.15	0.525	2.691	2.691	2.691	0.000	2.691	4.126	1100.190	7.003	-22.600
150	423.15	0.513	1.052	1.052	1.052	0.000	1.052	1.049	279.827	5.634	-19.821
200	473.15	0.498	0.631	0.632	0.631	0.001	0.631	0.269	71.623	4.271	-16.803

C6 <u>HEXANOIC ACID</u>											
T (°C)	T (Kelvin)	methane(t ₀)	RT ₁	RT ₂	RT ₃	stdev	avg RT	k	K (=kβ)	ln K	ΔG° (kJ/mol)
50	323.15	0.555	-	-	-	-	-	-	-	-	-
75	348.15	0.539	34.739	34.781	34.477	0.165	34.666	63.315	16883.941	9.734	-28.176
115	388.15	0.525	4.273	4.265	4.286	0.011	4.275	7.142	1904.593	7.552	-24.371
150	423.15	0.513	1.364	1.355	1.352	0.006	1.357	1.644	438.268	6.083	-21.400
200	473.15	0.498	0.681	0.681	0.679	0.001	0.680	0.367	97.879	4.584	-18.031
C7 <u>HEPTANOIC ACID</u>											
T (°C)	T (Kelvin)	methane(t ₀)	RT ₁	RT ₂	RT ₃	stdev	avg RT	k	K (=kβ)	ln K	ΔG° (kJ/mol)
50	323.15	0.555	-	-	-	-	-	-	-	-	-
75	348.15	0.539	-	-	-	-	-	-	-	-	-
115	388.15	0.525	7.067	7.083	7.084	0.010	7.078	12.482	3328.508	8.110	-26.173
150	423.15	0.513	1.848	1.850	1.850	0.001	1.850	2.604	694.372	6.543	-23.019
200	473.15	0.498	0.748	0.750	0.749	0.001	0.749	0.505	134.673	4.903	-19.287
C8 <u>OCTANOIC ACID</u>											
T (°C)	T (Kelvin)	methane(t ₀)	RT ₁	RT ₂	RT ₃	stdev	avg RT	k	K (=kβ)	ln K	ΔG° (kJ/mol)
50	323.15	0.555	-	-	-	-	-	-	-	-	-
75	348.15	0.539	-	-	-	-	-	-	-	-	-
115	388.15	0.525	11.784	11.794	11.794	0.006	11.791	21.458	5722.243	8.652	-27.921
150	423.15	0.513	2.599	2.603	2.603	0.002	2.602	4.068	1084.848	6.989	-24.588
200	473.15	0.498	0.848	0.848	0.848	0.000	0.848	0.704	187.720	5.235	-20.593
C9 <u>NONANOIC ACID</u>											
T (°C)	T (Kelvin)	methane(t ₀)	RT ₁	RT ₂	RT ₃	stdev	avg RT	k	K (=kβ)	ln K	ΔG° (kJ/mol)
50	323.15	0.555	-	-	-	-	-	-	-	-	-
75	348.15	0.539	-	-	-	-	-	-	-	-	-
115	388.15	0.525	19.681	19.692	19.694	0.007	19.689	36.503	9734.095	9.183	-29.636
150	423.15	0.513	3.764	3.764	3.763	0.001	3.764	6.332	1688.485	7.432	-26.145
200	473.15	0.498	0.984	0.984	0.984	0.000	0.984	0.977	260.594	5.563	-21.883
C10 <u>DECANOIC ACID</u>											
T (°C)	T (Kelvin)	methane(t ₀)	RT ₁	RT ₂	RT ₃	stdev	avg RT	k	K (=kβ)	ln K	ΔG° (kJ/mol)
50	323.15	0.555	-	-	-	-	-	-	-	-	-
75	348.15	0.539	-	-	-	-	-	-	-	-	-
115	388.15	0.525	32.049	32.057	32.063	0.007	32.056	60.060	16015.915	9.681	-31.242
150	423.15	0.513	5.418	5.423	5.420	0.003	5.420	9.559	2549.091	7.843	-27.594
200	473.15	0.498	1.159	1.160	1.159	0.001	1.159	1.330	354.543	5.871	-23.094

6.5 Raw Data for Ethyl Esters

6.5.1 SLB-IL60: Ethyl Esters

Table 20: Raw data for a homologous series of ethyl esters on the SLB-IL60 column. RT is the retention time measured in triplicate, β is the column phase volume ratio calculated according to equation 11, and ΔG° , the Gibbs Free Energy, was calculated according to equation 7.

C1 ETHYL FORMATE											
T (°C)	T (Kelvin)	methane(t_0)	RT ₁	RT ₂	RT ₃	stdev	avg RT	k	K (=k β)	ln K	ΔG° (kJ/mol)
50	323.15	2.026	-	-	-	-	-	-	-	-	-
75	348.15	1.904	2.385	2.384	2.385	0.001	2.385	0.253	78.959	4.369	-12.646
115	388.15	1.747	1.952	1.951	1.951	0.001	1.951	0.117	36.651	3.601	-11.622
150	423.15	1.645	1.768	1.768	1.767	0.001	1.768	0.075	23.303	3.149	-11.077
200	473.15	1.5245	1.598	1.597	1.597	0.001	1.597	0.048	14.930	2.703	-10.634
250	523.15	1.428	1.483	1.492	1.492	0.005	1.489	0.043	13.292	2.587	-11.253
C2 ETHYL ACETATE											
T (°C)	T (Kelvin)	methane(t_0)	RT ₁	RT ₂	RT ₃	stdev	avg RT	k	K (=k β)	ln K	ΔG° (kJ/mol)
50	323.15	2.026	-	-	-	-	-	-	-	-	-
75	348.15	1.904	2.929	2.930	2.928	0.001	2.929	0.539	168.316	5.126	-14.837
115	388.15	1.747	2.093	2.092	2.091	0.001	2.092	0.198	61.820	4.124	-13.309
150	423.15	1.645	1.828	1.825	1.826	0.002	1.826	0.110	34.448	3.539	-12.452
200	473.15	1.5245	1.614	1.613	1.661	0.028	1.629	0.069	21.510	3.069	-12.071
250	523.15	1.428	1.488	1.487	1.487	0.001	1.487	0.041	12.927	2.559	-11.132
C3 ETHYL PROPIONATE											
T (°C)	T (Kelvin)	methane(t_0)	RT ₁	RT ₂	RT ₃	stdev	avg RT	k	K (=k β)	ln K	ΔG° (kJ/mol)
50	323.15	2.026	-	-	-	-	-	-	-	-	-
75	348.15	1.904	3.442	3.441	3.441	0.001	3.441	0.808	252.419	5.531	-16.010
115	388.15	1.747	2.199	2.198	2.197	0.001	2.198	0.259	80.787	4.392	-14.173
150	423.15	1.645	1.863	1.860	1.858	0.003	1.860	0.131	40.907	3.711	-13.057
200	473.15	1.5245	1.623	1.623	1.623	0.000	1.623	0.065	20.191	3.005	-11.822
250	523.15	1.428	1.490	1.490	1.490	0.000	1.490	0.043	13.511	2.603	-11.324
C4 ETHYL BUTANOATE											
T (°C)	T (Kelvin)	methane(t_0)	RT ₁	RT ₂	RT ₃	stdev	avg RT	k	K (=k β)	ln K	ΔG° (kJ/mol)
50	323.15	2.026	-	-	-	-	-	-	-	-	-
75	348.15	1.904	4.408	4.408	4.406	0.001	4.407	1.315	410.994	6.019	-17.421
115	388.15	1.747	2.379	2.379	2.379	0.000	2.379	0.362	113.173	4.729	-15.261
150	423.15	1.645	1.927	1.928	1.930	0.002	1.928	0.172	53.825	3.986	-14.022

200	473.15	1.5245	1.626	1.636	1.637	0.006	1.633	0.071	22.241	3.102	-12.202
250	523.15	1.428	1.495	1.494	1.495	0.001	1.495	0.047	14.532	2.676	-11.641
C5 ETHYL PENTANOATE											
T (°C)	T (Kelvin)	methane(t ₀)	RT ₁	RT ₂	RT ₃	stdev	avg RT	k	K (=kβ)	ln K	ΔG° (kJ/mol)
50	323.15	2.026	-	-	-	-	-	-	-	-	-
75	348.15	1.904	6.557	6.553	6.557	0.002	6.556	2.444	763.658	6.638	-19.214
115	388.15	1.747	2.737	2.737	2.737	0.000	2.737	0.567	177.229	5.177	-16.708
150	423.15	1.645	2.047	2.052	2.051	0.003	2.050	0.246	76.938	4.343	-15.279
200	473.15	1.5245	1.664	1.664	1.663	0.001	1.664	0.091	28.527	3.351	-13.181
250	523.15	1.428	1.502	1.503	1.502	0.001	1.502	0.052	16.209	2.786	-12.116
C6 ETHYL HEXANOATE											
T (°C)	T (Kelvin)	methane(t ₀)	RT ₁	RT ₂	RT ₃	stdev	avg RT	k	K (=kβ)	ln K	ΔG° (kJ/mol)
50	323.15	2.026	-	-	-	-	-	-	-	-	-
75	348.15	1.904	10.614	10.546	10.545	0.040	10.568	4.552	1422.365	7.260	-21.014
115	388.15	1.747	3.294	3.294	3.294	0.000	3.294	0.886	276.893	5.624	-18.148
150	423.15	1.645	2.170	2.170	2.171	0.001	2.170	0.319	99.797	4.603	-16.194
200	473.15	1.5245	1.695	1.700	1.696	0.003	1.697	0.113	35.360	3.566	-14.026
250	523.15	1.428	1.511	1.511	1.511	0.000	1.511	0.058	18.106	2.896	-12.597
C7 ETHYL HEPTANOATE											
T (°C)	T (Kelvin)	methane(t ₀)	RT ₁	RT ₂	RT ₃	stdev	avg RT	k	K (=kβ)	ln K	ΔG° (kJ/mol)
50	323.15	2.026	-	-	-	-	-	-	-	-	-
75	348.15	1.904	17.704	17.666	17.665	0.022	17.678	8.286	2589.520	7.859	-22.749
115	388.15	1.747	4.200	4.202	4.203	0.002	4.202	1.406	439.301	6.085	-19.637
150	423.15	1.645	2.388	2.389	2.406	0.010	2.394	0.456	142.351	4.958	-17.444
200	473.15	1.5245	1.740	1.741	1.743	0.002	1.741	0.142	44.448	3.794	-14.926
250	523.15	1.428	1.523	1.522	1.523	0.001	1.523	0.066	20.658	3.028	-13.171
C8 ETHYL OCTANOATE											
T (°C)	T (Kelvin)	methane(t ₀)	RT ₁	RT ₂	RT ₃	stdev	avg RT	k	K (=kβ)	ln K	ΔG° (kJ/mol)
50	323.15	2.026	-	-	-	-	-	-	-	-	-
75	348.15	1.904	31.562	31.563	31.562	0.001	31.562	15.580	4868.674	8.491	-24.576
115	388.15	1.747	5.669	5.671	5.671	0.001	5.670	2.247	702.089	6.554	-21.150
150	423.15	1.645	2.712	2.712	2.734	0.013	2.719	0.653	204.091	5.319	-18.711
200	473.15	1.5245	1.798	1.797	1.798	0.001	1.798	0.179	55.995	4.025	-15.834
250	523.15	1.428	1.537	1.538	1.538	0.001	1.538	0.077	23.940	3.176	-13.812

C9 ETHYL NONANOATE											
T (°C)	T (Kelvin)	methane(t ₀)	RT ₁	RT ₂	RT ₃	stdev	avg RT	k	K (=kβ)	ln K	ΔG° (kJ/mol)
50	323.15	2.026	-	-	-	-	-	-	-	-	-
75	348.15	1.904	56.199	56.192	56.195	0.004	56.195	28.520	8912.351	9.095	-26.326
115	388.15	1.747	8.018	8.023	8.019	0.003	8.020	3.592	1122.513	7.023	-22.665
150	423.15	1.645	3.195	3.191	3.195	0.002	3.194	0.941	294.200	5.684	-19.998
200	473.15	1.5245	1.881	1.881	1.882	0.001	1.881	0.234	73.146	4.292	-16.886
250	523.15	1.428	1.556	1.556	1.555	0.001	1.556	0.089	27.879	3.328	-14.474
C10 ETHYL DECANOATE											
T (°C)	T (Kelvin)	methane(t ₀)	RT ₁	RT ₂	RT ₃	stdev	avg RT	k	K (=kβ)	ln K	ΔG° (kJ/mol)
50	323.15	2.026	-	-	-	-	-	-	-	-	-
75	348.15	1.904	100.200	100.199	100.198	0.001	100.199	51.635	16135.856	9.689	-28.044
115	388.15	1.747	12.171	12.171	12.173	0.001	12.172	5.969	1865.368	7.531	-24.304
150	423.15	1.645	3.878	3.879	3.876	0.002	3.878	1.357	424.139	6.050	-21.285
200	473.15	1.5245	1.976	1.975	1.973	0.002	1.975	0.295	92.278	4.525	-17.800
250	523.15	1.428	1.578	1.579	1.579	0.001	1.579	0.105	32.911	3.494	-15.196

6.5.2 HP-20M: Ethyl Esters

Table 21: Raw data for a homologous series of ethyl esters on the HP-20M. RT is the retention time measured in triplicate, β is the column phase volume ratio calculated according to equation 11, and ΔG° , the Gibbs Free Energy, was calculated according to equation 7.

C1 ETHYL FORMATE											
T (°C)	T (Kelvin)	methane(to)	RT ₁	RT ₂	RT ₃	stdev	avg RT	k	K (=k β)	ln K	ΔG° (kJ/mol)
50	323.15	0.555	-	-	-	-	-	-	-	-	-
75	348.15	0.539	0.610	0.611	0.611	0.001	0.611	0.133	35.457	3.568	-10.329
115	388.15	0.525	0.563	0.563	0.563	0.000	0.563	0.072	19.302	2.960	-9.553
150	423.15	0.513	0.542	0.542	0.542	0.000	0.542	0.056	14.892	2.701	-9.502
200	473.15	0.498	0.523	0.523	0.523	0.000	0.523	0.051	13.574	2.608	-10.260
C2 ETHYL ACETATE											
T (°C)	T (Kelvin)	methane(to)	RT ₁	RT ₂	RT ₃	stdev	avg RT	k	K (=k β)	ln K	ΔG° (kJ/mol)
50	323.15	0.555	-	-	-	-	-	-	-	-	-
75	348.15	0.539	0.638	0.638	0.638	0.000	0.638	0.184	48.980	3.891	-11.264
115	388.15	0.525	0.571	0.571	0.571	0.000	0.571	0.088	23.365	3.151	-10.169
150	423.15	0.513	0.545	0.545	0.545	0.000	0.545	0.062	16.450	2.800	-9.852
200	473.15	0.498	0.524	0.524	0.524	0.000	0.524	0.053	14.110	2.647	-10.412
C3 ETHYL PROPIONATE											
T (°C)	T (Kelvin)	methane(to)	RT ₁	RT ₂	RT ₃	stdev	avg RT	k	K (=k β)	ln K	ΔG° (kJ/mol)
50	323.15	0.555	-	-	-	-	-	-	-	-	-
75	348.15	0.539	0.688	0.688	0.688	0.000	0.688	0.276	73.717	4.300	-12.447
115	388.15	0.525	0.585	0.584	0.584	0.001	0.584	0.113	30.138	3.406	-10.991
150	423.15	0.513	0.551	0.551	0.551	0.000	0.551	0.073	19.567	2.974	-10.462
200	473.15	0.498	0.526	0.526	0.526	0.000	0.526	0.057	15.182	2.720	-10.700
C4 ETHYL BUTANOATE											
T (°C)	T (Kelvin)	methane(to)	RT ₁	RT ₂	RT ₃	stdev	avg RT	k	K (=k β)	ln K	ΔG° (kJ/mol)
50	323.15	0.555	-	-	-	-	-	-	-	-	-
75	348.15	0.539	0.779	0.779	0.779	0.000	0.779	0.445	118.738	4.777	-13.827
115	388.15	0.525	0.607	0.607	0.607	0.000	0.607	0.156	41.651	3.729	-12.035
150	423.15	0.513	0.560	0.560	0.560	0.000	0.560	0.091	24.242	3.188	-11.216
200	473.15	0.498	0.529	0.529	0.529	0.000	0.529	0.063	16.789	2.821	-11.096

C5 ETHYL PENTANOATE											
T (°C)	T (Kelvin)	methane(t ₀)	RT ₁	RT ₂	RT ₃	stdev	avg RT	k	K (=kβ)	ln K	ΔG° (kJ/mol)
50	323.15	0.555	-	-	-	-	-	-	-	-	-
75	348.15	0.539	0.987	0.986	0.987	0.001	0.987	0.831	221.480	5.400	-15.631
115	388.15	0.525	0.651	0.651	0.651	0.000	0.651	0.240	64.000	4.159	-13.421
150	423.15	0.513	0.575	0.575	0.575	0.000	0.575	0.120	32.035	3.467	-12.197
200	473.15	0.498	0.534	0.534	0.534	0.000	0.534	0.073	19.469	2.969	-11.679
C6 ETHYL HEXANOATE											
T (°C)	T (Kelvin)	methane(t ₀)	RT ₁	RT ₂	RT ₃	stdev	avg RT	k	K (=kβ)	ln K	ΔG° (kJ/mol)
50	323.15	0.555	-	-	-	-	-	-	-	-	-
75	348.15	0.539	1.380	1.380	1.380	0.000	1.380	1.560	416.079	6.031	-17.456
115	388.15	0.525	0.727	0.726	0.727	0.001	0.727	0.384	102.434	4.629	-14.939
150	423.15	0.513	0.599	0.599	0.599	0.000	0.599	0.167	44.502	3.796	-13.353
200	473.15	0.498	0.541	0.542	0.541	0.001	0.541	0.088	23.398	3.153	-12.402
C7 ETHYL HEPTANOATE											
T (°C)	T (Kelvin)	methane(t ₀)	RT ₁	RT ₂	RT ₃	stdev	avg RT	k	K (=kβ)	ln K	ΔG° (kJ/mol)
50	323.15	0.555	-	-	-	-	-	-	-	-	-
75	348.15	0.539	2.152	2.151	2.151	0.001	2.151	2.991	797.691	6.682	-19.340
115	388.15	0.525	0.855	0.855	0.855	0.000	0.855	0.629	167.619	5.122	-16.528
150	423.15	0.513	0.636	0.636	0.636	0.000	0.636	0.239	63.723	4.155	-14.616
200	473.15	0.498	0.551	0.552	0.551	0.001	0.551	0.108	28.756	3.359	-13.213
C8 ETHYL OCTANOATE											
T (°C)	T (Kelvin)	methane(t ₀)	RT ₁	RT ₂	RT ₃	stdev	avg RT	k	K (=kβ)	ln K	ΔG° (kJ/mol)
50	323.15	0.555	-	-	-	-	-	-	-	-	-
75	348.15	0.539	3.585	3.585	3.587	0.001	3.586	5.652	1507.318	7.318	-21.182
115	388.15	0.525	1.073	1.073	1.073	0.000	1.073	1.044	278.349	5.629	-18.165
150	423.15	0.513	0.694	0.694	0.694	0.000	0.694	0.352	93.853	4.542	-15.978
200	473.15	0.498	0.565	0.565	0.565	0.000	0.565	0.135	36.079	3.586	-14.105

C9 ETHYL NONANOATE											
T (°C)	T (Kelvin)	methane(t ₀)	RT ₁	RT ₂	RT ₃	stdev	avg RT	k	K (=kβ)	ln K	ΔG° (kJ/mol)
50	323.15	0.555	-	-	-	-	-	-	-	-	-
75	348.15	0.539	6.336	6.337	6.337	0.001	6.337	10.756	2868.35 7	7.961	-23.045
115	388.15	0.525	1.440	1.440	1.440	0.000	1.440	1.743	464.762	6.142	-19.819
150	423.15	0.513	0.784	0.784	0.784	0.000	0.784	0.527	140.606	4.946	-17.400
200	473.15	0.498	0.584	0.584	0.584	0.000	0.584	0.173	46.260	3.834	-15.083
C10 ETHYL DECANOATE											
T (°C)	T (Kelvin)	methane(t ₀)	RT ₁	RT ₂	RT ₃	stdev	avg RT	k	K (=kβ)	ln K	ΔG° (kJ/mol)
50	323.15	0.555	-	-	-	-	-	-	-	-	-
75	348.15	0.539	11.613	11.613	11.617	0.002	11.614	20.548	5479.44 8	8.609	-24.918
115	388.15	0.525	2.060	2.060	2.060	0.000	2.060	2.924	779.683	6.659	-21.489
150	423.15	0.513	0.924	0.924	0.924	0.000	0.924	0.800	213.333	5.363	-18.867
200	473.15	0.498	0.610	0.611	0.611	0.001	0.611	0.227	60.549	4.103	-16.142

6.6 Raw Data for Alkanes

6.6.1 SLB-IL60: Alkanes

Table 22: Raw data for a homologous series of alkanes on the SLB-IL60. RT is the retention time measured in triplicate, β is the column phase volume ratio calculated according to equation 11, and ΔG° , the Gibbs Free Energy, was calculated according to equation 7.

C5 PENTANE											
T (°C)	T (Kelvin)	methane(t_0)	RT ₁	RT ₂	RT ₃	stdev	avg RT	k	K (=k β)	ln K	ΔG° (kJ/mol)
50	323.15	2.026	-	-	-	-	-	-	-	-	-
75	348.15	1.904	2.006	2.007	2.006	0.001	2.006	0.054	16.853	2.825	-8.176
115	388.15	1.747	1.823	1.823	1.822	0.001	1.823	0.044	13.628	2.612	-8.430
150	423.15	1.645	1.702	1.701	1.701	0.001	1.701	0.034	10.702	2.370	-8.339
200	473.15	1.525	1.571	1.571	1.571	0.000	1.571	0.031	9.532	2.255	-8.869
250	523.15	1.428	1.468	1.468	1.468	0.000	1.468	0.028	8.697	2.163	-9.408
C6 HEXANE											
T (°C)	T (Kelvin)	methane(t_0)	RT ₁	RT ₂	RT ₃	stdev	avg RT	k	K (=k β)	ln K	ΔG° (kJ/mol)
50	323.15	2.026	-	-	-	-	-	-	-	-	-
75	348.15	1.904	2.027	2.027	2.027	0.000	2.027	0.065	20.246	3.008	-8.707
115	388.15	1.747	1.832	1.832	1.831	0.001	1.832	0.049	15.239	2.724	-8.790
150	423.15	1.645	1.706	1.706	1.706	0.000	1.706	0.037	11.588	2.450	-8.619
200	473.15	1.525	1.573	1.573	1.573	0.000	1.573	0.032	9.942	2.297	-9.035
250	523.15	1.428	1.469	1.469	1.470	0.001	1.469	0.029	8.989	2.196	-9.551
C10 DECANE											
T (°C)	T (Kelvin)	methane(t_0)	RT ₁	RT ₂	RT ₃	stdev	avg RT	k	K (=k β)	ln K	ΔG° (kJ/mol)
50	323.15	2.026	-	-	-	-	-	-	-	-	-
75	348.15	1.904	2.562	2.563	2.563	0.001	2.563	0.346	108.179	4.684	-13.557
115	388.15	1.747	1.955	1.955	1.956	0.001	1.955	0.120	37.366	3.621	-11.685
150	423.15	1.645	1.751	1.751	1.751	0.000	1.751	0.064	20.137	3.003	-10.563
200	473.15	1.525	1.589	1.590	1.589	0.001	1.589	0.043	13.290	2.587	-10.177
250	523.15	1.428	1.477	1.477	1.477	0.000	1.477	0.034	10.666	2.367	-10.296

C12 DODECANE											
T (°C)	T (Kelvin)	methane(t ₀)	RT ₁	RT ₂	RT ₃	stdev	avg RT	k	K (=kβ)	ln K	ΔG° (kJ/mol)
50	323.15	2.026	-	-	-	-	-	-	-	-	-
75	348.15	1.904	3.998	3.998	3.997	0.001	3.998	1.100	343.745	5.840	-16.904
115	388.15	1.747	2.190	2.190	2.190	0.000	2.190	0.254	79.355	4.374	-14.115
150	423.15	1.645	1.817	1.817	1.818	0.001	1.817	0.105	32.738	3.489	-12.273
200	473.15	1.525	1.607	1.607	1.607	0.000	1.607	0.054	16.911	2.828	-11.125
250	523.15	1.428	1.485	1.485	1.485	0.000	1.485	0.040	12.417	2.519	-10.957
C16 HEXADECANE											
T (°C)	T (Kelvin)	methane(t ₀)	RT ₁	RT ₂	RT ₃	stdev	avg RT	k	K (=kβ)	ln K	ΔG° (kJ/mol)
50	323.15	2.026	-	-	-	-	-	-	-	-	-
75	348.15	1.904	25.385	25.409	25.404	0.013	25.399	12.342	3856.976	8.258	-23.902
115	388.15	1.747	4.327	4.329	4.327	0.001	4.328	1.478	461.846	6.135	-19.799
150	423.15	1.645	2.268	2.267	2.268	0.001	2.268	0.379	118.288	4.773	-16.792
200	473.15	1.525	1.693	1.693	1.694	0.001	1.693	0.111	34.608	3.544	-13.942
250	523.15	1.428	1.514	1.513	1.513	0.001	1.513	0.060	18.616	2.924	-12.718
C18 OCTADECANE											
T (°C)	T (Kelvin)	methane(t ₀)	RT ₁	RT ₂	RT ₃	stdev	avg RT	k	K (=kβ)	ln K	ΔG° (kJ/mol)
50	323.15	2.026	-	-	-	-	-	-	-	-	-
75	348.15	1.904	-	-	-	-	-	-	-	-	-
115	388.15	1.747	8.170	8.161	8.167	0.005	8.166	3.676	1148.637	7.046	-22.739
150	423.15	1.645	2.894	2.895	2.894	0.001	2.894	0.759	237.335	5.469	-19.242
200	473.15	1.525	1.783	1.784	1.785	0.001	1.784	0.170	53.194	3.974	-15.633
250	523.15	1.428	1.538	1.538	1.538	0.000	1.538	0.077	24.013	3.179	-13.825
C20 EICOSANE											
T (°C)	T (Kelvin)	methane(t ₀)	RT ₁	RT ₂	RT ₃	stdev	avg RT	k	K (=kβ)	ln K	ΔG° (kJ/mol)
50	323.15	2.026	-	-	-	-	-	-	-	-	-
75	348.15	1.904	-	-	-	-	-	-	-	-	-
115	388.15	1.747	17.573	17.583	17.584	0.006	17.580	9.066	2833.077	7.949	-25.652
150	423.15	1.645	4.175	4.175	4.178	0.002	4.176	1.539	480.813	6.175	-21.726
200	473.15	1.525	1.927	1.927	1.927	0.000	1.927	0.264	82.507	4.413	-17.359
250	523.15	1.428	1.561	1.562	1.563	0.001	1.562	0.094	29.264	3.376	-14.685

C22 <u>DOCOSANE</u>											
T (°C)	T (Kelvin)	methane(t ₀)	RT ₁	RT ₂	RT ₃	stdev	avg RT	k	K (=kβ)	ln K	ΔG° (kJ/mol)
50	323.15	2.026	-	-	-	-	-	-	-	-	-
75	348.15	1.904	-	-	-	-	-	-	-	-	-
115	388.15	1.747	-	-	-	-	-	-	-	-	-
150	423.15	1.645	6.993	6.963	6.973	0.015	6.976	3.241	1012.791	6.920	-24.347
200	473.15	1.525	2.178	2.177	2.176	0.001	2.177	0.428	133.753	4.896	-19.260
250	523.15	1.428	1.602	1.602	1.602	0.000	1.602	0.122	38.016	3.638	-15.823
C24 <u>TETRACOSANE</u>											
T (°C)	T (Kelvin)	methane(t ₀)	RT ₁	RT ₂	RT ₃	stdev	avg RT	k	K (=kβ)	ln K	ΔG° (kJ/mol)
50	323.15	2.026	-	-	-	-	-	-	-	-	-
75	348.15	1.904	-	-	-	-	-	-	-	-	-
115	388.15	1.747	-	-	-	-	-	-	-	-	-
150	423.15	1.645	7.914	7.682	7.685	0.133	7.760	3.718	1161.727	7.058	-24.829
200	473.15	1.525	2.606	2.607	2.605	0.001	2.606	0.709	221.692	5.401	-21.247
250	523.15	1.428	1.669	1.669	1.668	0.001	1.669	0.168	52.603	3.963	-17.236
C26 <u>HEXACOSANE</u>											
T (°C)	T (Kelvin)	methane(t ₀)	RT ₁	RT ₂	RT ₃	stdev	avg RT	k	K (=kβ)	ln K	ΔG° (kJ/mol)
50	323.15	2.026	-	-	-	-	-	-	-	-	-
75	348.15	1.904	-	-	-	-	-	-	-	-	-
115	388.15	1.747	-	-	-	-	-	-	-	-	-
150	423.15	1.645	-	-	-	-	-	-	-	-	-
200	473.15	1.525	3.342	3.340	3.335	0.004	3.339	1.190	371.946	5.919	-23.283
250	523.15	1.428	1.771	1.771	1.770	0.001	1.771	0.240	74.921	4.316	-18.774

6.6.2 HP-20M: Alkanes

Table 23: Raw data for a homologous series of alkanes on the HP-20M. RT is the retention time measured in triplicate, β is the column phase volume ratio calculated according to equation 11, and ΔG° , the Gibbs Free Energy, was calculated according to equation 7.

C5 PENTANE											
T (°C)	T (Kelvin)	methane(t_0)	RT ₁	RT ₂	RT ₃	stdev	avg RT	k	K (=k β)	ln K	ΔG° (kJ/mol)
50	323.15	0.555	0.582	0.582	0.583	0.001	0.582	0.049	13.133	2.575	-6.919
75	348.15	0.539	0.567	0.566	0.566	0.001	0.566	0.051	13.523	2.604	-7.538
115	388.15	0.525	0.547	0.547	0.547	0.000	0.547	0.042	11.175	2.414	-7.789
150	423.15	0.513	0.534	0.534	0.534	0.000	0.534	0.040	10.736	2.374	-8.350
200	473.15	0.498	0.522	0.522	0.522	0.000	0.522	0.049	13.039	2.568	-10.102
C6 HEXANE											
T (°C)	T (Kelvin)	methane(t_0)	RT ₁	RT ₂	RT ₃	stdev	avg RT	k	K (=k β)	ln K	ΔG° (kJ/mol)
50	323.15	0.555	0.594	0.594	0.594	0.000	0.594	0.070	18.739	2.931	-7.874
75	348.15	0.539	0.572	0.573	0.572	0.001	0.572	0.062	16.491	2.803	-8.113
115	388.15	0.525	0.550	0.550	0.550	0.000	0.550	0.048	12.698	2.541	-8.202
150	423.15	0.513	0.536	0.536	0.536	0.000	0.536	0.044	11.775	2.466	-8.675
200	473.15	0.498	0.524	0.524	0.519	0.003	0.522	0.050	13.217	2.582	-10.155
C10 DECANE											
T (°C)	T (Kelvin)	methane(t_0)	RT ₁	RT ₂	RT ₃	stdev	avg RT	k	K (=k β)	ln K	ΔG° (kJ/mol)
50	323.15	0.555	1.086	1.088	1.089	0.002	1.088	0.960	255.936	5.545	-14.897
75	348.15	0.539	0.749	0.749	0.749	0.000	0.749	0.390	103.896	4.643	-13.440
115	388.15	0.525	0.598	0.598	0.598	0.000	0.598	0.139	37.079	3.613	-11.660
150	423.15	0.513	0.556	0.556	0.556	0.000	0.556	0.083	22.165	3.098	-10.901
200	473.15	0.498	0.528	0.528	0.528	0.000	0.528	0.061	16.254	2.788	-10.969
C12 DODECANE											
T (°C)	T (Kelvin)	methane(t_0)	RT ₁	RT ₂	RT ₃	stdev	avg RT	k	K (=k β)	ln K	ΔG° (kJ/mol)
50	323.15	0.555	3.072	3.070	3.070	0.001	3.071	4.533	1208.729	7.097	-19.068
75	348.15	0.539	1.302	1.302	1.302	0.000	1.302	1.416	377.489	5.934	-17.175
115	388.15	0.525	0.704	0.704	0.704	0.000	0.704	0.341	90.921	4.510	-14.554
150	423.15	0.513	0.591	0.591	0.591	0.000	0.591	0.151	40.346	3.698	-13.008
200	473.15	0.498	0.540	0.540	0.540	0.000	0.540	0.085	22.684	3.122	-12.280

C16 <u>HEXADECANE</u>											
T (°C)	T (Kelvin)	methane(t ₀)	RT ₁	RT ₂	RT ₃	stdev	avg RT	k	K (=kβ)	ln K	ΔG° (kJ/mol)
50	323.15	0.555	-	-	-	-	-	-	-	-	-
75	348.15	0.539	11.567	11.529	11.530	0.022	11.542	20.414	5443.661	8.602	-24.899
115	388.15	0.525	1.927	1.930	1.930	0.002	1.929	2.674	713.143	6.570	-21.201
150	423.15	0.513	0.876	0.877	0.877	0.001	0.877	0.708	188.745	5.240	-18.436
200	473.15	0.498	0.602	0.599	0.602	0.002	0.601	0.208	55.370	4.014	-15.790
C18 <u>OCTADECANE</u>											
T (°C)	T (Kelvin)	methane(t ₀)	RT ₁	RT ₂	RT ₃	stdev	avg RT	k	K (=kβ)	ln K	ΔG° (kJ/mol)
50	323.15	0.555	-	-	-	-	-	-	-	-	-
75	348.15	0.539	-	-	-	-	-	-	-	-	-
115	388.15	0.525	4.387	4.391	4.390	0.002	4.389	7.361	1962.836	7.582	-24.468
150	423.15	0.513	1.335	1.333	1.333	0.000	1.333	1.597	425.801	6.054	-21.298
200	473.15	0.498	0.672	0.672	0.674	0.001	0.673	0.352	93.771	4.541	-17.863
C20 <u>EICOSANE</u>											
T (°C)	T (Kelvin)	methane(t ₀)	RT ₁	RT ₂	RT ₃	stdev	avg RT	k	K (=kβ)	ln K	ΔG° (kJ/mol)
50	323.15	0.555	-	-	-	-	-	-	-	-	-
75	348.15	0.539	-	-	-	-	-	-	-	-	-
115	388.15	0.525	11.121	11.128	11.126	0.004	11.125	20.190	5384.127	8.591	-27.725
150	423.15	0.513	2.373	2.280	2.278	0.054	2.310	3.501	933.506	6.839	-24.060
200	473.15	0.498	0.805	0.805	0.804	0.001	0.805	0.617	164.501	5.103	-20.074
C22 <u>DOCOSANE</u>											
T (°C)	T (Kelvin)	methane(t ₀)	RT ₁	RT ₂	RT ₃	stdev	avg RT	k	K (=kβ)	ln K	ΔG° (kJ/mol)
50	323.15	0.555	-	-	-	-	-	-	-	-	-
75	348.15	0.539	-	-	-	-	-	-	-	-	-
115	388.15	0.525	27.224	26.829	26.829	0.228	26.961	50.354	13427.640	9.505	-30.674
150	423.15	0.513	4.502	4.503	4.450	0.030	4.485	7.737	2063.203	7.632	-26.850
200	473.15	0.498	1.056	1.056	1.056	0.000	1.056	1.122	299.174	5.701	-22.427
C24 <u>TETRACOSANE</u>											
T (°C)	T (Kelvin)	methane(t ₀)	RT ₁	RT ₂	RT ₃	stdev	avg RT	k	K (=kβ)	ln K	ΔG° (kJ/mol)
50	323.15	0.555	-	-	-	-	-	-	-	-	-
75	348.15	0.539	-	-	-	-	-	-	-	-	-
115	388.15	0.525	72.958	72.955	72.959	0.002	72.957	137.966	36791.026	10.513	-33.926
150	423.15	0.513	9.618	9.618	9.559	0.034	9.598	17.698	4719.481	8.459	-29.761
200	473.15	0.498	1.544	1.543	1.543	0.001	1.543	2.101	560.304	6.328	-24.895

C26 HEXACOSANE											
T (°C)	T (Kelvin)	methane(t ₀)	RT ₁	RT ₂	RT ₃	stdev	avg RT	k	K (=kβ)	ln K	ΔG° (kJ/mol)
50	323.15	0.555	-	-	-	-	-	-	-	-	-
75	348.15	0.539	-	-	-	-	-	-	-	-	-
115	388.15	0.525	-	-	-	-	-	-	-	-	-
150	423.15	0.513	21.323	21.320	21.319	0.002	21.321	40.534	10809.004	9.288	-32.676
200	473.15	0.498	2.481	2.449	2.449	0.018	2.460	3.942	1051.306	6.958	-27.370

“Knowledge comes by taking things apart: analysis.

But wisdom comes by putting things together.”

-John A Morrison